

*Epithelial to Mesenchymal Transition in Breast Cancer:  
A novel Murine Model System and  
the Regulatory Role of Tead Transcription Factors*

**Inauguraldissertation**

zur  
Erlangung der Würde eines Doktors der Philosophie  
vorgelegt der  
Philosophisch-Naturwissenschaftlichen Fakultät  
der Universität Basel

von

**Lorenz Waldmeier**

aus Basel (BS)

Basel, 2012

Originaldokument gespeichert auf dem Dokumentenserver  
der Universität Basel [edoc.unibas.ch](http://edoc.unibas.ch)

Dieses Werk ist unter dem Vertrag „Creative Commons Namensnennung-Keine kommerzielle Nutzung-Keine Bearbeitung 2.5 Schweiz“ lizenziert. Die vollständige Lizenz kann unter [creativecommons.org/licences/by-nc-nd/2.5/ch](http://creativecommons.org/licences/by-nc-nd/2.5/ch) eingesehen werden.



## Namensnennung-Keine kommerzielle Nutzung-Keine Bearbeitung 2.5 Schweiz

---

### Sie dürfen:



das Werk vervielfältigen, verbreiten und öffentlich zugänglich machen

### Zu den folgenden Bedingungen:



**Namensnennung.** Sie müssen den Namen des Autors/Rechteinhabers in der von ihm festgelegten Weise nennen (wodurch aber nicht der Eindruck entstehen darf, Sie oder die Nutzung des Werkes durch Sie würden entlohnt).



**Keine kommerzielle Nutzung.** Dieses Werk darf nicht für kommerzielle Zwecke verwendet werden.



**Keine Bearbeitung.** Dieses Werk darf nicht bearbeitet oder in anderer Weise verändert werden.

- Im Falle einer Verbreitung müssen Sie anderen die Lizenzbedingungen, unter welche dieses Werk fällt, mitteilen. Am Einfachsten ist es, einen Link auf diese Seite einzubinden.
- Jede der vorgenannten Bedingungen kann aufgehoben werden, sofern Sie die Einwilligung des Rechteinhabers dazu erhalten.
- Diese Lizenz lässt die Urheberpersönlichkeitsrechte unberührt.

#### Die gesetzlichen Schranken des Urheberrechts bleiben hiervon unberührt.

Die Commons Deed ist eine Zusammenfassung des Lizenzvertrags in allgemeinverständlicher Sprache: <http://creativecommons.org/licenses/by-nc-nd/2.5/ch/legalcode.de>

#### Haftungsausschluss:

Die Commons Deed ist kein Lizenzvertrag. Sie ist lediglich ein Referenztext, der den zugrundeliegenden Lizenzvertrag übersichtlich und in allgemeinverständlicher Sprache wiedergibt. Die Deed selbst entfaltet keine juristische Wirkung und erscheint im eigentlichen Lizenzvertrag nicht. Creative Commons ist keine Rechtsanwalts-gesellschaft und leistet keine Rechtsberatung. Die Weitergabe und Verlinkung des Commons Deeds führt zu keinem Mandatsverhältnis.



Genehmigt von der Philosophisch - Naturwissenschaftlichen Fakultät  
auf Antrag von

Prof. Dr. Gerhard Christofori

Prof. Dr. Markus Affolter

Basel, den 26. Juni 2012

Prof. Dr. Martin Spiess

Dekan

# Table of Contents

<b>List of abbreviations .....</b>	<b>i</b>
<b>Summary .....</b>	<b>ii</b>
<b>1. General Introduction.....</b>	<b>1</b>
<b>1.1 Cancer .....</b>	<b>1</b>
1.1.1 History and definition of cancer .....	1
1.1.2 Hallmarks of Cancer.....	3
<b>1.2 Breast cancer .....</b>	<b>8</b>
1.2.1 The normal breast .....	8
1.2.2 Breast cancer subtypes .....	9
1.2.3 Intratumoral heterogeneity .....	11
1.2.4 The tumor microenvironment.....	13
<b>1.3 Epithelial-mesenchymal transition (EMT) .....</b>	<b>14</b>
1.3.1 EMT is context-dependent .....	14
1.3.2 Mediators of EMT .....	16
1.3.3 TGF $\beta$ -induced EMT .....	18
<b>1.4 Tead transcription factors .....</b>	<b>25</b>
1.4.1 The Tead family .....	25
1.4.2 Tead functions .....	25
1.4.3 Tead transcriptional machinery .....	26
1.4.4 Regulation of Yap/Taz/Tead transcriptional activity .....	28
<b>1.5 MARA Analysis .....</b>	<b>34</b>
<b>2. Aim of the study .....</b>	<b>35</b>
<b>3. Results .....</b>	<b>36</b>
<b>3.1 Py2T murine breast cancer cells, a versatile model of TGF<math>\beta</math>-induced EMT in vitro and in vivo .....</b>	<b>36</b>
3.1.1 Abstract .....	36
3.1.2 Introduction .....	37
3.1.3 Results .....	38
3.1.3.1 Py2T, a novel breast cancer cell line undergoing TGF $\beta$ -induced EMT .....	38
3.1.3.2 EMT kinetics and plasticity in Py2T cells .....	41
3.1.3.3 Migratory and invasive properties upon EMT induction .....	43
3.1.3.4 Invasive tumor formation upon orthotopic transplantation into syngeneic mice .....	46
3.1.3.5 TGF $\beta$ -dependent EMT of Py2T tumors .....	47

3.1.4	Discussion .....	50
3.1.5	Conclusions .....	54
3.1.6	Supplemental Data .....	55
3.1.7	Materials and Methods .....	57
<b>3.2</b>	<b>Critical roles of Tead transcription factors in the EMT process .....</b>	<b>64</b>
3.2.1	Abstract .....	64
3.2.2	Introduction .....	65
3.2.3	Results .....	68
3.2.3.1	Increase of Tead transcriptional activity during EMT .....	68
3.2.3.2	Tead2 expression levels are upregulated during EMT .....	70
3.2.3.3	Increase of Tead2 activity is sufficient to induce EMT .....	72
3.2.3.4	Loss of Tead function attenuates EMT and inhibits migration and invasion .....	75
3.2.3.5	Tead2 is sufficient and required for Yap/Taz nuclear localization.....	77
3.2.3.6	Tead2 localization is regulated by cell density .....	81
3.2.3.7	Identification of Zyxin as a novel Tead2 target gene during EMT .....	82
3.2.4	Discussion .....	85
3.2.5	Supplementary Data .....	91
3.2.6	Materials and Methods .....	96
<b>4.</b>	<b>References.....</b>	<b>103</b>
<b>5.</b>	<b>Curriculum Vitae.....</b>	<b>117</b>
<b>6.</b>	<b>Acknowledgments .....</b>	<b>119</b>

## List of abbreviations

ChIP	Chromatin immunoprecipitation
EMT	Epithelial to mesenchymal transition
EnR	Engrailed
FL	Full length
IPA	Ingenuity pathway analysis
LT	Long-term
MARA	Motif activity response analysis
MMTV	Mouse mammary tumor virus
MT	Mammary tumor
NMuMG	Normal murine mammary gland
PyMT	Polyoma-middle-T
Py2T	Polyoma-middle-T tumor
Taz	Transcriptional co-activator with PDZ-domain
TBRDN	Dominant-negative TGF $\beta$ receptor II
Tead	TEA domain-containing
TF	Transcription factor
TGF $\beta$	Transforming growth factor $\beta$
Yap	Yes-associated protein

## Summary

Cancer is a leading cause of death worldwide, accounting for 7.6 million, or ~13% of all deaths in 2008. The majority of cancers arise from epithelia. Breast cancer, originating from the mammary epithelium, is the most frequent cancer in women worldwide. Breast cancer detection and treatment at early stages is an effective measure of counteracting the number of deaths, however at later stages, cancer cells may spread from the primary tumor to secondary organs, a multistage process called metastasis. This process involves the dissemination of cancer cells from the primary tumor, entrance into the vascular system, extravasation and re-growth (colonization) in the target organ. Metastasis is the actual cause of death in 90% of cancer patients.

Breast cancer treatment is complicated by the existence of substantial biological heterogeneity between and within tumors: At least five different subtypes of breast cancer with variable response to treatment and outcome have been proposed. The biological differences between these tumor subtypes are mainly determined by the nature of the oncogenic hit(s) and the cell type in which transformation originally occurred. In addition to different tumor types, progressing tumors (and also their metastatic outgrowth) consist of individual tumor cells with varying features, which can be evoked by acquisition of cumulative genetic/epigenetic alterations and/or by differential stimulation by components of the nearby tumor microenvironment.

These circumstances call for a better understanding of the underlying mechanisms that provide cancer cells with malignant features, such as the acquisition of a metastatic behavior and treatment resistance.

One mechanism that endows cancer cells with several pro-metastatic features and treatment resistance is the epithelial-mesenchymal transition (EMT). EMT is a latent embryonic program that can be aberrantly reactivated in epithelial tumor cells during tumor progression. Activation of EMT-like programs in tumor cells leads to dissolution of cell-cell adhesions, a loss of polarity and an acquisition of migratory, invasive and stem-cell-like traits.

Studies investigating the role of EMT in cancer have mainly employed a combination of different model systems for *in vitro* and *in vivo* experiments. Due to the lack of model systems that allow the study of breast cancer associated EMT *in vitro* and *in vivo* using the same cell line, I have established a stable cell line (Py2T) from a breast tumor of an MMTV-

PyMT transgenic mouse. I show here that this epithelial cell line undergoes *bona fide* EMT under cell culture conditions when stimulated with the well-known EMT-inducer transforming growth factor  $\beta$  (TGF $\beta$ ). TGF $\beta$  treatment of Py2T cells leads to downregulated expression of the epithelial marker E-cadherin and an upregulation of mesenchymal markers, concomitant with the induction of migratory and invasive properties. When orthotopically injected into mice, Py2T cells generate tumors that are highly invasive and display a mesenchymal phenotype characterized by the absence of E-cadherin expression, suggesting that these cells undergo spontaneous EMT-like changes *in vivo*. Interestingly, Py2T cells overexpressing a dominant-negative TGF $\beta$ -receptor, leading to a block of TGF $\beta$  responsiveness, also form tumors upon fat-pad transplantation, yet in these tumors a partial re-expression of E-cadherin can be observed, suggesting that TGF $\beta$  signaling contributes to the EMT phenotype *in vivo*. Together, my results show that the Py2T model system is a versatile tool to study EMT both *in vitro* and *in vivo*.

The second project presented in this thesis aimed at the identification of critical transcription factors (TFs) that mediate the widespread changes in gene expression observed during EMT. A genome-wide bioinformatics analysis has uncovered that the DNA-binding motif of Tead transcription factors (MCAT motif) is present in a large number of promoters of EMT-regulated genes. Here I show that Tead transcriptional activity is increased during EMT. Moreover, the expression levels of several Tead family members are also upregulated during EMT, and my results demonstrate that elevated transcriptional activity of Tead2 is sufficient to induce EMT. Furthermore, inhibition or depletion of Teads attenuates the EMT process. Moreover, Tead2 levels also can control the subcellular localization of the Tead co-activators Yap and Taz, a mechanism that possibly contributes to the increased Tead activity observed during EMT. I further demonstrate that Zyxin, a focal adhesion component and regulator of actin remodeling, which has previously been shown to be required for EMT-induced migration, is a direct target gene of Tead2. Collectively, these results demonstrate an important regulatory role of Tead transcription factors in the EMT process.

# 1. General Introduction

## 1.1 Cancer

### 1.1.1 History and definition of cancer

The origin of the term cancer dates back over 2,500 years and was first used by the Hippocratic school, where the prominent appearance of thick, dark veins on the surface of breast tumors were observed to appear like the limbs of a crab (Καρκίνος, Karkinos, greek for crab). Although difficult to interpret, documentations of what would nowadays possibly be identified as cancer reaches back to some of the first forms of documentation (Figure 1).

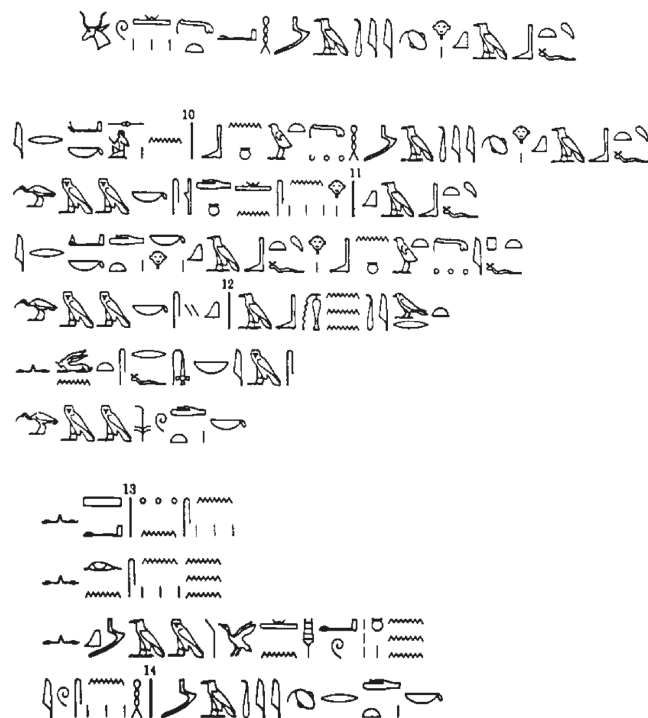


**Figure 1. Papyrus possibly describing a male breast cancer.**

This copy made in the 17th century b.c. of an older manuscript originally written during the period 3000-2500 b.c. (the „Pyramid“ age) was recovered by Edwin Smith in Luxor in 1862. The Hieroglyphs depicted are part of a five meters long roll describing several cases of illnesses, which could have been a physician’s hand- book, outlines of lectures, or a student’s notebook. Depicted is case 45, which was translated in 1930 by Breasted (Breasted, 1930): Upper hieroglyphs: “Instructions concerning bulging tumors on the breast”. Followed by “If thou examinest a man having bulging tumors on his breast, thou findest that swelling have spread over his breast; if thou puttest thy hand upon his breast upon those tumors, thou findest them very cool, there being no fever at all when thy hand touches him; they have no granulation, they form no fluid, they do not generate secretions of fluid, and they are bulging to thy hand . . . Swellings on his breast are large, spreading and hard; touching them is like touching a ball of wrappings; the comparison is to a green hemat-fruit, which is hard and cool under thy hand, like touching those swellings which are on his breast”. The most that can now be said, is that this was a *possible* case of cancer (Weiss, 2000).

Miscellaneous and ever changing theories had been postulated by different cultures of mankind about the origins and treatment of cancer (Weiss, 2000). The establishment of the concept that living organisms are composed of cells that can divide and therefore are able to multiply led to the understanding that cancers originate from somehow aberrantly multiplying cells of the own body, an idea pioneered by the German physicist Rudolf Virchow (Virchow, 1871). An understanding of why cells break free of their normal behavior and turn into cancer cells has only been elucidated in the last decades. Today we know that cancer is a disease of cells containing dysregulated genes and molecules, resulting in an imbalance between growth inhibitory signals and growth stimulatory signals. These imbalances ultimately result in abnormal, uncontrolled cell division (Neoplasia, greek for “new growth”).

Cancers can originate in virtually all tissues, including the blood. It should be specified that cancer is a general term encompassing a group of at least 100 diseases, with every cancer type originating from different tissues having its own characteristics and peculiarities. Cancers of the same original tissue are also diverse in their nature, and these differences are largely determined by the difference in nature of the underlying oncogenic event. Usually, cancers originate from just one single cell that then can give rise to the entire neoplastic tissue. Further genetic modifications of these cells, changes in differentiation state and cross-talk with normal cells and other surrounding factors further contributes to the diversity and complexity of cancers.

The majority of human tumors (or neoplasms) arises from epithelia, and can be benign or can be(come) malignant. Benign tumors remain confined to their location within the tissue they have originated. Malignant tumors can invade surrounding tissue and spread to different sites in the body via the blood and/or the lymphatic system, a process termed metastasis. These secondary metastatic outgrowths are usually the actual cause of death, rather than the primary tumors, which can often be removed by surgery. Importantly, only malignant tumors are correctly referred to cancers. Cancers of epithelial origin are termed carcinomas, which are responsible for over 80% of cancer deaths in the western world (Weinberg, 2006). According to the World Health Organization (WHO), cancer is one of the leading causes of death worldwide, accounting for 7.6 million deaths (around 13% of all deaths) in 2008.



### 1.1.2 Hallmarks of Cancer

Despite the above-described diversity among cancers, some features are common to most human cancers. These features are prerequisites that allow tumors to grow and progress to metastatic disease. A summary of such features, or hallmarks of cancer according to Hanahan and Weinberg (Hanahan and Weinberg, 2000; 2011), are briefly delineated below.

#### *Sustained proliferative signaling*

One general property of cancer cells is that they display a reduced or even completely abolished requirement of growth stimulatory signals for active proliferation. Normal cells rely on these stimuli to remain or enter into an active cell cycle. Such stimuli can come from the extracellular environment, other neighboring cells or are systemically distributed. A number of strategies are used by cancer cells to sustain proliferation the appropriate signals are limited: for example, overexpression of growth-factor receptors may lead to sufficient mitogenic signaling in response to low levels of growth factors, which would otherwise not suffice to elicit proliferative responses. Similarly, mutation of these receptors or in downstream elements of growth stimulatory pathways that lead to constitutive activation of signaling may allow proliferation in the absence of ligands. Conversely, cancer cells may aberrantly produce growth stimulatory factors to which they can respond themselves, which is rarely the case in normal cells. A large number of cancers of different origins display such alterations converging on activation of the mitogenic SOS-Ras-Raf-MAP kinase or the PI-3 Kinase/Akt pathways. Yet other strategies of cancer cells involve disruption of negative feedback loops, which are activated in normal cells upon mitogenic signaling in order to dampen these signals and to ensure well controlled transient signaling instead of overshooting. Examples are the disruption of negative feedback loops in the MAP kinase pathway mediated by Ras GTPases that directly counteract Ras activity, or loss of PTEN function, which normally dampens PI-3 kinase signaling. In addition, it has been observed that normal cells overstimulated by proliferative signals can enter into a quiescent state, while cancer cells sometimes lose the ability to do so to, thus “blindly” executing the given commands with fatal outcome.

*Evasion of growth suppressors*

Normal cells contain sensory mechanisms that mediate anti-proliferative signaling to ensure tissue homeostasis. Anti-proliferative signals are also elicited in situations where further proliferation would be detrimental due to cellular stress, lack of nutrients or DNA damage. Signals of this nature typically converge on two central “gatekeeper” proteins: cell extrinsic signals are usually directed onto the retinoblastoma protein pRB, while cell intrinsic cues to stop proliferation are propagated to p53. These two tumor suppressor proteins seem to be woven into a complex, situation- and tissue- specific web of sensory mechanisms in a functionally redundant manner. Upregulated and activated p53 transcriptionally upregulates the cell cycle inhibitor p21, which inhibits G1/S transition of the cell cycle by inhibition of Cyclin/CDK2 complexes. The anti-proliferative action of pRB is also affected by p21 expression: p21 inhibits pRB phosphorylation indirectly by inhibition of cyclin/CDK complexes, which normally phosphorylate pRB. Unphosphorylated pRB binds to and sequesters E2F transcription factors away from target promoters of cell cycle progression genes, thereby inhibiting cell cycle progression. Similarly, transforming growth factor  $\beta$  (TGF $\beta$ ) has been shown to potently inhibit proliferation by blocking c-myc expression, which prevents cell cycle arrest, and by induction of p15INK<sup>4B</sup> and p21. In cancers, both p53 and/or pRB inactivating mutations or loss can result in an evasion from growth suppressive stimuli. The tumor suppressive functions of TGF $\beta$  can be circumvented in tumor cells by either disruption of the core components like TGF $\beta$  receptors or by inactivation of the immediate downstream mediators like Smad4. On the other hand, only the tumor suppressor arm of the highly branched TGF $\beta$  pathway can be inactivated, leaving the core pathway and therefore the other downstream activities intact, which are well established to contribute to tumor progression. Another growth suppressive mechanism inherent to normal cells underlies their ability to „sense“ the contact of neighboring cells, instructing them to stop growing once the tissue reaches its correct size. This phenomenon of contact inhibition can also be observed with cultured cells in a dish (e.g. epithelial cells or fibroblasts), which will stop proliferating once the entire surface is covered and neighboring cells contact each other. Transformed cells often lose the ability to arrest proliferation under these circumstances and hence form foci (in a dish) or overgrow to form tumors.

*Resisting cell death*

Virtually all cells of the body are able to undergo cell “suicide” or apoptosis. This process is a highly ordered cellular program triggered by various physiological stresses and can also occur in response to elevated oncogenic signaling, therefore acting as a safeguard mechanism preventing the induction of cancer. The apoptotic machinery is composed of two parts. A sensing part, which monitors both the extracellular (e.g. Fas/Fas-ligand) and the intracellular environment (e.g. p53), and decides whether a cell should live or die. The executing part is responsible for degrading the cell in an orderly way. Whether apoptosis is executed depends on the balanced expression levels of the pro- (e.g. Bax, Bim) and anti-apoptotic (e.g. Bcl-2) proteins of the Bcl-2 family. The anti-apoptotic members bind and inhibit the activity of their apoptotic counterparts, which sit in the mitochondrial membrane. When activated, the pro-apoptotic members disrupt the mitochondrial membrane resulting in cytochrome-c release into the cytoplasm. This in turn activates a cascade of proteolytic caspases that execute the apoptotic program and degrade cellular components. Cancer cells have been shown to circumvent the induction of apoptosis in a multitude of ways, reflecting the importance of the apoptotic program as a barrier for cancer development. One of the most frequently observed ways to escape from apoptosis is the inactivation of p53, which acts as a critical sensor of DNA damage and whose activation induces either cell cycle arrest or apoptosis. Consequently, p53 is functionally inactivated in more than 50% of human cancers. Other strategies to circumvent apoptosis induction involve the misregulation of pro- or anti-apoptotic proteins, including the members of the pro-apoptotic Bcl-2 family, in the appropriate direction, or disruption of the FAS death signaling circuit.

*Limitless replicative potential*

The three hallmarks of cancer described above will usually not be sufficient to form a tumor, because most mammalian cells have a limited lifespan, clocked by an intrinsic, cell-autonomous program working independently of the above-mentioned signaling pathways. With each completed cell cycle, the chromosomal ends (telomeres) are shortened by 50-100 nucleotides. Cultured untransformed human cells may divide 60 – 70 times until telomeres are blunted. At this stage, a scrambling of the karyotype and crisis occurs, in which almost all cells undergo senescence and/or apoptosis. Under cell culture conditions, an estimated 1 in  $10^7$  cells however will survive the crisis and be “immortalized”, i.e. be able to divide without

limit. Most malignant cells display telomere maintenance, providing limitless growth potential and protection from crisis and apoptosis. Telomere maintenance is usually achieved by telomerase upregulation. Therefore, the lifetime “countdown” of normal cells represents a barrier to cancer development and has to be overcome by cancer cells.

### *Sustained angiogenesis*

During tissue and organ development, the formation of new blood vessels concomitant with growth of the respective organ or tissue is a prerequisite, and ensures that cells are supplied with nutrients and oxygen. At the same time, a well-developed vascular system also allows disposal of waste products and carbon dioxide. Neoplasms at the earliest stages lack the ability to encourage vessel recruitment by sprouting angiogenesis from the pre-existing surrounding vasculature, and must go through an “angiogenic switch” that allows sustained activation of angiogenesis. Only after an angiogenic switch a progression to larger tumor size is possible. Angiogenesis is balanced by both pro- and anti-angiogenic factors that signal via transmembrane receptors expressed on blood endothelial cells. Vascular endothelial growth factor A (VEGF-A) and Thrombospondin 1 (TSP-1) are the key representatives of the pro- and anti-angiogenic category, respectively. Therefore, one obvious strategy to overcome the cancer growth barriers of low oxygen and nutrients during the establishment of cancers is up- or downregulation of pro- and antiangiogenic factors, respectively. Some oncogenes like Ras and Myc can themselves upregulate pro-angiogenic factors, and are therefore an example for how some factors may influence multiple hallmarks of cancer at the same time.

### *Activating invasion and metastasis*

Most human cancers progress to a stage where cells are dissociating from the primary tumor to spread to different sites in the body, where they will colonize the foreign tissue to regrow as secondary tumors. This multistage process is called metastasis, which can be divided into a series of steps: First, cancer cells must break away from the primary tumor mass and reach the circulation, which provides a route to distant sites. To be able to do so, cancer cells need to loosen their cell-cell adhesions and acquire invasive and migratory properties. A process termed epithelial-mesenchymal transition (EMT) is implicated in facilitating these first steps, and possibly also later steps. Having survived the transport to secondary organs via the circulation, and having mastered the entrance into distant tissues, cancer cells may either rest at the new sites as clusters of a few cells residing in a dormant state (micrometastasis) or

they may re-grow. To be able to develop macroscopic tumors at the foreign sites (i.e. successful colonization), cancer cells have to adapt to these new sites, essentially requiring all the hallmarks described above, however in a different background with differing demands. As of yet, however, the mechanisms involved in colonization are poorly understood.

The signaling circuitry of normal cells that is reprogrammed in cancer cells to achieve the above discussed hallmarks of cancer can be portrayed as integrated signaling circuits consisting of interlinked subcircuits, each of which determining a subset of biological features that, when reprogrammed, make up the hallmarks of cancer cells (Figure 2).

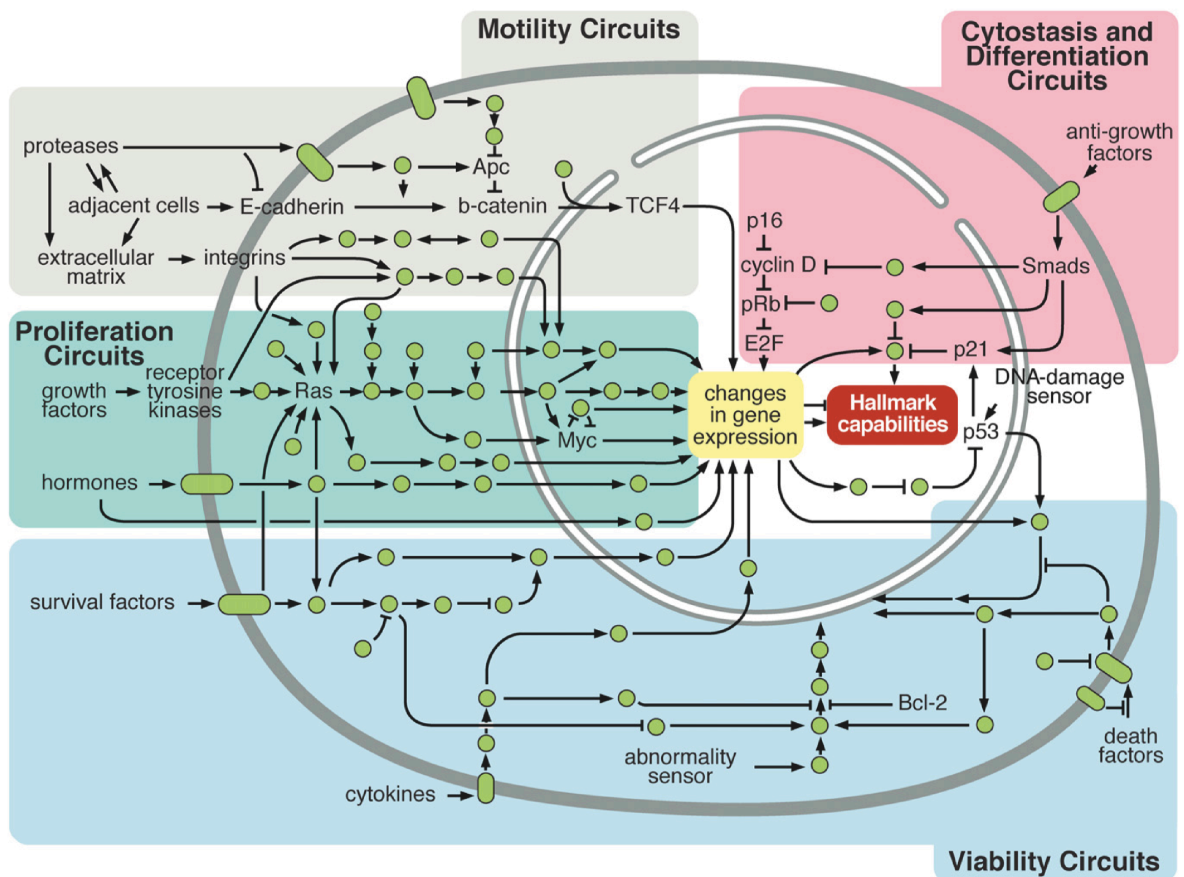


**Figure 2. Cellular circuitry reprogrammed in cancer cells.**

A simplified scheme showing the signaling pathways that operate in normal cells to regulate the balance of growth and apoptosis. Reprogramming of separate subcircuits, grouped according to their contribution to biological functions, can lead to acquisition of one or several hallmarks of cancer cells. Taken from (Hanahan and Weinberg, 2011).

## 1.2 Breast cancer

### 1.2.1 The normal breast

The normal breast is composed of a number of milk-producing terminal units (termed terminal ductal lobular units (TDLUs) in humans or terminal end buds (TEBs) in the mouse) that lead into a branched network of milk ducts converging at the nipple. These epithelial structures, in their entirety forming the mammary gland, are embedded in connective tissue mainly composed of adipocytes (fat cells) (Figure 3A).

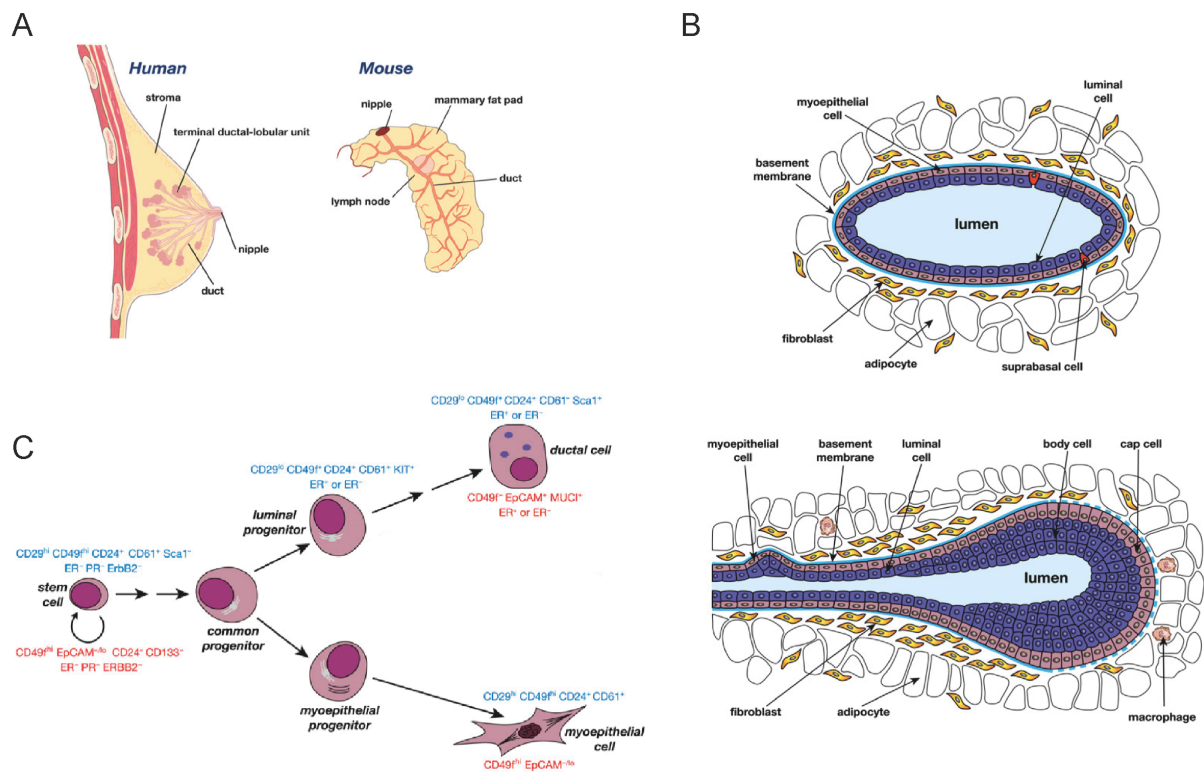


**Figure 3. The mammary gland.**

(A) Schematic representation of the human and mouse mammary gland. (B) Cross-sectional view of a duct (top) and a terminal end bud (bottom). (C) Hierarchical differentiation model of the mammary gland. Cell surface markers used to isolate subsets of cells at various differentiation stages are shown in red (human) and blue (mouse). Schemes are taken from (Visvader, 2009).

At a cellular level, ducts and end units are mainly composed of two separate cell types: an inner layer of luminal epithelial cells and an outer layer of contractile myoepithelial/basal epithelial cells, surrounded by a basement membrane (Figure 3B). It is becoming increasingly

clear that the mammary gland is developed in a hierarchical manner, much like the hematopoietic system. The two main cell types of the mammary epithelium have been found to be generated from adult mammary stem cells (MaSCs) that differentiate along the luminal or basal lineage via bipotential progenitors to give rise to differentiated luminal and basal cells (Visvader, 2009); (Figure 3C).

### **1.2.2 Breast cancer subtypes**

#### *Classification of breast cancer subtypes*

Breast cancer is a generic term that encompasses neoplasms of the normal breast tissue which are of considerably varied type. These different subtypes of breast tumors have distinct disease courses and react differentially to treatment. In order to deal with this complexity, classification schemes are used which categorize similar tumor types according to histological and immunopathological features, and, more recently, also by their gene expression profiles. These classification schemes are summarized hereafter.

Classical pathology segregates breast tumors according to overall morphology and structural organization: Invasive ductal carcinomas (IDCs) are the most commonly identified (~75% of all cases), followed by invasive lobular carcinoma (ILC); (~10% of all cases). The remaining types not listed here are referred to as „special types“. In general, these subtypes can be correlated with disease prognosis. Immunopathological categorization as used in clinics nowadays, segregates tumor types according to expression of certain markers, which helps to predict prognosis and to choose appropriate treatment. The most important markers used are estrogen receptor (ER), human epidermal receptor 2 (HER2, also called ErbB2 or Neu) and progesterone receptor (PR). Tumors that are ER-positive may respond to anti-estrogen treatment, while HER2-positive tumors can be treated with targeted therapies (e.g. Trastuzumab, an antibody targeting HER2). Tumors are classified according to marker combinations: ER+ (ER+/HER2-), HER2+ (ER-/HER2+), triple-negative (ER-/PR-/HER2-) and triple-positive (ER+/PR+/HER2+). The ER+ cases have the best outcome, while triple-negative cases have the worst prognosis (Bertos and Park, 2011).

Gene expression profiling of breast tumors using microarray technology has led to identification of transcriptional signatures and therefore molecularly defined subtypes (Perou et al., 2000; Sørlie et al., 2001; Weigelt et al., 2010; Colombo et al., 2011). These partially

recapitulate the immunopathological subtypes, however also allowed refined classifications. The main molecular subgroups defined have been termed luminal A, luminal B, basal-like, HER2, and normal breast-like. Luminal A and B subtypes are only slightly distinct and contain ER-positive cases, where tumors of subtype A are characterized by higher expression of ER-regulated genes, lower proliferation and improved overall outcome with respect to tumors of subtype B. Luminal subtypes, in comparison to HER2 and basal-like subtypes, are generally associated with a good prognosis. The remaining three subtypes are ER-negative. The HER2 subtype is similar to HER2-positive tumors identified by immunopathological means, and the very heterogeneous, most aggressive basal-like subtype corresponds to triple-negative tumors. The normal-like subgroup resembles expression profiles of normal breast tissue. Another subgroup within the ER-negative group of tumors, called claudin-low, has been defined recently and was linked to metaplastic breast cancers belonging to the above mentioned “special types” of tumors according to histological analyses (Hennessy et al., 2009). The claudin-low subtype is characterized by low expression of tight junction and adhesions molecules (e.g. several claudins, occludins and E-cadherin) and diminished expression of luminal differentiation markers. Furthermore, the gene expression profile of this subtype correlates with gene signatures of epithelial-mesenchymal transition (EMT) and putative breast cancer stem cells (Prat et al., 2010a; Taube et al., 2010; Herschkowitz et al., 2012).

#### *Origins of breast cancer subtypes*

Two main mechanisms have been proposed that may lead to heterogeneity between tumors (Visvader, 2011). The genetic/epigenetic model suggests that the nature of the oncogenic hit(s) determines tumor phenotype (Figure 4A). On the other hand, the cell-of-origin model states that the same oncogenic hit in distinct cells with different differentiation status may lead to tumors with different phenotypes (Figure 4B). Interestingly, gene expression profiles of different subtypes of breast cancers overlap with those of normal mammary cells at distinct differentiation stages (Lim et al., 2009; Prat and Perou, 2009), allowing the assignment of a potential cell of origin to each tumor subtype. Figure 4C illustrates these potential relationships.



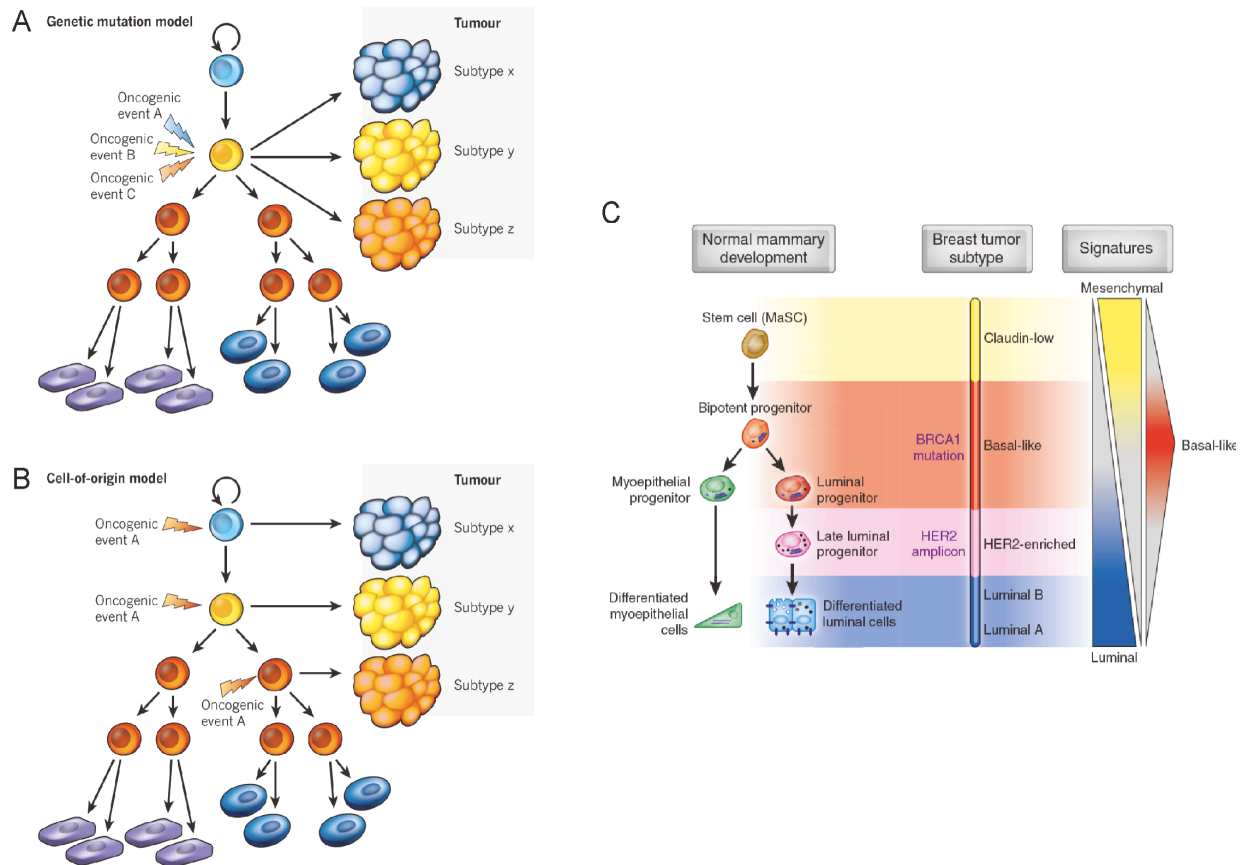


**Figure 4. Origins of breast cancer subtypes.**

(A) In the genetic/epigenetic mutation model, the nature of the cancer-initiating mutations primarily determines the phenotype of the tumor, such that different mutations result in different tumor morphology. (B) In the cell-of-origin model, transformation of cells residing in distinct differentiation stages results in different tumor subtypes. (A) and (B) are from (Visvader, 2011). (C) Similarities between breast tumor subtypes and cells in distinct stages of mammary lineage differentiation as determined by gene expression profiling. Taken from (Prat and Perou, 2009).

### 1.2.3 Intratumoral heterogeneity

The classification of tumors into subtypes should not mislead from the fact that considerable heterogeneity of tumor cell phenotypes within the same tumor exists (intratumoral heterogeneity). Cells within a tumor can be different in size, morphology and cell-cell interaction, marker expression, proliferation rate, metastatic properties, and sensitivity to therapy, thereby complicating treatment. As tumors progress, this heterogeneity generally increases. Intratumoral heterogeneity can be created by several means. At least two models are currently discussed, which are summarized below.

*The clonal evolution model*

Heterogeneity elicited by genetic/epigenetic changes in tumor cells can be described by the „clonal evolution model“ initially proposed by Nowell in 1976 (Nowell, 1976). According to this model, a tumor arises because a single cell acquires one or a few genetic/epigenetic alterations, allowing it to acquire one or several of the hallmarks that are required for tumor initiation as described above. During tumor progression, tumor cells acquire increasing amounts of genetic/epigenetic modifications, facilitated for example by increased genomic instability. Some of these mutations provide advantages for further growth, and others result in a disadvantage. Cells carrying disadvantageous alterations are negatively selected and those that have gained advantageous changes are positively selected according to the laws of Darwinian evolution. These evolutionary mechanisms eventually result in a tumor that is composed of an array of heterogeneous cell clones, each carrying different genetic/epigenetic changes provoking different phenotypes.

*The cancer stem cell model*

Alternatively, tumor heterogeneity can also be generated by other means. An underlying concept that has emerged in recent years is that breast and other solid cancers may contain tumor cells with stem cell-like properties, similar to leukemic malignancies (Al-Hajj et al., 2003; Campbell and Polyak, 2007; Polyak, 2007; Visvader and Lindeman, 2008). According to the proposed „cancer stem cell“ model, tumors are organized in a hierarchical manner much like normal tissues, where indefinitely self-renewing adult tissue stem cells differentiate into phenotypically diverse progenitor cells that make up the bulk of the tumor, thereby creating intratumoral heterogeneity (Blanpain et al., 2007; Clevers, 2011).

Notably, by definition only the cancer stem cells are able to initiate new tumors when transplanted into immunocompromised mice because of their self-renewal properties, and are therefore regarded as the drivers of tumor growth, whereas their descendants are generally non-tumorigenic because of differentiation and associated loss of self-renewal capacity. It is also important to note that the cancer stem cell concept assumes the presence of stem cells in tumors but does not address the provenance of these stem-like cells. Cancer stem cells could emerge by transformation of normal tissue stem cells. In this case the resulting cancer stem cells would at the same time be the tumor cell of origin. Alternatively, stem-like cells may also arise from differentiated tumor cells by secondary acquisition of stemness. The latter

possibility may involve intrinsic factors as for example additional genetic/epigenetic lesions, but can also be influenced by external cues from the microenvironment. For example, recent evidence suggests that EMT can be a mechanism that enhances stemness (Mani et al., 2008; Morel et al., 2008; Asiedu et al., 2011). This example indicates that the clonal evolution model and the cancer stem cell model do not have to be mutually exclusive, and that combinations of those two models may be at work to create the heterogeneity observed within individual tumors (Clevers, 2011; Visvader, 2011).

#### **1.2.4 The tumor microenvironment**

A unified concept of not only breast cancer but of all solid cancers is not possible without considering the other major constituents of tumors apart from the cancer cells themselves. These other constituents are collectively referred to the tumor microenvironment, which includes various cell types like endothelial cells making up the blood- and lymphatic system, pericytes that cover blood vessels, infiltrating immune cells and tumor-associated fibroblasts, as well as the complex proteinaceous space between cells, the extracellular matrix (ECM). All of these constituents are reciprocally influencing each other as well as the tumor cells to promote or inhibit tumor growth and progression in complex ways. Examples are paracrine signaling, signaling by cell-cell interactions and cell-matrix interactions, sequestering of signaling molecules by ECM proteins, activation of signaling molecules by secreted proteases, immune surveillance and so on. In addition, the composition and activities of the tumor environment are significantly changing during tumor progression, adding another layer of complexity to the tumor “ecosystem”, which is one of the reasons that microenvironmental regulation of tumor growth and progression is only beginning to be understood (Joyce and Pollard, 2009; Sleeman et al., 2012). One well-studied example of microenvironmental regulation however is the ability of microenvironmental factors to induce an epithelial-mesenchymal transition in tumor cells, which is discussed below.

### 1.3 Epithelial-mesenchymal transition (EMT)

#### 1.3.1 EMT is context-dependent

##### *The EMT concept*

EMT is a latent embryonic program that encompasses plastic changes in phenotype (Figure 5). During EMT, epithelial cells lose their cell-cell adhesions and apical-basal polarity, adopt a mesenchymal appearance with front-rear polarity, produce increased amounts of extracellular matrix and acquire migratory and invasive properties. The transition is accompanied by a replacement of the epithelial intermediate filament network that is based on cytokeratins by vimentin filaments, along with the remodeling of cortical actin in epithelial cells into stress fibers in mesenchymal cells (Nieto, 2011). The prototypical component of epithelial adherens junctions, E-cadherin, is downregulated and replaced by the mesenchymal N-cadherin, an event termed “cadherin switch” (Cavallaro and Christofori, 2004).

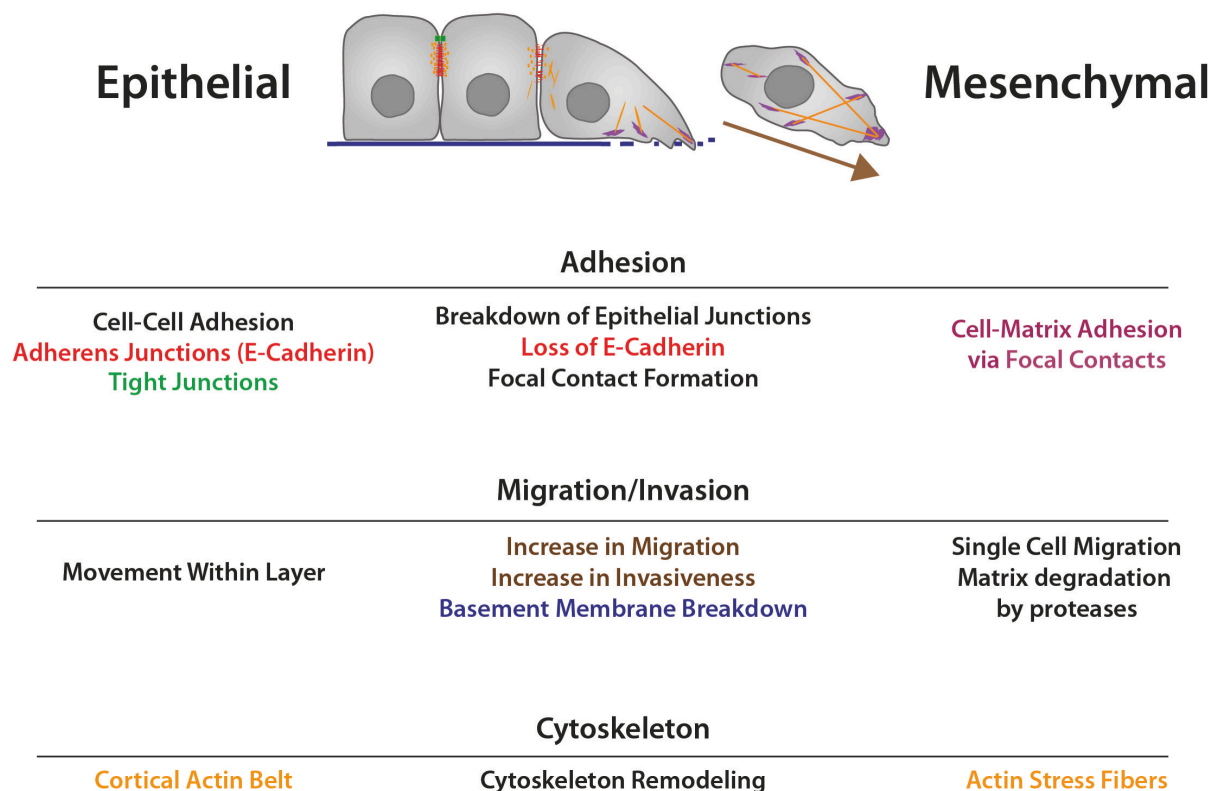


**Figure 5. Phenotypic hallmarks of the Epithelial-mesenchymal transition.**

Schematic drawing showing the conversion of epithelial cells (*top left*) into mesenchymal cells (*top right*) during EMT. Hallmark characteristics of each state are described in the bottom panel (*left and right*), and the changes occurring during EMT are indicated in between (*middle*). Text is color-coded and refers to the colors used in the drawing.

### *Developmental EMTs*

Classical EMT is observed at several stages during early development, where it allows dispersion of cells in the embryo. The first event of EMT occurs at the gastrulation stage, where cells of the primitive streak undergo EMT and leave the epithelial layer to form endoderm and mesoderm, while the remaining cells not undergoing EMT form the ectoderm. Thus, EMT is necessary to produce the three germ layers. Later in development, EMT is required for formation of neural crest cells, which delaminate from the neural tube and migrate to distant sites to differentiate into various specialized cell types such as bone or pigment cells (Acloque et al., 2009). In the adult, EMT is transiently activated in inflammatory contexts and tissue wounding, and produces mesenchymal cells/fibroblasts associated with tissue repair from epithelial cells. Chronic inflammation can result in sustained activation of EMT and the continued generation of extracellular matrix-producing fibroblasts, leading to excess deposition of matrix that eventually results in organ destruction (Kalluri and Weinberg, 2009).

### *Oncogenic EMT*

Most important for this work is the observation that similar changes in epithelial phenotype and migratory/invasive behavior have also been observed in cancer cells (Thiery, 2002; Klymkowsky and Savagner, 2009), including breast cancer (Trimboli et al., 2008; Tomaskovic-Crook et al., 2009). A reactivation of the EMT program or at least a partial activation of some features of EMT in cancer cells (oncogenic EMT), is thought to provide cancer cells with the ability to leave the primary tumor, to invade the surrounding tissue and to enter the vascular system, thereby facilitating the first steps in the metastatic cascade (Chaffer and Weinberg, 2011). It is envisioned that, once cancer cells arrive at distant sites, a secondary outgrowth involves re-differentiation into an epithelial phenotype (MET), as metastatic lesions usually mimic the phenotype of primary tumors (Brabletz et al., 2005). Additionally, oncogenic EMT has been linked to resistance to chemo- and radiation therapy, evasion from immune-surveillance, evasion from apoptosis, self-renewal and resistance to treatment (Singh and Settleman, 2010; May et al., 2011; Tiwari et al., 2012). Because EMT is a transient process and in addition may involve only a few cells at once, signs of EMT have been difficult to detect in human tumor samples by standard pathological procedures. Importantly, oncogenic EMT rarely represents the full EMT like it is observed during

organism development (Lee et al., 2006; Klymkowsky and Savagner, 2009). Rather, through reactivation of “subroutines” of developmental EMT, a variable number of processes and phenotypic subsets are activated during oncogenic EMT. For example, it is often observed that parts of tumors with a mesenchymal appearance are still positive for epithelial cytokeratins, like cytokeratin 8/18, while concomitantly expressing mesenchymal markers like vimentin (Derksen et al., 2006; Damonte et al., 2007; Creighton et al., 2009; McCoy et al., 2009; Cardiff, 2010; Prat et al., 2010a).

### *EMT in breast cancers*

EMT in human breast cancer appears to preferentially occur in distinct subtypes, namely within the heterotypic triple-negative or basal subgroup (Sarrió et al., 2008). Recent further stratification of the basal-like subgroup by transcriptional profiling uncovered that EMT signatures can be found in rare but highly aggressive metaplastic type and claudin-low type breast cancers of the basal-like subgroup (Hennessy et al., 2009; Taube et al., 2010; Prat et al., 2010a). Interestingly, cells undergoing EMT-like changes in human tumors, as determined by gene expression profiles, do not always display the same cellular phenotypes and metastatic behavior as cells that undergo EMT in murine breast cancers: the formation of highly invasive “EMT-tumors” characterized by spindloid appearance of tumor cells has been documented in many mouse models of breast cancer, while in most human breast cancers, spindloid cells seem to be less apparent, even though their gene expression profiles may overlap with EMT signatures and cell express mesenchymal markers (Cardiff et al., 2000; 2011). Additionally, spindle cell EMT tumors in mice have been observed to be only locally invasive and have not been observed to metastasize (Cardiff, 2010), while EMT in human breast cancer has been correlated with metastasis and poor prognosis (Sarrió et al., 2008; Hennessy et al., 2009; Taube et al., 2010). The reason for this apparent discrepancy between species is currently not known.

### **1.3.2 Mediators of EMT**

Numerous mediators of EMT have been uncovered, many of which are functionally conserved between oncogenic and developmental EMTs (Micalizzi et al., 2010; Drasin et al., 2011; Takebe et al., 2011). The main players identified thus far that control and execute the EMT program range from a plethora of signaling molecules to various transcription factors

and some microRNA families, as well as molecules composing structural components like adherens junctions and polarity complexes.

### *E-cadherin and EMT*

Perhaps the most critical player and also marker of EMT is the adherens junction component E-cadherin, encoded by the *CDH1* gene. A loss of E-cadherin mediated cell-cell adhesion in epithelial cells, by either delocalization from adherens junctions via endocytosis (Janda et al., 2006) or transcriptional inactivation by transcriptional repressors (Thiery et al., 2009) or promoter hypermethylation (Polyak and Weinberg, 2009), is sufficient to induce EMT (Perl et al., 1998; Onder et al., 2008). Moreover, loss of *CDH1* heterozygosity occurs in invasive lobular carcinoma, which contains highly invasive tumor cells infiltrating the tumor stroma (Vos et al., 1997). Invasive lobular carcinoma is phenocopied in p53 null breast cancer mice with conditionally inactivated E-cadherin (Derksen et al., 2006). The loss of E-cadherin leads to activation of numerous signaling events, a prototypical one being the release of E-cadherin associated  $\beta$ -catenin into the cytoplasm, resulting in activation of the canonical Wnt pathway (Cavallaro and Christofori, 2004). Not surprisingly, a number of E-cadherin transcriptional repressors are also implicated in EMT.

### *Transcription factors and EMT*

The zinc-finger transcriptional repressors Snail1, Snail2, Zeb1 and Zeb2 and the basic helix-loop-helix repressors E12/E47 and Twist can directly repress E-cadherin transcription by binding to palindromic E-boxes (CANNTG) in the *CDH1* promoter (Peinado et al., 2007). A plethora of signaling molecules is known to be sufficient to induce EMT via signaling through their cell surface receptors. These signals mainly converge on the upregulation of the above mentioned “master transcription factors”. These signaling molecules include transforming growth factor  $\beta$  (TGF $\beta$ ), epidermal growth factor (EGF), fibroblast growth factor (FGF), hepatocyte growth factor (HGF), insulin-like growth factor (IGF) and platelet-derived growth factor (PDGF). Other signaling pathways capable of inducing EMT include the Notch, Hedgehog and Wnt pathway (Thiery and Sleeman, 2006; Sleeman and Thiery, 2011).

### 1.3.3 TGF $\beta$ -induced EMT

#### *The dual role of TGF $\beta$ in cancer*

TGF $\beta$  is a ubiquitously expressed cytokine with a diverse spectrum of roles in tissue development, differentiation and homeostasis. In normal tissues, TGF $\beta$  exerts a tumor suppressive effect by inhibiting proliferation. However, during tumor progression, cancer cells frequently acquire resistance to TGF $\beta$  mediated cytostasis, while remaining responsive to other aspects of TGF $\beta$  signaling, such as the induction of EMT, a functional switch known as the „TGF $\beta$  paradox“. Therefore, TGF $\beta$  exerts a dual role during tumor progression. In normal tissue and in early lesions, TGF $\beta$  acts as a tumor suppressor, while at later stages, when cancer cells have lost responsiveness to the tumor suppressive arm of TGF $\beta$ -signaling, it contributes to tumor malignancy, in part by induction of EMT (Massagué and Gomis, 2006; Massagué, 2008).

#### *The TGF $\beta$ pathway*

Mammals have three genes encoding highly similar TGF $\beta$ -ligands (TGF $\beta$  1-3), which can bind to three receptors (T $\beta$ R-I to III). T $\beta$ R-III is usually the most highly expressed and functions as an accessory receptor, which binds and modulates TGF $\beta$  function, however it lacks enzymatic activity. T $\beta$ R-I and II harbor a Ser/Thr kinase in their cytoplasmic domains and are enzymatically active. Upon ligand binding, T $\beta$ R-II transphosphorylates T $\beta$ R-I, which leads to binding of the intracellular receptor Smad (R-Smad) proteins Smad2 and Smad3 and activation by phosphorylation. Activated Smad2 and Smad3 are then complexing with the common Smad (Co-Smad) Smad4, which enables the translocation of the Smad2/3/4 complex into the nucleus, where it binds to gene promoters and regulates their transcription. This pathway is termed the „canonical“ TGF $\beta$  pathway (Feng and Derynck, 2005). Non-canonical (i.e. Smad2/3-independent) signaling is also elicited upon ligand binding to TGF $\beta$ -receptors, and includes activation of the mitogen activated protein kinases (MAPK) ERK1/2, p38 and JNK, activation of the PI3K-AKT-mTOR pathway, activation of the NF- $\kappa$ B pathway and activation of the small GTP-binding proteins RhoA, Rac1 and Cdc42 (2009).

#### *TGF $\beta$ stimulation induces EMT*

EMT induction by TGF $\beta$  has first been described by Derynck and colleagues in 1994 (Miettinen et al., 1994). Following this discovery, TGF $\beta$  has been established as a master



inducer of EMT in a variety of contexts (Zavadil and Böttinger, 2005; Taylor et al., 2010; Moses and Barcellos-Hoff, 2011). To achieve EMT activation and progression, TGF $\beta$  signaling must coordinate the various phenotypic changes occurring during EMT, such as the loss of epithelial junctions, the remodeling of the cytoskeleton and the gain in migratory and invasive properties by controlling a complex regulatory network of effectors downstream of the activated canonical and non-canonical pathways. Some of the principal mechanisms involved are delineated hereafter.

### *Canonical TGF $\beta$ signaling calls up EMT transcription factors*

A critical part of this regulatory network that drives EMT are the Snail, ZEB and bHLH families of master transcription factors (TFs) of EMT, which are upregulated in response to TGF $\beta$  signaling either through a Smad-dependent mechanism or indirectly. In turn, these TFs repress epithelial gene expression and concomitantly activate mesenchymal gene expression through activation of downstream transcriptional networks (Figure 6).

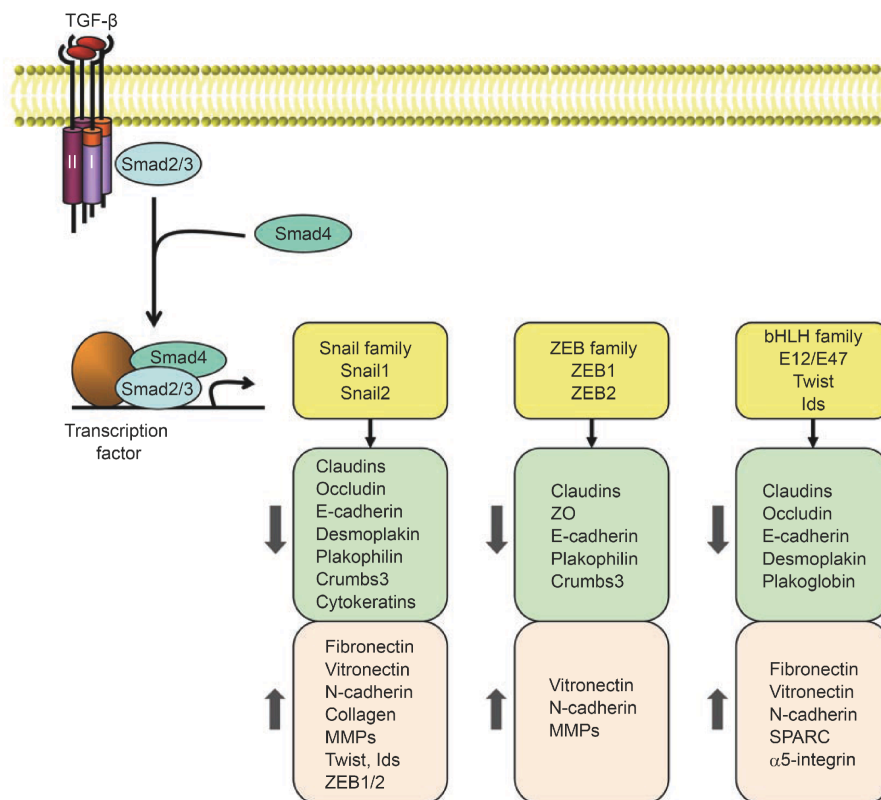


**Figure 6. Canonical TGF $\beta$  signaling and downstream effects.**

In response to TGF- $\beta$ , the receptor associated Smad2 and 3 are activated, and form complexes with the common Smad4. This complex then regulates the transcription of target genes through interactions with other DNA binding transcription factors. Activated Smads mediate transcriptional regulation through three families of transcription factors, resulting in repression of epithelial marker gene expression and activation of mesenchymal gene expression. Taken from (Xu et al., 2009).

The Snail family consists of Snail1 (initially called Snail), Snail2 (Slug) and the less characterized Snail3 (Smuc) (Herreros et al., 2010). Snail1 upregulation during EMT is directly mediated by Smad3, which binds to the Snail1 promoter and stimulates its transcription (Hoot et al., 2008). In addition, Snails are regulated at the post-transcriptional level via phosphorylation by GSK3, which regulates their stability and nuclear-cytoplasmic localization (Barrallo-Gimeno and Nieto, 2005). The zinc-finger proteins of the Snail family act as transcriptional repressors, and as such they mediate transcriptional downregulation of E-cadherin by recruitment of co-repressors such as HDACs, thereby inducing EMT. In addition, Snail represses the expression of various other cell-cell junction proteins like several claudins and occludins, as well as the polarity complex component Crumbs3 (Peinado et al., 2007). The ZEB family of transcriptional repressors consists of two members in vertebrates: ZEB1, (also known as  $\delta$ EF1) and ZEB2 (also known as SIP1). Transcriptional repression by ZEBs is achieved by repressor motifs in the central homeodomain and by recruitment of CTBP as a co-repressor. However, interaction of ZEB1 with co-activators PCAF and p300 can switch ZEB1 function from repression to activation (Postigo et al., 2003; Peinado et al., 2007). TGF $\beta$  signaling induces ZEB proteins through Smad-independent mechanism mediated in part by Ets-1. ZEBs subsequently downregulate epithelial genes by interacting with Smad3 and by recruiting the co-repressor CTBP (Shirakihara et al., 2007). ZEBs are regulated at the post-transcriptional level by the microRNA-200 family, which are dramatically downregulated during TGF $\beta$ -induced EMT and EMT in general (Burk et al., 2008; Gregory et al., 2008; Korpala et al., 2008). As the Snails, ZEBs are also repressors of E-cadherin and bind to E-boxes in the E-cadherin promoter (Comijn et al., 2001; Eger et al., 2005). A third class of transcriptional E-cadherin repressors that act via E-boxes is represented by the basic helix-loop-helix transcription factors E12/E47 (TCF3) and Twist. E12 and E47 are different splice variants of the E2A gene (Peinado et al., 2007). Another direct target of TGF $\beta$  signaling is HMGA2 (high mobility group A2). This factor is upregulated upon activation of TGF $\beta$  signaling by direct binding of Smad4 to its promoter, and at the same time appears to control expression of Snails and Twist, exemplifying the elaborate transcriptional network architecture that controls the execution of EMT (Thuault et al., 2006).

*The role of non-canonical TGF $\beta$  signaling in EMT*

Apart from the effects elicited via canonical TGF $\beta$  signaling, the non-canonical arms of the pathway not involving Smad proteins also contribute to the diverse phenotypic and functional changes occurring during TGF $\beta$ -induced EMT (Figure 7). The activation of these pathways occurs through protein-protein interactions of signaling mediators with the T $\beta$ Rs receptors, which can be direct or mediated by adaptor proteins.

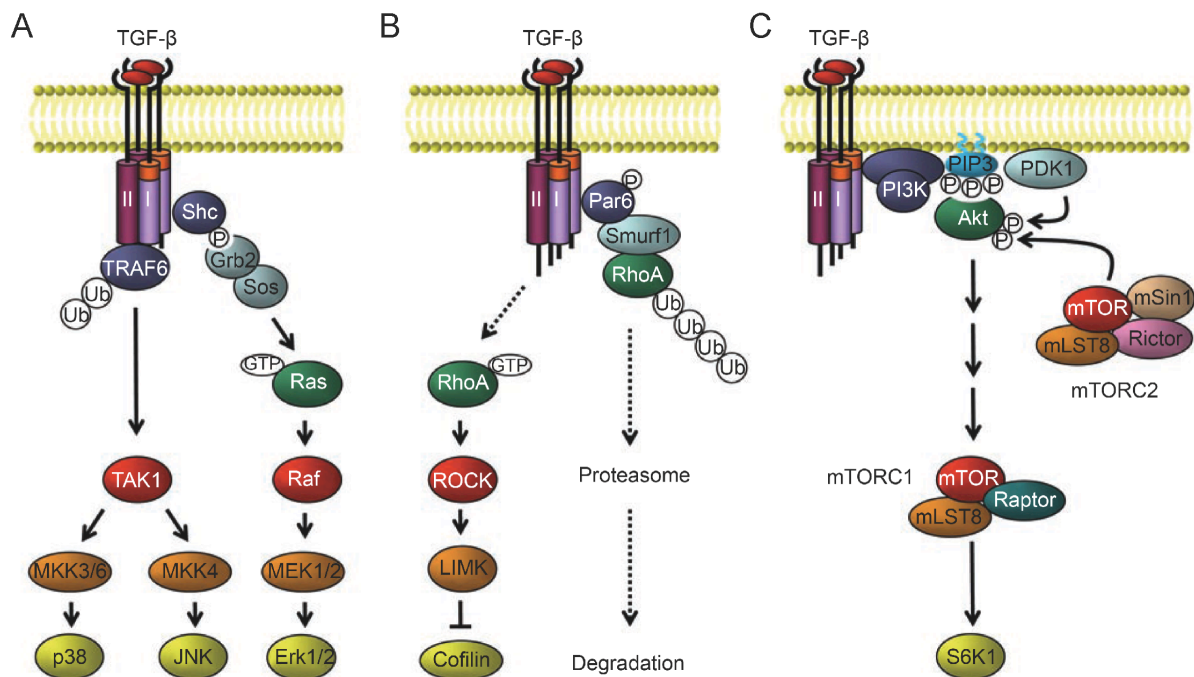


**Figure 7. Non-canonical TGF $\beta$  signals**

(A) TGF- $\beta$  mediates p38 MAP kinase and JNK MAP kinase activation through activation of the MAPKKK TAK1 by receptor-associated TRAF6. Erk MAP kinase is activated through recruitment and phosphorylation of Shc by T $\beta$ RI. (B) RhoA is activated in response to TGF- $\beta$  and at the same time is also locally targeted for proteasomal degradation at tight junctions by the E3 ubiquitin-ligase Smurf1. (C) TGF- $\beta$  induces PI3-kinase signaling, leading to the activation of Akt-mTOR signaling. Dashed lines represent indirect actions. Taken from (Xu et al., 2009).

Activation of the MAPK pathway by TGF $\beta$ , although generally lower compared to activation by other growth factors, is achieved in the following way (Figure 7A): The adaptor protein ShcA binds to T $\beta$ RI and is tyrosine-phosphorylated, which creates a docking site for the recruitment of Grb2 and Sos. This complex then initiates Ras activation, leading to the activation of a Raf, MEK and ERK1 and 2 kinase activation cascade (Lee et al., 2007). Pre-activated MAPK signaling cooperates with TGF $\beta$  to enhance EMT induction, as activated

Ras or activated Raf, which are upstream of MAP kinases, is required for TGF $\beta$  induction of EMT in otherwise unresponsive Eph4 cells (Oft et al., 1996; Janda et al., 2002; 2006). Furthermore, blocking MEK1/2 activity using a chemical inhibitor, inhibits TGF- $\beta$ -induced EMT (Xie et al., 2004). TGF $\beta$  also induces activation of the MAP kinases p38 and JNK. This activation is initiated by T $\beta$ RI-associated TRAF6, an E3 ubiquitin ligase, which is autoubiquitinated upon TGF $\beta$  stimulation and mediates TGF $\beta$  associated kinase 1 (TAK1) activation (Sorrentino et al., 2008; Yamashita et al., 2008). Activated TAK1, then activates the MAP kinase kinases MKK3 and MKK6, which activate p38, and MKK4, which activates JNK (Xu et al., 2009). Activation of p38 is usually required for EMT induction, as treatment with a chemical inhibitor prevents TGF $\beta$ -induced EMT in some but not all mammary epithelial cells (Bakin et al., 2002; Yu et al., 2002; Xie et al., 2004). Also JNK has been demonstrated to be required for EMT (Santibañez, 2006; Alcorn et al., 2008). JNK, among other targets, activates c-Jun, a component of the transcription complex AP-1, which cooperates with Smads, for example in transcriptionally upregulating urokinase-like plasminogen activator (uPA), an inducer of extracellular matrix degradation (Santibañez, 2006).

TGF $\beta$  signals to the small Rho-like GTPase RhoA in at least two ways (Figure 7B). First, TGF $\beta$  signaling provokes an increase in RhoA activity, leading to activation of its downstream target ROCK, which induces the formation of actin stress fibers. In addition, ROCK activation also leads to activation of LIM kinase which that inactivates cofilin, an actin depolymerizing factor important for actin reorganization during EMT (Bhowmick et al., 2001). Second, the polarity complex protein Par6 was found to be phosphorylated upon TGF $\beta$  stimulation by T $\beta$ RII while bound to T $\beta$ RI. This results in Smad2/3-dependent upregulation and recruitment of the E3 ubiquitin ligase Smurf1, which is responsible for degradation of RhoA at tight junctions (Ozdamar et al., 2005). This contrasts with the increased overall activation of RhoA by TGF $\beta$ , but might be explained by spatio-temporal differences of RhoA activity during EMT.

TGF $\beta$  stimulation leads to rapid activation of PI3 kinase and downstream activation of protein kinase B/Akt (PKB/Akt);(Figure 7C). Activation of the PI3K/Akt pathway was shown to be required for Smad2 activation and general Smad transcriptional response, as well as for junction breakdown during EMT (Bakin et al., 2000). PI3 kinase activation is achieved by

indirect association of the PI3K regulatory subunit p85 with T $\beta$ RII and T $\beta$ RI receptors, which is necessary for PI3 kinase activation by TGF $\beta$  (Yi et al., 2005).

Together, these all these findings illustrate the extensive functional cross-talks between canonical and non-canonical TGF $\beta$  pathways, and leave the impression that a finely tuned network of players orchestrates the diverse downstream processes elicited by TGF $\beta$  stimulation, ultimately leading to the transdifferentiation from an epithelial into a mesenchymal cellular state.

### *TGF $\beta$ in mouse models of breast cancer*

Early experiments using genetically engineered mice (GEM) assessing the role of TGF $\beta$  in breast cancer uncovered the tumor suppressive action of this cytokine. For example, transgenic mice constitutively expressing TGF $\beta$ 1 in the mammary gland under the control of the MMTV promoter did not develop tumors, and when treated with DMBA to induce mammary tumors, tumor latency was increased in comparison to non-transgenic control mice. Similarly, when MMTV-TGF $\beta$ 1 mice were crossed with MMTV-TGF- $\alpha$  mice that are prone to tumor formation, tumors in double-transgenic mice developed later in comparison to single-transgenic mice (Pierce et al. 1995). Additionally, MMTV-TGF $\beta$ 1 single-transgenic mice showed a decreased incidence of tumorigenesis when infected with the tumor inducing mouse mammary tumor virus (Boulanger and Smith, 2001). Conversely, overexpression of a dominant-negative TGF $\beta$ -receptor II (dnT $\beta$ RII) in mammary glands of MMTV-neu breast cancer mice led to faster tumor development. Interestingly, in the same double-transgenic mice, lung metastasis was decreased. Conversely, expression of TGF $\beta$  in neu-induced tumors resulted in an increase in metastasis formation, suggesting that TGF $\beta$  signaling positively contributes to the metastatic process (Siegel et al., 2003). Moreover, systemic administration of TGF $\beta$  neutralizing antibodies applied to a variety of murine breast cancer models consistently resulted in a reduction of metastatic spread (Biswas et al., 2007; Nam et al., 2008; Padua and Massagué, 2009). Collectively, these studies illustrate the dual nature of TGF $\beta$ , acting as a tumor suppressor in normal tissue and promoting metastatic disease in tumors.

What is the source of TGF $\beta$  *in vivo*? Under conditions of tissue injury, TGF $\beta$  is released by blood platelets and stromal components in order to prevent overproliferation and inflammation (Massagué, 2008). As tumors can be viewed as wounds that do not heal

(Dvorak, 1986), much the same is true in tumors. TGF $\beta$  is often present in the tumor microenvironment, and its presence, which can be indirectly detected by Smad phosphorylation, has been documented in many subsets of tumors (Xie et al., 2002). TGF $\beta$  in tumors can be produced by the tumor cells themselves, thereby activating TGF $\beta$  signaling in an autocrine fashion, or by a variety cell types of the tumor stroma. Examples herefore are tumor-infiltrating leukocytes, macrophages, and bone marrow-derived endothelial, mesenchymal, and myeloid precursor cells. The preferential presence of TGF $\beta$ 1 at the invasive fronts of tumors observed in a study of invasive ductal mammary carcinoma may be due to higher concentrations of tumor infiltrating cells at this location (Dalal et al., 1993).

## ***1.4 Tead transcription factors***

### **1.4.1 The Tead family**

The Tead/TEF (TEA domain-containing/transcription enhancer factor) family of transcription factors comprises four (Tead1-4) members in mice and humans, which are highly conserved between species (Jacquemin et al., 1996; Kaneko and DePamphilis, 1998). Even though at least one family member is expressed in virtually every tissue, single members exhibit differential expression patterns across tissues and during development. Members of this family are also found in yeast, birds, fungi, worms and flies (Jacquemin et al., 1996; Kaneko and DePamphilis, 1998; Wu et al., 2001). In *Drosophila*, only one homolog named Scalloped (Sd) was identified (Campbell et al., 1992). Tead1 (TEF-1) was first identified in human cells as an activator of the simian virus 40 enhancer (SV40)(Davidson et al., 1988). Subsequently, murine Tead1 (Blatt and DePamphilis, 1993; Shimizu et al., 1993) and the three other members Tead2 (TEF4) (Yasunami et al., 1995; Jacquemin et al., 1996; Kaneko et al., 1997), Tead3 (TEF5)(Yasunami et al., 1996; Yockey et al., 1996; Kaneko et al., 1997) and Tead4 (TEF3)(Jacquemin et al., 1996; Yasunami et al., 1996; Yockey et al., 1996) were identified.

### **1.4.2 Tead functions**

After their discovery, Tead proteins were subsequently characterized as being important for gene expression during cardiac and skeletal muscle development and regeneration (Chen et al., 1994; Stewart et al., 1994; Gupta et al., 1997; Butler and Ordahl, 1999; Ueyama et al., 2000; Milewski et al., 2004; Zhao et al., 2006; Benhaddou et al., 2012). Tead2 was found to bind to an enhancer region of Pax3 and to activate its expression in pre-migratory neural crest cells (Milewski et al., 2004). Notably, neural crest cell delamination from the neural tube is an example of developmental EMT, and requires Pax3 expression. Interestingly, Tead2 has been shown to be the only Tead family member and one of the first transcription factors overall that is transcribed after egg fertilization at the two-cell stage of embryonic development, where global gene transcription commences (Kaneko et al., 1997; Kaneko and DePamphilis, 1998). The exact role of Tead2 at this stage has not been determined. It is interesting to note however that Tead2, along with one of its co-activators (Yap) is selectively and highly expressed in undifferentiated embryonic, neural and hematopoietic stem cells (Ramalho-Santos et al., 2002), indicating that transcriptional activity mediated by Tead2 may be

involved in the production or maintenance of these cells. However, Tead2 homozygous mutant mice appear relatively normal (Sawada et al., 2008), although they display an increased risk of exencephaly, a defect that results in brain protrusion into the amniotic cavity and is attributed to incomplete neural tube closure (Kaneko et al., 2007). Tead1 homozygous mutant embryos die at embryonic day 11.5 (E11.5) because of heart defects (Chen et al., 1994). Notably, Tead1/Tead2 double mutant embryos are small at E8.5 due to reduced cell proliferation and increased apoptosis, lack a closed neural tube, a notochord and somites and die at E9.5 with severe defects. These observations suggest that Tead1 and Tead2 have redundant roles *in vivo*. Tead4 mutant embryos do not develop further than E3.5, due to defects in trophectoderm specification and therefore are unable to form blastocysts, which consist of outer trophectoderm and inner cell mass (Yagi et al., 2007). Together, it appears that Tead family members may functionally compensate for each other in some contexts, but also have specific roles at certain stages of development.

### **1.4.3 Tead transcriptional machinery**

#### *Tead DNA binding*

All Tead family members contain an evolutionarily conserved TEA (TEF-1, TEC1 and AbaA) DNA binding domain, consisting of a three-helix bundle with a homeodomain fold (Anbanandam et al., 2006). The 72 amino acid long TEA domain localizes to the N-terminal half and is highly conserved between different Tead family members (Jacquemin et al., 1996; Kaneko and DePamphilis, 1998) and species (Jacquemin et al., 1996; Kaneko and DePamphilis, 1998). The Tead1 and Tead2 TEA domain sequences in mouse and humans are identical. Interestingly, human Tead1 can substitute for *Drosophila* Scalloped in wing formation, illustrating a high grade of conservation also on the functional level (Deshpande et al., 1997). All four Tead proteins bind to MCAT DNA binding motifs with the core sequence CATTCCCT (Larkin et al., 1996; Yoshida, 2008), as well as to the highly similar GTIIC motifs with the core sequence CATTCCCT (Davidson et al., 1988), with similar affinity (Kaneko and DePamphilis, 1998).

#### *Tead co-activators*

Transcriptional activation by Tead transcription factors requires the recruitment of co-activator proteins. Tead1 can bind TATA-box binding protein (TBP), although this interaction



seems to rather repress gene transcription (Jiang and Eberhardt, 1996). Furthermore, Tead2 can bind the nuclear receptor coactivator protein SRC1 that belongs to the p160 coactivator protein family (Belandia and Parker, 2000). The effects of these interactions on Tead mediated transcription are subtle and in the range of 2-3 fold. In *Drosophila*, the nuclearly localized protein Vestigial (Vg) has been established to specify and to be required for wing formation (Brook et al., 1996). Vg has been shown to exert its function by direct binding to the Tead homolog Scalloped, which binds to wing-specific enhancers (Halder et al., 1998; Simmonds et al., 1998; Guss et al., 2001). There are four mammalian homologs of Vg called vestigial-like (Vgll) 1-4. Human Vgll1 (also called TONDU) can substitute for Vg in *Drosophila* (Vaudin et al., 1999), however the functional contribution of Vgll proteins to Tead activation in mammalian cells has not been evaluated. The Vg/Sd complex only operates in the wing-disc, yet Sd was also shown to direct gene expression during leg, eye and optic lobe development (Srivastava et al., 2004; Garg et al., 2007), indicating that other co-factors must exist that mediate Sd activity in these tissues.

An *in vitro* study identified binding of Yap (Yes-associated protein, also called Yap65 or Yap1) to Tead2 and further showed the binding and requirement of Yap for transcriptional activity of all four Tead family members (Vassilev et al., 2001). Yap interacts with Teads via its N-terminal region, and contains a transcriptional activation domain at its C-terminus, which is similar to that found in the herpes simplex virus protein VP16 and is almost equally potent in transcriptional activation (Yagi et al., 1999). Importantly, Vll proteins do not contain a transcriptional activation domain, and their transcriptional activation of Teads is generally weaker compared to that of Yap (Vassilev et al., 2001; Maeda et al., 2002). The Yap-related protein Taz (transcriptional co-activator with PDZ-domain, also named Wwtr1) has also been shown to be able to bind to Teads, and activates their transcriptional activity to a similar extent as Yap (Mahoney et al., 2005). Yap and Taz are about 45% identical and share a common domain structure (Kanai et al., 2000). They both contain 1) a 14-3-3 protein binding motif important for cytoplasmic retention, 2) one (Taz) or two (Yap) WW domains, 3) a transcriptional activation domain in the C-terminal half, 4) a Tead-binding region in the N-terminal half, 5) multiple phosphorylation sites and 6) a C-terminal motif that mediates interaction with PDZ domain containing proteins. The WW domains can strongly bind to proteins containing the Pro-Pro-X-Tyr (PPXY) motif. This motif can be found in a large number of transcription factors, some of which have been shown to be regulated by either

Yap or Taz, like PPAR $\gamma$ , Runx2 and members of the Smad, Sox and Forkhead families (Pan, 2010). Therefore, Yap and Taz do not only regulate Teads, but are also involved in transcriptional regulation via other DNA-binding TFs.

Reciprocally, it has been suggested that Yap and Taz are among the main regulators of Tead TFs, based on the following observations: transgenic embryos in which Tead1 and Tead2 were disrupted showed many phenotypic similarities to embryos with disrupted Yap, such as small size at E8.5, a discontinuous notochord and defective yolk sac vasculogenesis. In addition, compound mutants of Tead1, Tead2 and Yap demonstrated genetic interaction among Tead and Yap (Morin-Kensicki et al., 2006; Sawada et al., 2008). In *Drosophila*, the Yap/Taz homolog Yorkie (yki) has also been shown to genetically interact with Scalloped (Goulev et al., 2008; Wu et al., 2008; Zhang et al., 2008). Furthermore, Yap and Tead1/Tea2 were shown to regulate a largely overlapping sets of genes in cultured cells (Ota and Sasaki, 2008; Zhao et al., 2008b).

Functional studies using the untransformed mammary epithelial cell line MCF10A, have demonstrated that artificial overexpression of Yap or Taz promotes cell proliferation, anchorage-independent growth, loss-of-contact inhibition and EMT in a Tead-dependent manner (Overholtzer et al., 2006; Zhao et al., 2007; Lei et al., 2008; Zhao et al., 2008b; Zhang et al., 2009a). Similarly, increased proliferation and loss of contact inhibition mediated by Tead activation has also been observed with fibroblasts and was shown to be Yap-dependent. Furthermore, overexpression of Yap or an activated version of Tead2 rendered these cells tumorigenic (Ota and Sasaki, 2008). Therefore, Tead activity mediated by Yap/Taz is an important determinant of oncogenic features. But how is Tead activity regulated in an endogenous setting?

#### **1.4.4 Regulation of Yap/Taz/Tea2 transcriptional activity**

Yap and Taz nuclear localization, which determines Tead activity, can be regulated by the rather recently discovered Hippo tumor suppressor pathway, as well as by other means that seem to be independent of canonical Hippo signaling.

##### *The core Hippo pathway*

The Hippo pathway regulates the levels of proliferation and apoptosis in growing tissues, and its deregulation is implicated in cancer. The first members of the pathway were initially

identified in *Drosophila*, however the core of the pathway is highly conserved in mammals, and consists of Mst1/2 (Hippo, Hpo in flies), WW45 (Salvador, Sav in flies), Lats1/2 (Warts, Wts in flies) and Mob (Mats in flies). These proteins form a complex, which negatively regulates Yap and Taz. Biochemical experiments showed that, when the pathway is activated, Mst phosphorylates Lats, which in turn phosphorylates Yap/Taz at several key serine residues, thereby creating a docking site for 14-3-3 proteins that mediate cytoplasmic retention of Yap/Taz. The exclusion of Yap and Taz from the nucleus results in abrogated Tead activity and discontinued target gene expression (Figure 8).

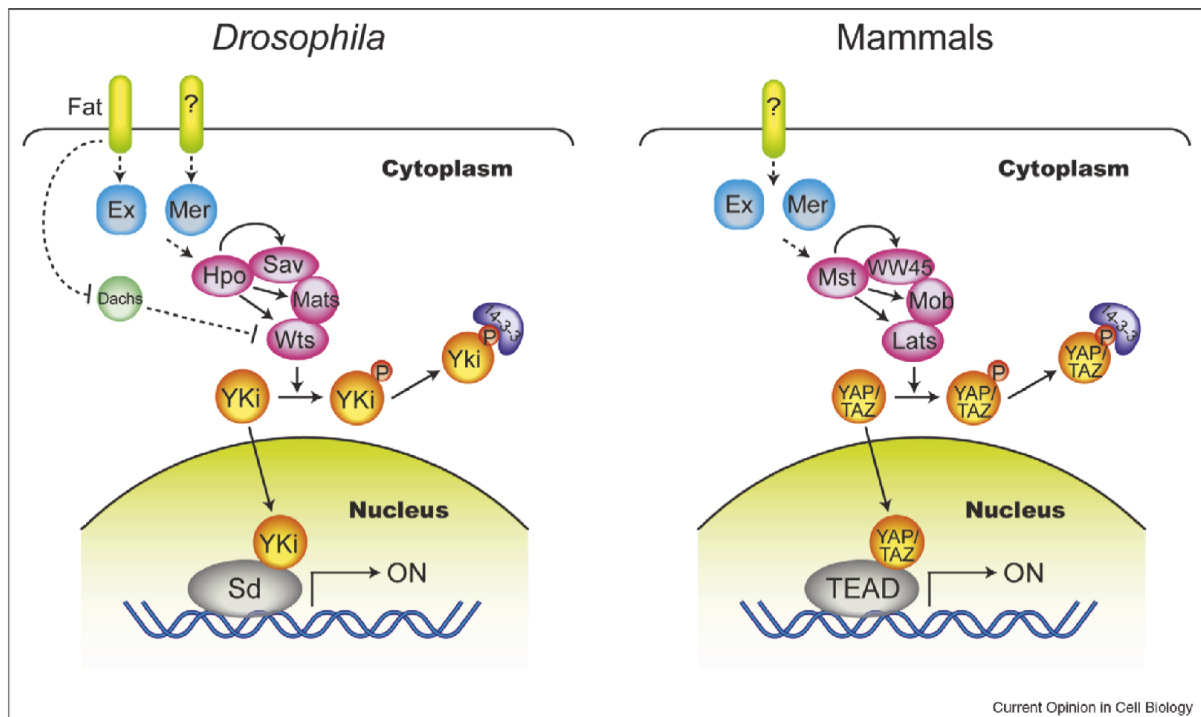


**Figure 8. Hippo signaling in *Drosophila* and mammals.**

Corresponding components in *Drosophila* and mammals are shown in the same color. The abbreviations used are as follows: Ex (Expanded), Mer (Merlin, also called NF2), Hpo (Hippo), Sav (Salvador), Mats (Mob as tumor suppressor), Wts (Warts), Yki (Yorkie), Sd (Scalloped), Mst (Mst1/2, also called STK4 and STK3, Hpo homolog), WW45 (Sav homolog), Mob (Mps One Binder kinase activator-like 1A/B, MOBKL1A/B, Mats homolog), Lats (Lats1/2, Wts homolog), YAP (Yes-associated protein, Yki homolog), TAZ (transcriptional co-activator with PDZ binding motif, also called WWTR1, Yki homolog), and TEAD (TEA domain family member 1/2/3/4). Dashed arrows indicate unknown biochemical mechanism and question marks denote unknown components. Taken from (Zhao et al., 2008a).

The mechanisms of Hippo signaling activation and the mechanisms that control Yap/Taz localization were largely unclear a few years ago, however during the last three years, significant progress in elucidating the regulatory signals has been achieved. An emerging

view is that Yap/Taz mediated Tead activity is largely controlled by three main cellular components: cell-cell junctions, the actin cytoskeleton, and polarity complexes. These cellular structures may act through activation of canonical Hippo signaling to control Yap/Taz localization or may influence Yap/Taz localization independently of the core Hippo components (Pan, 2010; Zhao et al., 2010; 2011b; Boggiano and Fehon, 2012). An overview of these mechanisms is given hereafter.

#### *Regulation by intercellular junctions*

Intercellular junctions are not only structural components of cells but also participate in cellular signaling. The classical example hereof is the role of adherens junctions in sequestering  $\beta$ -catenin, thereby preventing its nuclear translocation where it acts as a transcriptional regulator together with TCF/Lef transcription factors (Jeanes et al., 2008). In order to prevent overgrowth, polarized cells in growing epithelial tissues need to monitor their surroundings and cease proliferation once a certain cell density or organ size is reached. Intercellular junctions are ideally positioned to appoint this task. First evidence that cells signal through the Hippo pathway to control proliferation came from the observations that Yap phosphorylation was increased when cells were grown to high densities in cell culture dishes, leading to cytoplasmic translocation of Yap and decreased Tead activity (Zhao et al., 2007; Ota and Sasaki, 2008). These observations suggested that the core Hippo Mst and Lats kinases are activated upon high cell density, however this has not been directly demonstrated. Early models of the Hippo pathway suggested a hierarchical transmission of signals from transmembrane proteins acting as density „sensors“, to intracellular proteins which convey the signal along a cascade to the core Hippo components (Hamaratoglu et al., 2006; Zeng and Hong, 2008; Zhao et al., 2008a); (Figure 8). However it was later found that Yki (Yap in *Drosophila*) can form a complex with the adherens junction localized „upstream“ component Expanded (Ex) in a phosphorylation-independent manner, leading to sequestering of Yki from the nucleus (Badouel et al., 2009). Moreover, the same complex was found to contain Hpo (Mst) and Wts (Lats), and again the nuclear function of Yki was shown to be inhibited by formation of this complex, notably in a phosphorylation-independent manner (Oh et al., 2009). These findings suggested that membrane sequestration of Yap (Yki) by Hippo pathway components represents a mechanism for Yap inhibition in addition to phosphorylation (Figure 9).

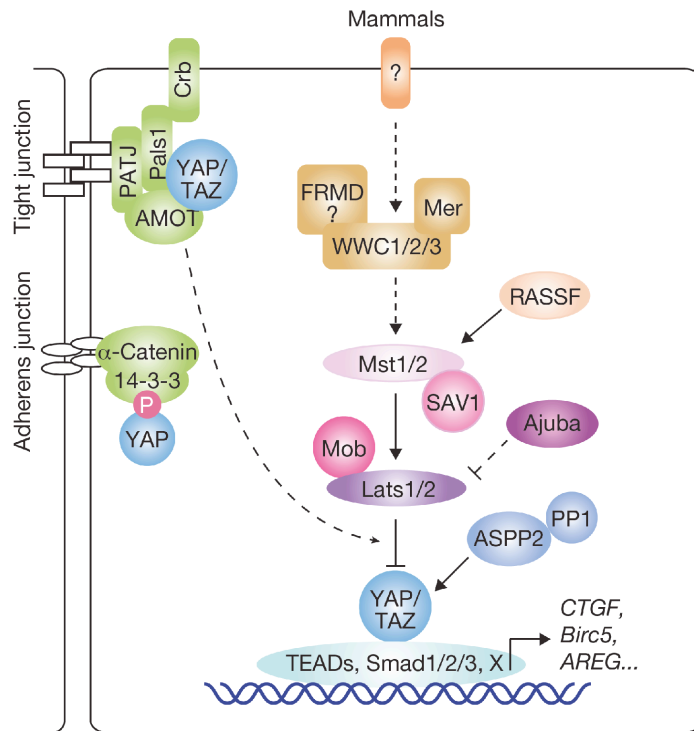


**Figure 9. Updated concept of Hippo signaling in mammals**

Sequestering of Yap/Taz by intercellular junctions and the crumbs polarity complex is added (compare to Figure 8). Participation of Smads is also indicated. Arrowed or blunted ends indicate activation or inhibition, respectively. Dashed lines indicate unknown mechanisms. Taken from (Zhao et al., 2011b).

Several studies in mammalian systems have confirmed the existence of similar mechanisms of Yap inhibition. Two studies showed that Yap interacts with the adherens junction protein  $\alpha$ -catenin, which links E-cadherin to the actin cytoskeleton, in mouse keratinocytes (Schlegelmilch et al., 2011; Silvis et al., 2011). In dense cells, Yap is phosphorylated and bound by 14-3-3, and this complex binds to  $\alpha$ -catenin (Schlegelmilch et al., 2011); (Figure 9). Loss of  $\alpha$ -catenin or adherens junction disruption by EGTA, but interestingly not E-cadherin depletion, leads to dissociation of the complex, dephosphorylation of Yap by the phosphatase PP2A and subsequent nuclear accumulation and transcriptional activity. Of note, Yap phosphorylation upon increased cell density was neither Mst- nor Lats-dependent, suggesting that another kinase must accomplish this task in keratinocytes. A study performed in breast epithelial cells presented evidence that E-cadherin can regulate Yap localization via catenins and Hippo components (Kim et al., 2011). When beads coated with E-cadherin were added to these cells to create homophilic E-cadherin interactions in a defined way, a moderate but measurable reduction of proliferation was observed. This phenotype could be blocked by siRNA depletion of either  $\alpha$ - or  $\beta$ -catenin, or by depletion of the Hippo pathway components Merlin/NF2, Lats, and Kibra. Additionally, E-cadherin overexpression led to cytoplasmic retention of Yap, which was dependent on the E-

cadherin catenin-binding domain. Conversely, depletion of  $\beta$ -catenin or Lats in densely cultured cells led to nuclear accumulation and reduced phosphorylation of Yap. Notably, the anti-proliferative effect of E-cadherin ligation was independent of Mst, again suggesting that an additional kinase must mediate Yap phosphorylation under these circumstances. Yap/Taz regulation that is completely independent of phosphorylation by the Hippo pathway has also been shown to be mediated by Yap/Taz binding to angiomin family (AMOT) proteins localized in tight junctions (Chan et al., 2011; Wang et al., 2011b; Zhao et al., 2011a); (Figure 9). Interestingly, knockdown of AMOTL2 in MCF10A cells leads to induction of EMT-like changes (Wang et al., 2011b). Collectively, these data suggest that Yap/Taz sequestration to tight- and adherens-junctions provides a mechanism for inhibition of Yap/Taz mediated Tead activity.

#### *Regulation by the cytoskeleton*

Experiments from mammalian tissue culture suggest that Yap/Taz subcellular localization and activity is regulated by changes in cell morphology and the actin cytoskeleton. Whether this is mediated by canonical Hippo signaling is currently debated. Wada et al. showed that Yap/Taz nuclear localization and activity is increased upon cell spreading (i.e. cell morphology) and concomitant formation of stress fibers (F-actin), in a Lats-dependent manner (Wada et al., 2011). In addition, pharmacological inhibition of F-actin and also of microtubules also suggested that the cytoskeletal state influences Yap phosphorylation via Lats (Zhao et al., 2012). Differential regulation of Yap localization and transcriptional activity was also shown to be dependent on extracellular matrix stiffness, although the authors of this study did not find differences in Yap phosphorylation, and the effects of matrix stiffness and stress fiber formation upon cell spreading were still observed in Lats-depleted cells (DuPont et al., 2011). Additionally, increased amounts of F-actin in the *Drosophila* wing disc promoted by loss of capping proteins results in increased Yki activity and tissue overgrowth (Fernández et al., 2011; Sansores-Garcia et al., 2011).

#### *Regulation by polarity complexes*

Finally, Yap/Taz localization and activity has been shown to be modulated by the crumbs (Crb) apical polarity complex (Varelas et al., 2010). Similar to  $\alpha$ -catenin and AMOT, the Crb complex sequesters Yap/Taz from the nucleus by direct interaction in cells grown to high density and inhibits Yap/Taz target gene expression, which is dependent on canonical Hippo

signaling. Interestingly, AMOT was also found in the apical complex identified by Varelas and colleagues (Varelas et al., 2010), suggesting that regulation by AMOT and the Crb complex could be related (Figure 9). A study by the same group previously established physical binding of Taz and Smads, and showed that presence of Taz in the nucleus is required for the ability of Smad2/3/4 complexes to accumulate in the nucleus after TGF $\beta$  stimulation (Varelas et al., 2008). The newer study then established that in densely grown Eph4 mammary epithelial cells, Smad2/3 were activated upon TGF $\beta$  treatment but failed to accumulate in the nucleus to regulate TGF $\beta$  target genes. The authors further showed that in dense cells treated with TGF $\beta$ , a complex encompassing pSmad2/3 and pYap exists. Under these conditions, inactivation of Hippo signaling by depletion of Lats, disruption of the crumbs complex by knockdown of its components Pals1 or Crumbs3, or calcium chelation resulted in nuclear accumulation of activated Smads and restored target gene transcription (Varelas et al., 2010); (Figure 9). These results suggest that the Hippo pathway can control the response to canonical TGF $\beta$  signaling.

Collectively, the extensive number of studies during the last few years have shown that Yap/Taz/TeaD transcriptional control is exerted through a combination of at least two mechanisms: 1) the phosphorylation of Yap/Taz by the canonical Hippo pathway, and 2) the sequestration of Yap/Taz at the cell cortex by direct binding to components of adherens- and tight junctions and polarity complexes (Figure 9).

#### *Transcriptional targets of TeaD*

Although much research has been directed towards understanding the upstream regulatory mechanisms of Yap/Taz/TeaD transcriptional activity, and several functional consequences have been documented, mechanistic insights into the downstream effects of this transcriptional complex are limited. Several direct Yap/Taz/TeaD target genes have been identified in mammalian cells (Ota and Sasaki, 2008; Zhao et al., 2008b; Lai et al., 2011) and *Drosophila* (Wu et al., 2008; Zhang et al., 2008; Neto-Silva et al., 2010; Ziosi et al., 2010). However, these target genes appear to be highly species- and context specific (Ota and Sasaki, 2008). CTGF and Cyr61 are direct target genes in mammalian cells. CTGF was determined to be important for Yap-induced anchorage-independent growth and proliferation in MCF10A cells (Zhao et al., 2008b). Cyr61, together with CTGF has been shown to be responsible for Yap/Taz/TeaD-mediated Taxol resistance of breast cancer cells (Lai et al., 2011). Further

evaluation of the individual functions of Yap/Taz/Tead target genes will be an interesting area for future research.

### ***1.5 MARA Analysis***

MARA is a computational method that allows prediction of transcription factor activity across different samples from gene expression profiling data. To infer differential activity of transcription factors, MARA uses human and mouse ‘promoteromes’, i.e. annotations of the genomic location of promoter regions from genome-wide transcription start site data obtained from cap analysis of gene expression (CAGE); (Balwierz et al., 2009). To predict functional transcription factor binding sites (TFBSs) within these promoter regions, MARA uses the MotEvo algorithm (van Nimwegen, 2007), which maps known regulatory motifs to the promoterome by comparative genomic sequence analysis and predicts functionality of these mapped sites by considering their evolutionary conservation.

The output of MARA include a list of regulatory motifs and corresponding TFs, sorted by a z-value that quantifies the contribution of the motif to the observed expression changes of target genes. MARA also provides a list of target promoters for each motif, as well as the location of binding sites in the promoters through which the corresponding TFs are predicted to act. Additionally, an activity profile across all input samples is generated which quantifies the difference in expression of all predicted target genes between samples.



## 2. Aim of the study

Metastasis is the cause of death in 90% of cancer patients, yet this process is one of the most enigmatic aspects of the disease. Uncovering the mechanisms that contribute to metastatic disease is likely to pave the way for the development of prevention- and treatment-strategies. Increasing evidence suggests that a cell-biological program termed epithelial-mesenchymal transition (EMT) plays a key role in the metastatic process.

The work presented here represents several approaches to advance the knowledge about the biological processes important for metastasis formation by

- Establishing new tools that allow a better characterization of the role of EMT in tumor progression and metastasis
- Identifying and characterizing key molecular regulatory mechanisms that control the EMT transdifferentiation process

To achieve these goals, we established a novel model system of EMT, which we demonstrate to be a versatile tool to study EMT both in a cell culture environment and also under more physiological conditions in mice. In addition, we set out to identify critical transcription factors that are responsible for essential gene expression changes associated with the EMT process, and identified the Tead transcription factor family as critical regulators of the EMT program.

## 3. Results

### *3.1 Py2T murine breast cancer cells, a versatile model of TGF $\beta$ -induced EMT in vitro and in vivo*

#### 3.1.1 Abstract

Introduction: Increasing evidence supports a role of an epithelial to mesenchymal transition (EMT) process in endowing subsets of tumor cells with properties driving malignant tumor progression and resistance to therapy. To advance our understanding of the underlying mechanisms, we sought to generate a transplantable cellular model system that allows defined experimental manipulation and analysis of EMT *in vitro* and at the same time recapitulates oncogenic EMT *in vivo*. Methods: A cell line (Py2T) was established from a breast tumor of an MMTV-PyMT transgenic mouse. TGF $\beta$ -induced EMT and cell migration and invasion were assessed by cellular assays *in vitro*, and the expression of epithelial and mesenchymal markers in Py2T cells was determined by immunofluorescence staining, immunoblotting and quantitative RT-PCR. Tumor formation of Py2T cells was evaluated by orthotopic transplantation into syngeneic mice, and tumors were characterized for an EMT-like phenotype by histopathological and gene expression analysis. TGF $\beta$  signaling in Py2T cells was modulated by stable lentiviral expression of a dominant-negative TGF $\beta$  receptor, and effects on primary tumor formation, tumor progression and metastasis was evaluated upon orthotopic transplantation into immunocompromised mice. Results: We have established a novel murine breast cancer cell line (Py2T), which displays a metastable epithelial phenotype, concomitantly expresses luminal and basal cytokeratins, and can be induced to undergo reversible EMT by exposure to TGF $\beta$  *in vitro*. Upon TGF $\beta$ -induced EMT, Py2T cells also gain in single cell motility and invasiveness. Py2T cells give rise to tumors after orthotopic injection into syngeneic mice. Notably, transplantation of epithelial Py2T cells results into invasive primary tumors, indicating that the cells undergo EMT *in vivo*, a process that appears to depend on TGF $\beta$  signaling. Conclusions: Together, the data demonstrate that the Py2T cell line represents a versatile model system to study the EMT process *in vitro* and *in vivo*. The observations that Py2T cells give rise to tumors and collectively undergo EMT-like changes *in vivo* highlight the suitability of the Py2T model system as a tool to study tumor-related EMT. In particular, Py2T cells may serve to corroborate recent findings relating EMT to cancer cell stemness, to therapy resistance and to tumor recurrence.

### 3.1.2 Introduction

Epithelial to mesenchymal transition (EMT) is an embryonic cellular program during which polarized epithelial cells lose their cell-cell adhesions and convert into a motile mesenchymal cell type (Thiery et al., 2009; Nieto, 2011). These phenotypic changes can be induced by a plethora of signals, including hypoxia, Wnt signaling, epidermal growth factor (EGF), hepatocyte growth factor (HGF), transforming growth factor  $\beta$  (TGF $\beta$ ), and many more (Huber et al., 2005; Moustakas and Heldin, 2007). Intracellular signaling pathways then integrate these signals to initiate the acquisition of mesenchymal traits via an elaborate network of EMT-related transcription factors (Moreno-Bueno et al., 2008), culminating in the loss of E-cadherin, a central hallmark of EMT (Thiery, 2002). In the adult, an analogous program can be reactivated in the setting of solid tumors (termed oncogenic or Type III EMT) (Kalluri and Weinberg, 2009). During the last two decades, EMT has been in the focus of many research fields and laboratories (Nieto, 2011). One longstanding interest is based on the concept that EMT of cancer cells facilitates their dissociation from primary tumors and their invasion of surrounding tissue and intravasation, thereby contributing to the initial steps of metastasis (Thiery et al., 2009; Chaffer and Weinberg, 2011; Valastyan and Weinberg, 2011). Consistent with the metastatic role of EMT, recent results have indicated that EMT confers stem cell-like traits to tumor cells (Mani et al., 2008; Morel et al., 2008; Polyak and Weinberg, 2009). These results have also provided an attractive explanation for the findings that oncogenic EMT contributes to resistance against cancer therapy, escape from oncogene addiction and recurrence of tumor growth (Singh and Settleman, 2010; Cardiff et al., 2011; May et al., 2011; Dave et al., 2012). A number of normal and transformed cell lines of murine and human origin have been described and used to study EMT *in vitro*, yet model systems that allow the study of breast cancer EMT both *in vitro* and *in vivo* have remained scarce.

To meet this need, we set out to establish a cellular model of breast cancer EMT that with one cellular system allows the study of epithelial plasticity *in vitro* and of EMT, malignant tumor progression and metastasis *in vivo*. We here report the establishment of a cell line (Py2T) derived from a primary breast tumor of MMTV-PyMT transgenic mice. Py2T cells undergo EMT *in vitro* upon TGF $\beta$  stimulation and, upon orthotopic injection into syngeneic or nude mice, they form primary tumors with an EMT-like phenotype, which is at least in part dependent on the responsiveness of the transplanted tumor cells to TGF $\beta$  signaling.

### 3.1.3 Results

#### 3.1.3.1 Py2T, a novel breast cancer cell line undergoing TGF $\beta$ -induced EMT

To establish a cellular model system that could be used to study epithelial to mesenchymal transition (EMT) *in vitro* and also *in vivo*, we sought to establish stable cancer cell lines from primary breast tumors. Since EMT is regarded as a prerequisite in the early steps of metastasis, we chose to isolate cells from tumors of the highly metastatic MMTV-PyMT mouse model of breast cancer (Guy et al., 1992; Lin et al., 2003). After recovery from culture shock and passaging for 2 months, an isolated pool of cells displayed a uniform cobblestone-like morphology typical of differentiated epithelial cells (Figure 1A). We termed this cell line Py2T (Polyoma-middle-T tumor). The presence of the MMTV-PyMT transgene in these cells could be confirmed by genotyping (Figure 1B). Curiously, PyMT transgene expression was not maintained during extended culturing (Figure 1C).

Next, we investigated whether treatment with a selection of known inducers of EMT (Huber et al., 2005) could induce EMT-like morphological changes in cultured Py2T cells. Both transforming growth factor  $\beta$  (TGF $\beta$ ) and hepatocyte growth factor/scatter factor (HGF) provoked loss of cell-cell contacts, which was not observed with other treatments, even after prolonged treatment for 10 days (Figure 1D). Interestingly, only TGF $\beta$  treatment resulted in a classical „cadherin-switch“, a hallmark of EMT in which expression of the epithelial cell adhesion molecule E-cadherin is lost and expression of mesenchymal N-cadherin is gained (Cavallaro and Christofori, 2004). Furthermore, we observed an upregulation of the mesenchymal marker fibronectin only in TGF $\beta$ -treated cells and to a lesser extent in EGF-treated cells (Figure 1E). Therefore, among all the factors tested, only TGF $\beta$  induced a *bona fide* EMT in Py2T cells.

TGF $\beta$  is known to exert cytostatic effects via effector arms downstream of the canonical Smad2/3 pathway in normal cells. However, cancer cells often develop resistance to TGF $\beta$ -induced cell cycle arrest (Massagué, 2008). The canonical TGF $\beta$  pathway was activated in Py2T cells upon TGF $\beta$  treatment, indicated by the nuclear translocation of the Smad2/3 complex and the activation of Smad3 by phosphorylation (Figure S1A). Furthermore, transient transfection of a promoter reporter construct in which firefly luciferase expression was under the control of a Smad-binding element (SBE) revealed a dramatic induction of transcriptional activity upon TGF $\beta$  stimulation, while there was no detectable activity in

untreated cells (Figure S1B); (Dennler et al., 1998). Despite an intact canonical pathway, we did not observe any significant increase in cell cycle arrest or apoptosis upon TGF $\beta$  treatment of Py2T cells (data not shown).

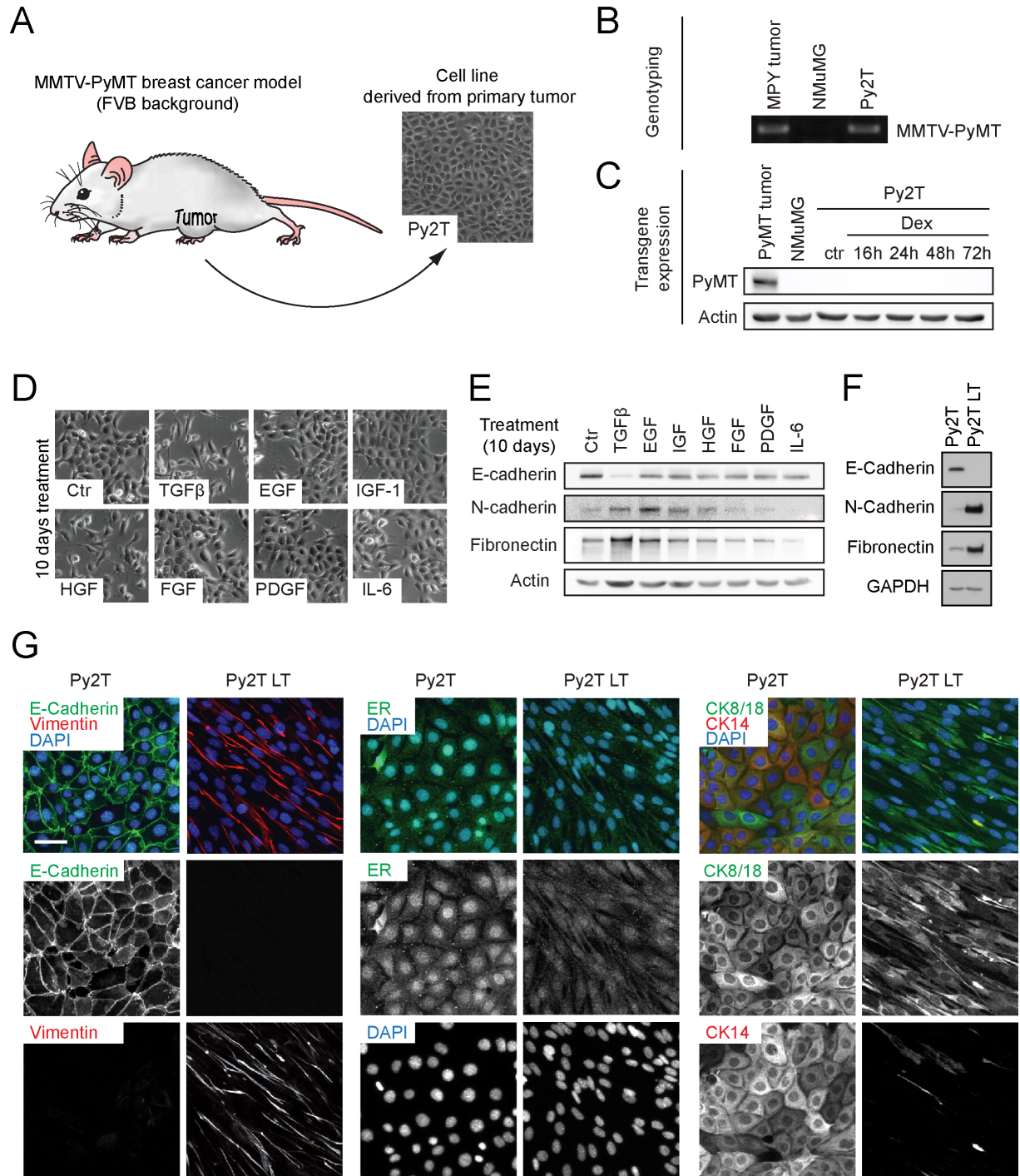


**Figure 1. Establishment of a murine breast cancer cell line undergoing TGF $\beta$ -induced EMT.**

(A) Primary tumor cells were isolated from an advanced breast tumor of a MMTV-PyMT transgenic female mouse and were cultured for at least 2 months prior to further experimentation, resulting in a novel cell line termed Py2T.

(B) Py2T cells maintain the MMTV-PyMT transgene. The MMTV-PyMT transgene was detected by PCR and agarose gel electrophoresis. DNA from an MMTV-PyMT tumor and from normal murine mammary gland (NMuMG) cells served as positive and negative controls, respectively.

(C) Py2T cells lost the expression of the MMTV-PyMT transgene. Immunoblotting for the PyMT protein was performed on lysates of Py2T cells untreated or treated with 0.1  $\mu$ M Dexamethasone for up to 72h to induce the MMTV promoter. Lysates of an MMTV-PyMT tumor and NMuMG cells served as positive and negative controls, respectively.

(D) Treatment of Py2T cells with known EMT inducers. Cells were continuously treated with the indicated growth factors and cytokines for 10 days (2ng/mL TGF $\beta$ 1; 50ng/mL EGF; 10ng/mL IGF-I; 50ng/mL HGF; 20ng/mL FGF-2; 20ng/mL PDGF-BB; 50ng/mL IL-6). Potential morphological changes were analyzed by phase-contrast microscopy.

(E) Expression of epithelial (E-cadherin) and mesenchymal (N-cadherin, fibronectin) markers were analyzed by immunoblotting of the lysates of cells treated in (D).

(F) Immunoblotting analysis of EMT marker expression in Py2T and Py2T LT cells. The mesenchymal subline Py2T LT (long-term) was generated by TGF $\beta$ -treatment of Py2T cells for at least 20 days, and was subsequently maintained in TGF $\beta$  containing growth medium (see also Additional files 3 and 4 for live cell imaging of Py2T and Py2T LT).

(G) Analysis of markers for EMT and breast cell type before and after TGF $\beta$ -induced EMT. Immunofluorescence staining was performed with antibodies against E-Cadherin (epithelial marker), vimentin (mesenchymal marker), estrogen receptor alpha (ER $\alpha$ ), cytokeratin 8/18 (luminal markers) and cytokeratin 14 (basal marker). Scale bar, 20  $\mu$ m.

To establish an experimental system that allowed direct comparison of epithelial versus mesenchymal cells without prior lengthy TGF $\beta$  treatment, Py2T cells were treated with TGF $\beta$  for 20 days and subsequently maintained as mesenchymal subline (Py2T LT) in growth medium containing TGF $\beta$ . Conveniently, Py2T LT cells preserved their mesenchymal phenotype, even when frozen and re-cultured in the presence of TGF $\beta$ . As confirmed by immunoblotting analysis, Py2T LT cells displayed a lack of E-cadherin expression, along with high expression of the mesenchymal markers N-cadherin and fibronectin (Figure 1F). Furthermore, immunofluorescence staining against E-cadherin and the mesenchymal marker vimentin were mutually exclusive in Py2T and Py2T LT cells, respectively, further verifying their distinct epithelial and mesenchymal states (Figure 1G *left*).

To determine the cell type represented by Py2T cells and to further characterize the effects of TGF $\beta$ -induced EMT on cellular identity, we stained for relevant breast cancer and mammary gland cell lineage markers. As the bulk of MMTV-PyMT tumors consist of luminal, estrogen receptor  $\alpha$  (ER $\alpha$ )-positive epithelial cells, we expected Py2T cells to display a similar expression pattern. Indeed, we could detect nuclear ER $\alpha$  staining in untreated cells, indicative of luminal differentiation (Figure 1G *middle*). Py2T LT cells however did not stain positive for ER $\alpha$ , consistent with a role of ER $\alpha$  in maintaining an epithelial phenotype and suppressing EMT (Guttilla et al., 2012). To determine whether Py2T cells represent a luminal or a basal mammary gland cell subtype, we stained for luminal cytokeratin 8/18 (CK8/18) and for basal cytokeratin 14 (CK14). Interestingly, Py2T cells were double positive for these markers, while, consistent with the loss of the epithelial phenotype, Py2T LT cells only weakly stained for CK8/18 and lacked CK14 (Figure 1G *right*, see also Figure 2B).

We also performed a gene expression profiling by Affymetrix DNA oligonucleotide microarray analysis of Py2T and Py2T LT cells. The gene expression profiles were compared to molecular breast cancer subtypes using the PAM50 predictor established by Parker and colleagues (Parker et al., 2009), followed by the 9-cell line claudin-low predictor (Prat et al., 2010b). This bioinformatic analysis revealed that the gene expression profile of Py2T cells resembles a Her2-enriched breast cancer subtype, whereas the Py2T LT cell line represents the highly invasive claudin-low subtype (data not shown).

### *3.1.3.2 EMT kinetics and plasticity in Py2T cells*

To characterize the transition from an epithelial to a mesenchymal phenotype in a time-resolved fashion, we analyzed various hallmarks of EMT upon TGF $\beta$  treatment of Py2T cells over time. On a morphological level, TGF $\beta$  treatment led to a gradual loss of cell-cell contacts and scattering already after 1 day of TGF $\beta$  treatment, while cell elongation and filopodia formation gradually increased over several days (Figure 2A). Immunoblotting analysis revealed a downregulation of E-cadherin expression over seven days, whereas N-cadherin levels began to increase between four and seven days, illustrating a classical cadherin switch (Figure 2B) (Cavallaro and Christofori, 2004). Maximum fibronectin expression was observed already after one day of TGF $\beta$  treatment. Expression of the luminal CK8/18 was found reduced yet with significant expression remaining even after thirteen days of treatment, whereas the expression of basal CK14 was completely lost after seven days. We further examined the transcriptional regulation of well-known EMT markers by quantitative RT-PCR (Figure 2C). The kinetics of mRNA levels of E-cadherin, N-cadherin and fibronectin closely correlated with the immunoblotting analysis (Figure 2B). Furthermore, we observed a strong and gradual increase in mRNA levels of vimentin and the E-cadherin gene repressors Zeb1 and Zeb2, a robust early induction of Snail mRNA, and only a modest increase in mRNA levels of the other E-cadherin repressors Slug, E47 and Twist (Figure 2C). Overall, these time-course experiments demonstrated that in Py2T cells, TGF $\beta$ -induced EMT involves gradual changes in gene expression, with early events occurring already after one day (loss of cell-cell contact, upregulation of fibronectin and Snail), while others are observed at later stages of EMT (cadherin switch, expression of vimentin, Zeb1 and Zeb2).

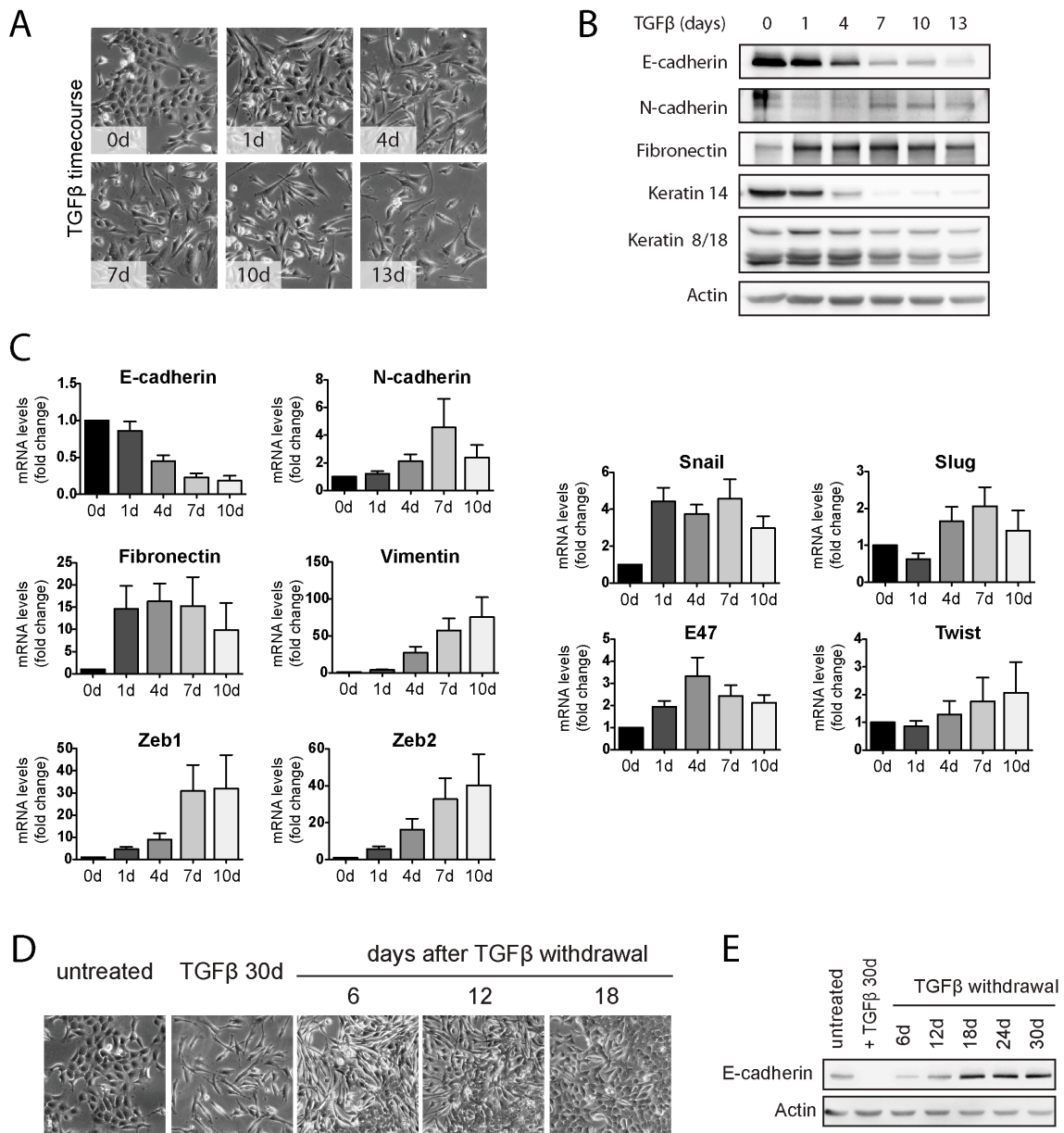


**Figure 2. Kinetics and reversibility of TGFβ-induced EMT in Py2T cells.**

(A) Morphological changes of Py2T cells during a time-course of TGFβ-treatment. Cells were cultured in growth medium containing TGFβ (2ng/ml) and phase-contrast microscopy pictures were taken at the indicated times.

(B) Immunoblotting analysis of lysates prepared from Py2T cells treated as in (A). The expression of epithelial (E-cadherin), mesenchymal (N-cadherin, fibronectin), luminal (CK8/18) and basal (CK14) markers was analyzed.

(C) Changes in the expression of EMT markers during TGFβ-induced EMT of Py2T cells. Py2T cells were treated for 10 days with TGFβ as described in (A). RNA was extracted at the indicated time points and quantitative RT-PCR was performed with primers specific for the EMT markers indicated. Expression levels are shown as mean fold difference of untreated cells (0d) ± S.E.M of 5 independent experiments.

(D-E) Reversibility of TGFβ-induced EMT. Py2T cells were treated with TGFβ for 30 days to induce EMT and were then further cultured without TGFβ for additional 30 days. Phase-contrast microscopy images were taken at the indicated time points (D). E-cadherin expression levels were analyzed throughout the experiment by immunoblotting (E).



After having studied the transition from an epithelial to a mesenchymal state, we wondered whether Py2T cells that have undergone EMT can also revert back to the epithelial state and undergo a mesenchymal to epithelial transition (MET) upon withdrawal of TGF $\beta$ . We observed that Py2T cells cultured for up to 30 days in growth medium containing TGF $\beta$  were still able to revert to the original epithelial morphology when TGF $\beta$  was withdrawn from the medium. The MET process took approximately 18 days (Figure 2D), with a gradual re-establishment of E-cadherin expression during this time (Figure 2E). These results indicate that Py2T cells offer a valuable experimental system to study the multiple stages of EMT and its reversion, MET.

### 3.1.3.3 *Migratory and invasive properties upon EMT induction*

To evaluate whether Py2T cells could be a suitable *in vitro* model system to study functional consequences of EMT, we assessed the migratory and invasive capabilities of these cells before, during and after EMT. First, we employed a modified Boyden chamber assay to analyze whether and to what extent Py2T cells become migratory and invasive during EMT. Cells previously treated with TGF $\beta$  for different times were seeded into Boyden chamber inserts without (migration assay) or with matrigel coating (invasion assay) and were allowed to move towards a gradient of fetal bovine serum as single cells. Quantification of cells that traversed the membrane revealed that cells treated with TGF $\beta$  for seven or more days were more migratory compared to untreated cells, and the migratory capacity dramatically increased with longer TGF $\beta$  treatment (Figure 3A *top left*). Similarly, when we seeded cells into Boyden chambers pre-coated with matrigel, cells passed through the bottom of the chambers with a similar increase over time of TGF $\beta$  treatment (Figure 3A *top right*). To illustrate these results, we stained cells located on the bottom side of the insert membranes with crystal violet (Figure 3A *bottom*). These findings clearly demonstrate that Py2T cells display a dramatic increase in chemotactic, single cell migration and invasion upon induction of EMT.

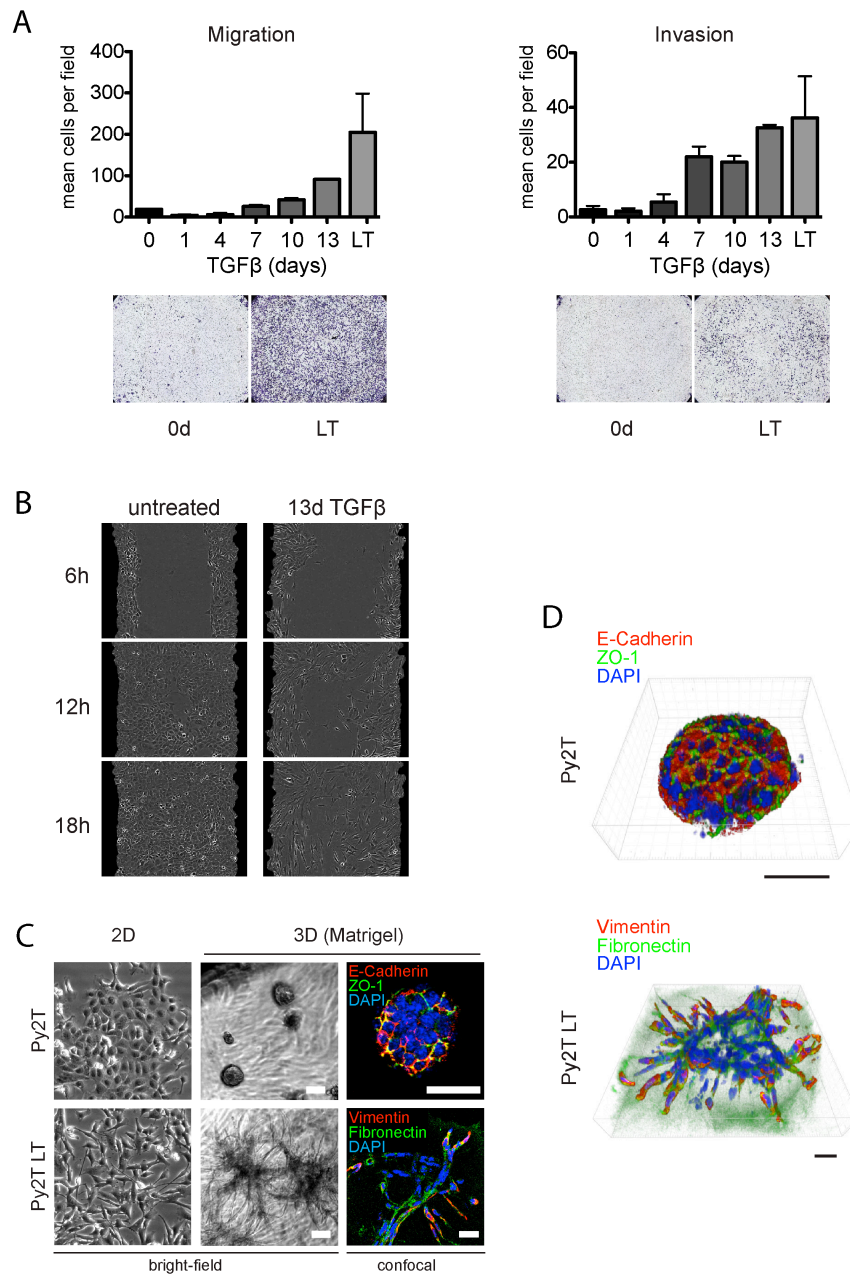


**Figure 3. Changes of migratory and invasive properties of Py2T cells before, during and after TGFβ-induced EMT.**

(A) Boyden chamber migration and invasion assay. Cells were treated with TGFβ for the indicated times (LT=long term treatment, as described in Fig 1F). 25'000 cells were seeded into migration or invasion chambers in duplicate in the absence or presence of TGFβ and allowed to pass through the membrane pores for 24 hours along an FBS gradient. Invasion chambers were pre-coated with growth-factor reduced Matrigel (BD BioCoat chambers). Cells that passed through the membrane pores were stained with crystal violet and photographed (*bottom panels*) and then counted (*top graphs*). Results are expressed as mean ± S.E.M of three independent experiments.

(B) Scratch wound healing assay. Cells pre-treated with TGFβ or not as indicated were starved over night and scratch wounds were introduced into confluent monolayers. Scratch wound closure was monitored by an IncuCyte™ live cell imaging system. Black masking represents initial gap width at 0 hours. Note the collective, sheet-like wound closure by untreated Py2T cells in contrast to single cell wound infiltration of TGFβ-treated cells (also see Additional files 1 and 2 for live imaging data of this experiment).

(C) Morphology of epithelial Py2T cells and mesenchymal Py2T LT cells grown on plastic tissue culture dishes (2D) and in Matrigel (4mg/ml; 3D). Structures were grown for 6 days, and stained directly in Matrigel with antibodies against epithelial E-cadherin and ZO-1 or against mesenchymal vimentin and fibronectin. Immunofluorescence images were acquired by confocal microscopy. Scale bars, 25μm.

(D) Three-dimensional reconstruction of confocal imaging stacks from cells grown in Matrigel as described in (A) (See also Additional files 5 and 6 for rotating 3D models). Scale bars, 25μm.

Scratch wound closure is another frequently used assay to assess the migratory capacity of cells on tissue culture plastic. Untreated and TGF $\beta$ -treated Py2T cells were grown to confluency and then starved in serum-free medium. After scratching a gap into confluent monolayers, we followed gap closure by live cell imaging (Additional file 1 and 2). Figure 3B shows images at different time points after wounding. Interestingly, untreated Py2T cells closed the scratch wound already after 12 hours in a sheet-like fashion, demonstrating that they are capable of a collective mode of migration, indicative of a metastable state (Lee et al., 2006). Py2T cells treated with TGF $\beta$  closed the scratch wound much slower, moving in a mesenchymal mode of single cell migration and displaying front-rear polarity. These observations indicate that TGF $\beta$  treatment switches Py2T cells from a collective to a single cell migration mode (Friedl, 2004).

To compare the migratory and invasive capabilities of Py2T and Py2T LT cells in a more physiological setting, the cells were seeded into a three-dimensional extracellular matrix (*Matrigel*; Figure 3C). Cells cultured on plastic are shown for comparison (Figure 3C, *left*; see also Additional file 3 and 4 for live imaging). When cultured for 6 days in growth factor-reduced Matrigel, Py2T cells formed spheres. In contrast, Py2T LT cells invaded the surrounding matrix (Figure 3C *middle*). To further examine these different phenotypes, we performed in-gel immunofluorescence staining of intact three-dimensional structures, followed by confocal microscopy. Double-labeling of Py2T spheres with antibodies against E-cadherin and ZO-1 revealed densely packed cells with intact adherens and tight junctions, respectively (Figure 3C *top right*). In contrast, Py2T LT structures, stained against vimentin and fibronectin, invaded the matrix as single cells or as cell trails (Figure 3C *bottom right*). The phenotypic differences between Py2T and Py2T LT cells grown in extracellular matrix became even more apparent upon reconstructing the confocal microscopy stacks to three-dimensional models using Imaris software (Figure 3D, see also Additional file 5 and 6 for animation). This analysis revealed the invasion and indian-file-like trailing of Py2T LT cells as single cells. Interestingly, only the leading cells expressed vimentin, while all Py2T LT cells cultured on a two-dimensional surface were positive for vimentin (Figure 1G) and moved as single cells rather than being organized in trails (Additional file 4). Taken together, these data demonstrate that the Py2T cell line represents a valuable model system to study various aspects of cell migration and invasion in the context of EMT.

### 3.1.3.4 Invasive tumor formation upon orthotopic transplantation into syngeneic mice

We next orthotopically transplanted Py2T cells into fat pads of mice to evaluate their tumorigenicity. Since Py2T cells have been derived from tumors of MMTV-PyMT mice in an FVB/N background and because the PyMT transgene was no more expressed in cultured cells, we transplanted Py2T cells into syngeneic FVB/N mice. Three mice were injected with  $1 \times 10^6$  cells, all of which developed tumors. After 27 days of growth, tumors were harvested and analyzed. Hematoxylin & Eosin (H&E) staining of histological sections of a Py2T tumor (Figure 4A, *right*) and a late stage MMTV-PyMT tumor (Figure 4A, *left*) revealed that MMTV-PyMT tumors were mainly well differentiated with some less well-differentiated areas and necrosis towards the tumor center.

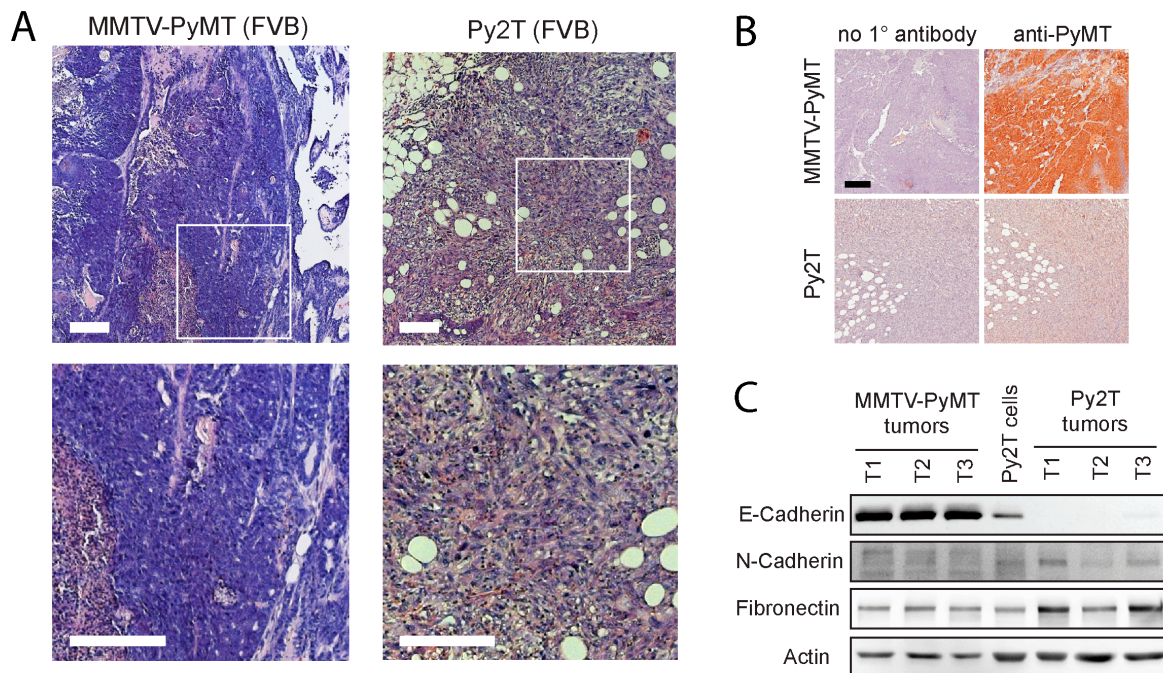


**Figure 4. Orthotopic transplantation of Py2T cells into syngeneic mice results in the formation of invasive tumors.**

(A) H&E staining of histological sections from tumors of MMTV-PyMT transgenic mice and from transplanted Py2T tumors.  $1 \times 10^6$  Py2T cells were transplanted into the fat pad of 8 weeks old female FVB/N mice and allowed to grow tumors for 27 days. Late-stage MMTV-PyMT tumors were from 12 weeks old female mice. *Bottom panels*: enlarged regions indicated by the white squares in the top panels. Note the typical pushing borders in MMTV-PyMT tumors in contrast to stream-like invasion of fat tissue in Py2T tumors. Scale bars, 200 $\mu$ m.

(B) Polyoma-middle-T (PyMT) expression in MMTV-PyMT and Py2T tumors. Paraffin sections were stained with an antibody against PyMT. Immunohistochemical staining in the absence of primary antibody (1°) was used as negative control. Scale bar, 100 $\mu$ m.

(C) Immunoblotting analysis for EMT markers in tumor lysates of MMTV-PyMT and Py2T tumors. Lysate from cultured Py2T cells is included as a control. Note the loss of E-cadherin expression and upregulation of mesenchymal markers (N-cadherin, fibronectin) in Py2T tumors.

The tumor borders were passively invading the fat pad by proliferation (pushing borders). In contrast, Py2T tumors were characterized by streams of elongated cells that were actively invading the surrounding fat tissue. Of note, Py2T tumors lacked excessive necrosis, possibly because they were well vascularized as determined by staining for the blood vessel marker CD31 (data not shown). Furthermore, Py2T tumors contained a high stromal component intermixed with tumor cells. To exclude the possibility that immune cell infiltration was due to a possible re-expression of the PyMT transgene, tumor tissue sections were stained with an antibody against the PyMT protein. As expected, PyMT expression could be detected in MMTV-PyMT tumors (Figure 4B, *left*), but not in Py2T tumors (Figure 4B, *right*). Notably, when Py2T cells were orthotopically implanted into immuno-deficient nude mice, all mice developed tumors with a substantial infiltration of CD45-positive stromal cells, with a high content of macrophages (Figure S2).

The spindle-like appearance of cells in the Py2T tumors suggested that Py2T cells may have undergone an EMT in these tumors. We thus compared lysates from mainly epithelial MMTV-PyMT tumors with lysates from mainly invasive Py2T tumors for expression of EMT markers. Indeed, expression of E-cadherin in MMTV-PyMT tumors was readily detectable as expected, however, very little if any E-cadherin expression was detectable in lysates of Py2T tumors (Figure 4C), supporting the hypothesis that Py2T cells had undergone EMT-like changes *in vivo*. Expression of the mesenchymal markers fibronectin and N-cadherin was also higher in some but not all Py2T tumors as compared to MMTV-PyMT tumors. Collectively, these results demonstrate that Py2T cells are tumorigenic, despite the absence of PyMT expression, and that they undergo oncogenic EMT-like changes *in vivo*. Notably, neither FVB/N nor immunodeficient mice bearing Py2T tumors had detectable metastasis, as determined by organ sectioning and luciferase activity measurement of organ lysates from mice injected with luciferase-tagged Py2T cells (data not shown, see also discussion).

#### 3.1.3.5 *TGF $\beta$ -dependent EMT of Py2T tumors*

We next assessed whether the EMT occurring during Py2T tumor growth in the mammary fat pad of mice could be attributed to stimulation by host-derived TGF $\beta$ . First, we generated Py2T cell lines that stably express GFP for their distinction from host stromal cells. Next, we superinfected these cells with a lentiviral construct encoding a dominant-negative form of TGF $\beta$  receptor II (TBRDN); (Oft et al., 1998) or empty vector as control. Cultured Py2T

TBRDN-expressing cells did not show any apparent changes in phenotype as compared to control cells in the absence of TGF $\beta$ , but were resistant against TGF $\beta$ -induced EMT (Figure S3A). In a next step, we transplanted untreated Py2T control and Py2T TBRDN into fat pads of immunodeficient nude mice to evaluate their ability to undergo EMT *in vivo*.

All mice developed tumors, and tumor growth was not significantly different between the two experimental groups (Figure S3B). H&E staining of Py2T control tumors revealed the same stream-like cellular growth pattern as observed in Py2T tumors in FVB/N mice (Figure 5A *top left*), with cells displaying a spindle-like morphology (Figure 5A *bottom left*). In contrast, tumors formed by Py2T TBRDN contained areas of differentiated appearance (Figure 5A *top right*), with cells adopting a round, differentiated morphology (Figure 5A *bottom right*).

Analysis of the expression of EMT markers revealed that, indeed, Py2T control tumors were negative for E-cadherin expression (Figure 5B, *top left*), whereas Py2T TBRDN tumors widely expressed E-cadherin, corresponding to the more differentiated regions observed by H&E staining (Figure 5B, *top right*). These results indicated that the inhibition of TGF $\beta$  signaling in Py2T TBRDN cells was sufficient to prevent a loss of E-cadherin expression and to preserve an epithelial phenotype. Immunofluorescence microscopy analysis of E-cadherin staining of GFP-expressing Py2T and Py2T TBRDN tumor cells, respectively, confirmed these observations (Figure 5C). Furthermore, immunoblotting analysis demonstrated higher E-cadherin expression in Py2T TBRDN tumors in contrast to Py2T control tumors (Figure 5E). Py2T tumors also stained positive for the mesenchymal marker vimentin, however, the vimentin expressing cells observed were stromal cells rather than Py2T cells, as revealed by a lack of GFP expression (Figure 5D). This result suggested that Py2T cells, although capable of vimentin upregulation upon EMT induction *in vitro* (Figure 2C), did not undergo a complete EMT in transplanted tumors, which is often reported as a hallmark of oncogenic EMT.

As Py2T cells expressed both luminal (CK8/18) and basal (CK14) markers in culture (Figure 1G, Figure 2B), we were curious to see whether the EMT-like changes observed in tumors would be accompanied by changes in the expression of these lineage markers. Immunofluorescence staining (Figure 5B) and immunoblotting analysis (Figure 5E) revealed a switch-like change in expression: a loss of CK14 expression was observed in favor of



CK8/18 expression in Py2T tumors. On the other hand, Py2T TBRDN tumors were strongly positive for CK14 expression and displayed a reduction or even a loss of CK8/18 expression. Together, these results demonstrate that Py2T tumors display EMT-like changes characterized by a loss of E-cadherin expression, and suggest an apparent differentiation along the luminal lineage, both of which is inhibited by blocking the TGF $\beta$  responsiveness of the tumor cells.

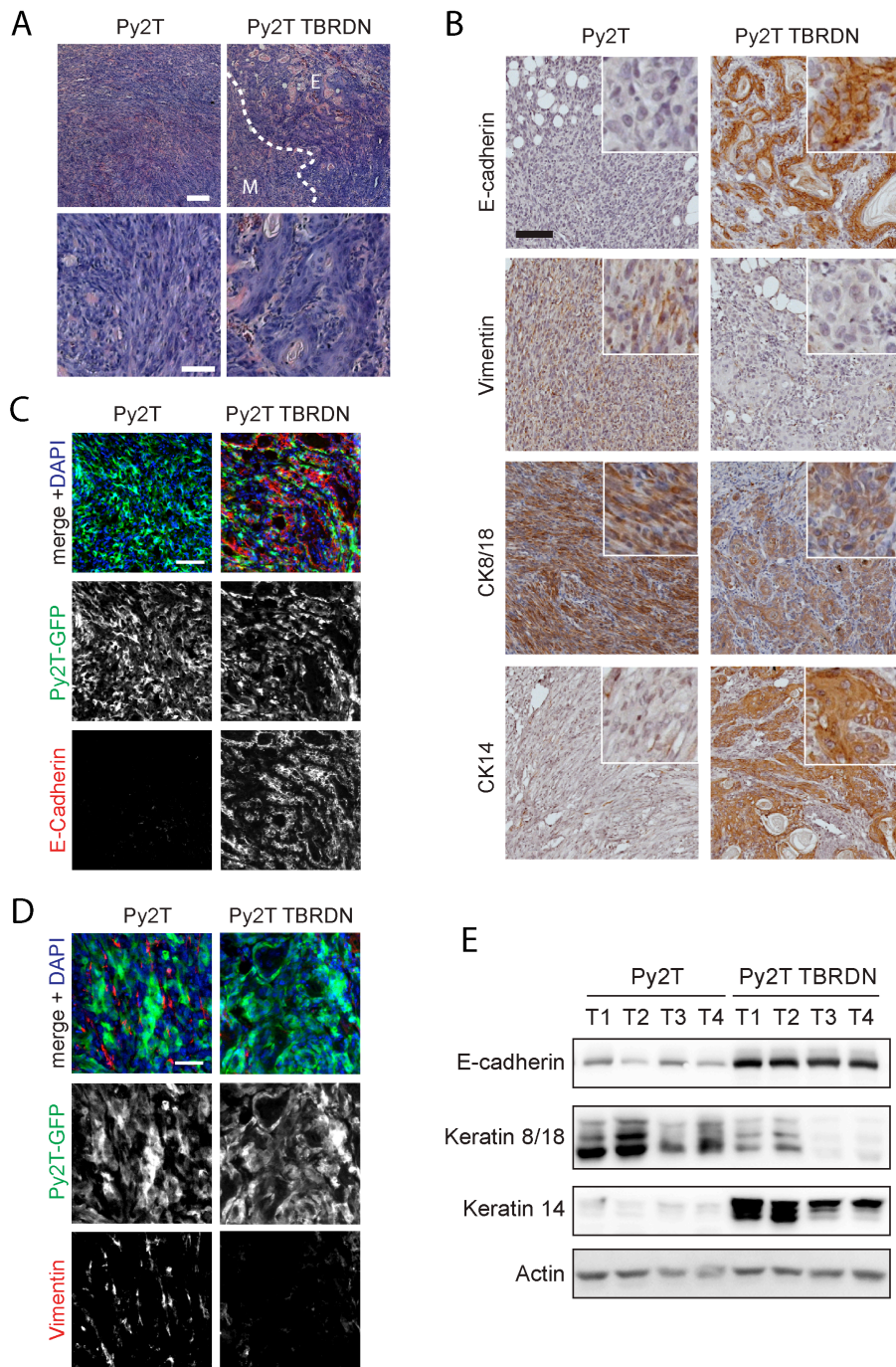


**Figure 5. Tumors of TGF $\beta$ -resistant Py2T cells display a more epithelial phenotype.**

(A) Morphology of tumors generated from Py2T cells stably overexpressing a dominant-negative TGF $\beta$ R2 (Py2T TBRDN) or empty vector control cells (Py2T).  $1 \times 10^6$  cells were injected into fat pads of nude mice and tumors were grown for 24 days. Paraffin sections were stained with H&E. Note the appearance of more differentiated epithelial areas in Py2T TBRDN tumors. *Top*: Epithelial (E) and mesenchymal (M) regions are separated by the dashed line (Scale bar, 200  $\mu$ m). Bottom panels show larger magnification (Scale bar, 50  $\mu$ m).

(B) Expression of EMT and lineage markers in Py2T and Py2T TBRDN tumors. Immunohistochemical staining of paraffin sections was performed using the specified antibodies. White squares show higher magnification. Scale bar, 100  $\mu$ m.

(C-D) Immunofluorescence staining of frozen sections of GFP-labeled Py2T and Py2T TBRDN tumors described in (A) with antibodies against E-cadherin or vimentin (*red*) and Py2T tumor cells (*green*). Scale bar, 20  $\mu$ m.

(E) Immunoblotting analysis of epithelial and cytokeratin lineage markers in a series of Py2T and Py2T TBRDN tumors as indicated.

### 3.1.4 Discussion

We here report the generation and characterization of a stable murine breast cancer cell line, named Py2T, from a primary breast tumor of MMTV-PyMT transgenic mice. Cultured Py2T cells can be induced to undergo a full EMT by TGF $\beta$  treatment, a multistage process that takes up to ten days and results in a complete loss of epithelial morphology and epithelial marker expression and the gain of mesenchymal marker expression and increased cell migration and invasion. Upon long-term treatment with TGF $\beta$ , Py2T cells maintain the mesenchymal differentiation status (Py2T LT), allowing the direct comparison between the extreme stages of epithelial-mesenchymal plasticity. Upon removal of TGF $\beta$ , Py2T LT cells revert to their epithelial origin by undergoing an MET, with the gain of epithelial morphology and marker expression.

Py2T cells also offer a novel syngeneic orthotopic transplantation model of malignant breast cancer progression. Upon injection into the fat pads of syngeneic FVB/N mice or into immuno-deficient nude mice, Py2T cells form primary tumors and spontaneously undergo EMT-like changes *in vivo*. As a proof of concept for the dual *in vitro* and *in vivo* use of Py2T cells as models of murine breast cancer cells undergoing EMT, we blocked TGF $\beta$  responsiveness of Py2T cells by stable expression of a dominant-negative version of TGF $\beta$ R2. Transplantation of these cells yielded tumors with an epithelial phenotype, showing that the EMT-like changes in Py2T cell-derived tumors are, at least in part, dependent on TGF $\beta$  stimulation. These experiments approve Py2T cells as a versatile model for functional studies of murine breast cancer cells undergoing EMT *in vitro* and *in vivo*.

It has been recognized that breast cancer is not a single, but a heterogeneous disease of various subtypes, which can be categorized according to staining for marker combinations, or, more recently, by molecular subtyping according to gene expression profiles. The type of



breast cancer is largely dictated by the transforming oncogene and the cell of origin being transformed (Petersen et al., 2001; Vargo-Gogola and Rosen, 2007; Visvader, 2009; Bertos and Park, 2011). We therefore characterized the cell type represented by Py2T cells. Molecular subtyping of MMTV-PyMT tumors has previously shown that these tumors resemble the luminal subtype of human breast cancer (Herschkowitz et al., 2007; Vargo-Gogola and Rosen, 2007), as would be expected from the fact that the MMTV promoter is active in luminal epithelial cells (Wagner et al., 2001; Andrechek et al., 2005). Consistent with their origin from a tumor of an MMTV-PyMT transgenic mouse, Py2T cells are positive for the luminal markers estrogen receptor (ER) and CK8/18 (Figure 1G). Interestingly, Py2T cells also co-express the basal marker CK14 (Figure 1G) and therefore do not display a purely luminal phenotype. Concomitant basal and luminal cytokeratin expression has also been observed in a luminal breast cancer model where the MMTV promoter has been used to drive mutant PIK3CA H1047R oncogene expression (Meyer et al., 2011), and one of the pathways activated by PyMT is the PI3K pathway (Dilworth, 2002), suggesting that similar mechanisms are involved. Our observations and those of others show that MMTV-PyMT tumors also contain a fraction of CK14-positive tumor cells (data not shown)(Maglione et al., 2001). Furthermore, double positivity for CK8/18 and CK14 has been established as a hallmark of basal cell lines (Keller et al., 2010).

Together, these considerations suggest that Py2T cells should be categorized as a basal cell line with luminal origin, although comparative molecular subtyping could further clarify this issue. It is interesting to note in this context that EMT-like changes have most commonly been observed in the basal-like subgroup of breast cancers, indicating that this subgroup is predisposed for EMT-like changes (Mahler-Araujo et al., 2008; Sarrió et al., 2008). Basal-like tumors also encompass the recently determined claudin-low subtype, now considered to be a distinct entity, which is clearly enriched in EMT marker expression (Lim et al., 2010; Taube et al., 2010; Prat et al., 2010a). Our gene expression profiling and subsequent bioinformatic analysis according to the PAM50 and 9-cell line claudin-low predictor (Parker et al., 2009; Prat et al., 2010b) revealed that Py2T cells most closely resemble Her2-enriched breast cancer of patients. In contrast, Py2T cells that have undergone TGF $\beta$ -induced EMT (Py2T LT) resemble basal-like, claudin-low breast cancer, a highly invasive breast cancer subtype that has been shown to correlate with EMT in a variety of experimental systems (Taube et al., 2010; Prat et al., 2010b; Asiedu et al., 2011; Herschkowitz et al., 2012).

Expression of basal cytokeratins 5 and 14 has also been linked to a hybrid or metastable differentiation state, in which cells display considerably more plasticity than fully differentiated cells, residing in a dynamic continuum between epithelial and mesenchymal states (Lee et al., 2006; Klymkowsky and Savagner, 2009). One feature that characterizes metastable cells is that they display loose but intact cell-cell adhesions and show migratory properties in the form of collective movement as a sheet. Indeed, when grown to confluency, Py2T cells close a scratch wound as a cellular sheet (Figure 3C and Additional file 1). A further indicator for a metastable state is the observation that, when grown under sparse culture conditions on plastic, Py2T cells are able to transiently leave the epithelial sheet and move as single cells in a spontaneous manner (Additional file 3). This single cell mode of migration resembles amoeboid movement, characterized by a rounding of cell bodies and a fast change in direction, and is distinct from the mesenchymal mode of migration characterized by front-rear polarity which we observed with Py2T LT cells (Additional file 4) (Friedl, 2004; Sahai, 2005). The reversibility of TGF $\beta$ -induced EMT of Py2T cells further illustrates the plasticity of Py2T cells and has also been proposed as a hallmark of metastability (Figure 2E) (Lee et al., 2006; Klymkowsky and Savagner, 2009; Savagner, 2010). From these observations we conclude that cultured Py2T cells do not represent fully differentiated epithelial cells, but that they are rather in a metastable state that is readily shifted towards a mesenchymal phenotype by TGF $\beta$  treatment.

When implanted into the mammary fat pad microenvironment, Py2T cells eventually develop tumors with an EMT-like phenotype (Figures 4 and 5). We believe that the term „EMT-like“ is accurate, since we have noticed that in these tumors, Py2T cells do not completely convert into mesenchymal cells as they do under culture conditions in the presence of TGF $\beta$ . Breast cancers can display a range of stages of EMT, in fact, tumor-associated EMT appears less complete than developmental EMT (Kalluri and Weinberg, 2009; Drasin et al., 2011). A staging scheme has been proposed based on the state of cell polarization, cell cohesiveness and intermediate filament expression, categorizing oncogenic EMT into four distinct stages (P0-P3), with P0 designating full epithelial differentiation and P3 indicating a fully mesenchymal state (Klymkowsky and Savagner, 2009). Py2T tumors correspond to the P2 stage, where cells have lost polarization and cohesive cell-cell contacts, but retain cytokeratin expression (at least CK8/18) and fail to upregulate vimentin (Figure 5). When we block TGF $\beta$ -responsiveness in Py2T cells, epithelial morphology is widely

retained, and tumor cells appear to be organized as dynamic cohesive sheets or strand-like structures, however not regaining full epithelial polarization (Figure 5). This phenotype is again consistent with a metastable state rather than full epithelial differentiation, and corresponds to the P1 stage of oncogenic EMT according to (Klymkowsky and Savagner, 2009).

Despite the fact that Py2T cells form locally invasive tumors and that MMTV-PyMT tumors give rise to distant metastases, we were unable to detect any metastasis evoked by Py2T tumors. One conceivable reason for this apparent discrepancy could be the following: Py2T tumors are fast growing and aggressive, and, due to animal welfare considerations, mice have to be sacrificed approximately 25 days after implantation (Figure S3). Therefore, the timeframe to establish detectable metastasis may be simply too short. In comparison, the metastasis latency in MMTV-PyMT tumors is about 3.5 months (Fantozzi and Christofori, 2006).

We have observed that PyMT transgene expression is absent in Py2T cells both *in vitro* (Figure 1C) and *in vivo* (Figure 4B). This finding has important implications. First, it allows the transplantation of Py2T cells (derived from MMTV-PyMT mice in a FVB/N background) into syngeneic FVB/N mice (Figure 4). Second, the loss of PyMT expression together with the fact that these cells are nevertheless tumorigenic suggests that outgrowing Py2T cells have escaped oncogene addiction. Intriguingly, in several other mouse models of breast cancer, discontinued oncogene expression is followed by the appearance of tumors that display EMT-like features (see (Cardiff, 2010) for review). For example, after turning off Her2/neu expression in tumors induced by this oncogene in the mammary gland, tumors regress, yet regrow as spindle cell „EMT“ tumors that are strikingly similar if not identical in phenotype to the tumors we describe here (Moody et al., 2002). In agreement with our study, these tumors have not been observed to metastasize (Cardiff, 2010). It is likely that our model recapitulates these events, whose underlying mechanisms have yet to be determined. If so, the Py2T model system could be instrumental in elucidating mechanisms of tumor recurrence and resistance to therapy, which has been previously attributed to EMT (Creighton et al., 2009; Singh and Settleman, 2010; Drasin et al., 2011; Biddle and Mackenzie, 2012; Dave et al., 2012). Finally, in light of the recent findings that EMT confers stem cell-like traits to cancer cells (Mani et al., 2008; Morel et al., 2008), Py2T cells also offer a unique system to study these events *in vitro* and *in vivo*.

### 3.1.5 Conclusions

We have established and functionally characterized a novel cellular model of murine breast cancer EMT (Py2T). While Py2T cells undergo EMT in response to TGF $\beta$  stimulation *in vitro*, orthotopic transplantation into mice results in tumors displaying oncogenic, TGF $\beta$ -dependent EMT. Py2T cells thus represent a versatile model to investigate the molecular mechanisms underlying EMT and to delineate how EMT contributes to therapy resistance, loss of oncogene addiction and tumor recurrence.

## 3.1.6 Supplemental Data

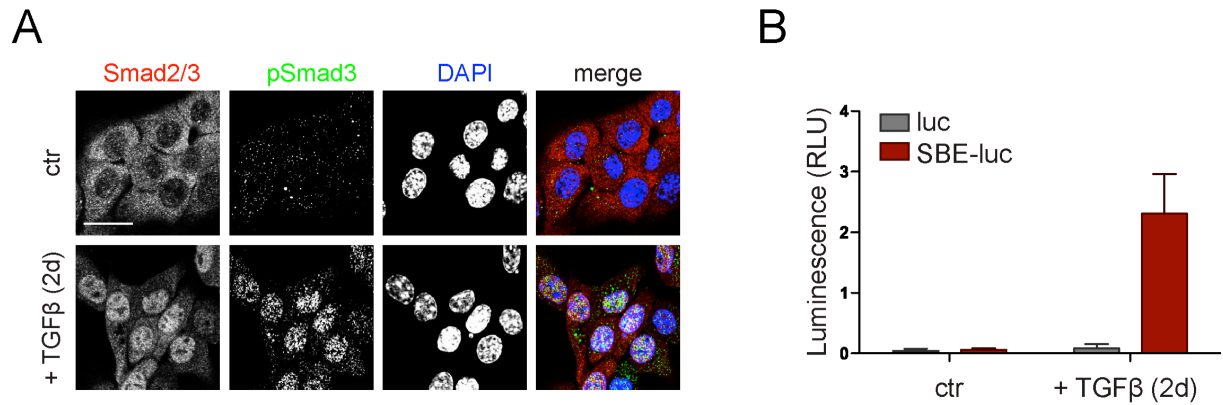


**Figure S1. Canonical TGFβ signaling in untreated versus TGFβ-treated Py2T cells.**

(A) Immunofluorescence staining for total Smad2/3 (red) and phosphorylated (activated) pSmad3 (green). Nuclei are visualized by DAPI staining. Scale bar, 20μm.

(B) Transcriptional Smad activity was determined by a dual luciferase reporter assay. Cells were transfected with a Smad4 luciferase reporter containing a Smad-binding element (SBE-luc) or a control plasmid lacking the SBE (luc), along with Renilla luciferase for normalization. Relative luminescence units (RLU) are expressed as mean +/- SEM from 2 independent experiments.

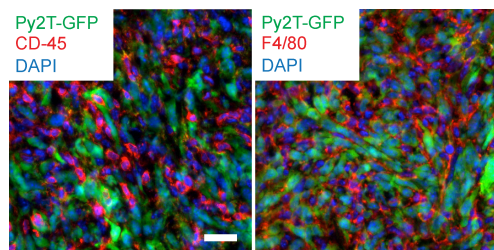


**Figure S2. Py2T tumors are characterized by a high immune cell infiltration.**

Immunofluorescence staining of a Py2T tumor for the leukocyte marker CD45 and the macrophage marker F4/80. Images show a central region of a tumor grown in nude mice as described in Figure 5. Scale bar, 50μm.

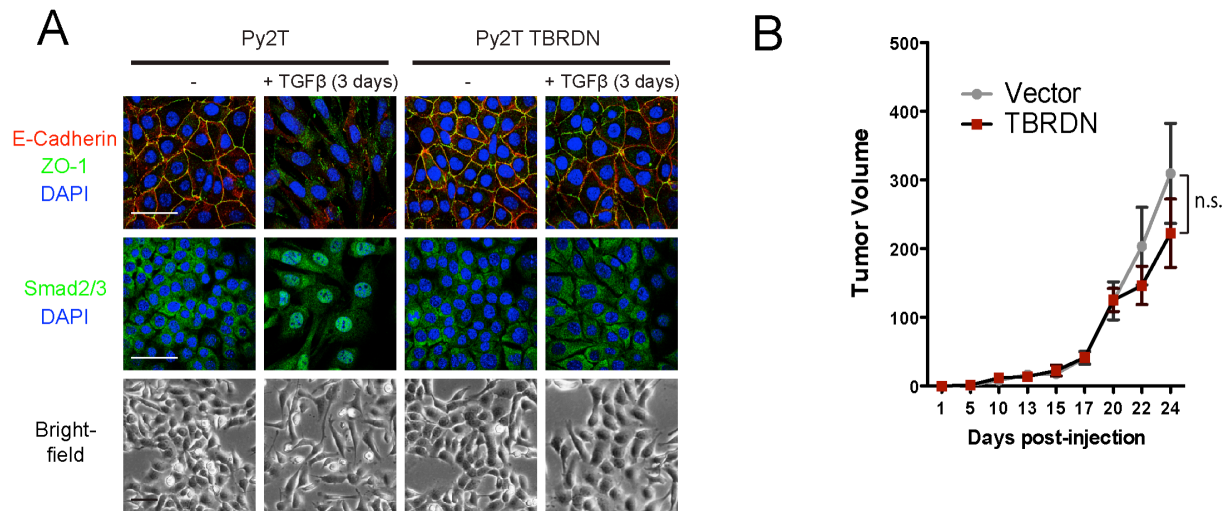


**Figure S3. Expression of a dominant-negative TGFβRII in Py2T cells prevents EMT *in vitro* and *in vivo*.**

(A) Py2T cells stably expressing a dominant-negative TGFβRII (Py2T TBRDN) or cells transfected with empty vector control were treated with TGFβ (2ng/mL). To assess activation of canonical TGFβ signaling and nuclear accumulation of Smad proteins, cells were stained with antibodies against Smad2/3. To evaluate the breakdown of cell junctions downstream of TGFβ signaling, cells were stained with E-cadherin (adherens junctions) and ZO-1 (tight junctions). Scale bars, 50μm.

(B) Tumor growth of Py2T TBRDN and control cells (Experiment is described in Figure 5). N=10 mice per group. Data is presented as mean ± S.E.M. Statistical values are calculated by using an unpaired, two-tailed t-test. A p-value > 0.05 was considered not significant.

Additional files containing digital data (movies, spreadsheet files) are available upon request.

### 3.1.7 Materials and Methods

#### *Antibodies and reagents*

Antibodies: PyMT (mouse monoclonal Pab762, a kind gift of Dr. S. Dilworth, Imperial College London), Actin (sc-1616, SantaCruz Biotechnology), E-cadherin (610182, Transduction Laboratories), N-cadherin (M142, Takara Bio), fibronectin (F3648 Sigma-Aldrich), GAPDH (ab9485, Abcam), cytokeratin 14 (RB-9020-P0, NeoMarkers), cytokeratin 8/18 (20R-CP004, Fitzgerald), vimentin (V2258, Sigma-Aldrich), ER $\alpha$  (sc-542, Santa Cruz Biotechnology), ZO-1 (617300, Zymed), F4/80 (MCAP497, Serotec), CD45 (550539, BD), Smad2/3 (610842, BD), Smad3 pSer423/425 (9520, Cell Signalling).

Reagents: recombinant human (rh) TGF $\beta$ 1 (240-B-010, R&D Systems), recombinant mouse (rm) EGF (PMG8041, Invitrogen), rmIGF-1 (250-19, Peprotech), rmHGF (2207-HG, R&D Systems), rmbasicFGF (3139-FB-025, R&D Systems), rhPDGF-BB (220-BB, R&D Systems), rhIL-6 (200-06 Peprotech), Dexamethasone (800-437-7500, Chemicon), Matrigel, growth factor reduced (356230, BD).

#### *Cells and cell lines*

A subclone of NMuMG cells (NMuMG/E9; hereafter NMuMG) has been previously described (Maeda et al., 2005). NMuMG and Py2T cells were cultured in DMEM supplemented with glutamine, penicillin, streptomycin, and 10% FBS (Sigma).

#### *Mouse strains*

MMTV-PyMT (Guy et al., 1992; Lin et al., 2003) were received from N. Hynes (FMI, Basel, Switzerland). BALB/c nude mice were purchased from JANVIER SAS (Le Genest Saint Isle, France).

#### *Primers*

For genotyping of the MMTV-PyMT transgene, the following primers were used: MMTV-PyMT (forward: 5'-cggcggagcggaggaactgagg-3', reverse: 5'-tcagaagactcggcagtcttag-3').

For quantitative RT-PCR, the following primers were used:

mRNA	Forward primer (5'-3')	Reverse primer (5'-3')
Rpl19	ctcgttgccggaaaaaca	tcaccaggtcaccttctca
E-cadherin	cgacctgcctctgaatcc	tacacgctgggaaacatgagc
N-cadherin	ctgccatgactttctacggaga	caatgacgtccaccctgttct
Fibronectin	cccagacttatgggtgcaatt	aattccgcctcgagtctga
Vimentin	ccaaccttttctccctgaa	ttgagtgggtgtcaaccaga
Zeb1	gccagcagtcgatgaaaa	tatcacaatacgggcaggtg
Zeb2	ggaggaaaaacgtgtgaactat	gcaatgtgaagctgtcctctt
Snail	ctctgaagatcacatccgaa	ggcttctcaccagttgtgggt
Slug	tgtgtctgcaagatctgtggc	tccccagttgagttctaattg
E47	ggacattaacgagccttccg	tggggttcaggtgcgttct
Twist	gccggagacctagatgcattg	cacgcctgattctgtgaa

### *Genotyping*

To extract DNA, cells from a confluent 10cm dish were trypsinized, washed in PBS and pelleted. To the pellet, 450 $\mu$ L tail tip buffer (50mM Tris-HCl pH 8, 100mM NaCl, 100mM EDTA, 1% SDS) and 180 $\mu$ L 6M NaCl were added, the samples were mixed and spun at full speed in a tabletop centrifuge. Supernatant was added to 600 $\mu$ L isopropanol, vortexed and spun for 5 min at full speed. Supernatant was discarded and 500 $\mu$ L of 70% EtOH was added, vortexed and spun for 3 min at full speed. Supernatant was discarded and the pellet was dried and resuspended in TE buffer. Samples were analyzed using standard PCR procedure.

### *Quantitative RT-PCR*

Total RNA was prepared using Tri Reagent (Sigma-Aldrich), reverse transcribed with M-MLV reverse transcriptase (Promega, Wallisellen, Switzerland), and transcripts were quantified by PCR using SYBR-green PCR MasterMix (Applied Biosystems, Rotkreuz, Switzerland). Riboprotein L19 primers were used for normalization. PCR assays were performed in triplicates, and fold induction was calculated using the comparative Ct method ( $\Delta\Delta C_t$ ).



*Luciferase reporter assay*

$5 \times 10^4$  Py2T cells were plated in triplicate in a 24 well plate. One day after plating, cells were transfected with 800ng reporter and 5ng Renilla encoding plasmids using Lipofectamine 2000. Fresh growth medium was added after 5 hours of transfection containing 2ng/mL TGF $\beta$  or not. After 2 days, cells were lysed directly in plates using 1x passive lysis buffer (#E194, Promega) and lysates were analyzed using the Dual-Luciferase Reporter Assay System (#E1960, Promega) and a Berthold Luminometer LB960. Measured luciferase values were normalized to internal Renilla control. The Smad4 reporter was kindly provided by P. ten Dijke (Leiden University; (Dennler et al., 1998)).

*Cell line isolation*

A piece (~200mg) of freshly isolated tumors was transferred into collection medium (DMEM supplemented with 10% FBS, 2mM glutamine, supplemented with Gentamycin (50ug/mL)) and minced into very small pieces using sterile technique with a scalpel. Pieces were collected by rinsing with pre-digestion buffer (10mM HEPES pH7.4, 142mM NaCl, 0.67mM KCl, 1mM EDTA) supplemented with Gentamycin (50ug/mL)(G1397, Sigma-Aldrich) and 1x Antibiotic-Antimycotic (15240-096, Invitrogen), and transferred to a 15mL Falcon tube. Pieces were predigested in horizontal position at 200rpm at 37°C for 30min on a bacterial shaker. Predigested tissue was pelleted by spinning at 900xg for 5min, the supernatant was removed and the pellet was resuspended in digestion mix (10mM HEPES pH7.4, 142mM NaCl, 0.67mM KCl, 0.67mM CaCl<sub>2</sub>, 20mM Glucose, 1mg/mL Collagenase Type I, 0.1mg/mL DNaseI) supplemented with Gentamycin (50ug/mL) and 1x Antibiotic-Antimycotic. The tissue was digested by shaking in horizontal position at 200rpm at 37°C for 30min on a bacterial shaker. For final single cell dissociation, tissue was pipetted up and down for 5 min using a 1mL pipette. Digested tissue was pelleted, washed twice in PBS and plated into multiple wells of a 24 well plate in normal growth medium (DMEM supplemented with 10% FBS, 2mM glutamine, 100U penicillin and 0.2mg/ml streptomycin). Growth medium was exchanged the next day, and subsequently exchanged every three to four days until epithelial cultures without Fibroblast contamination emerged.

*Immunofluorescence staining of cultured cells*

Cells were plated on glass coverslips and treated for the indicated times with TGF $\beta$ . The following steps were all done at room temperature. After fixation using 4 %

paraformaldehyde /PBS for 15 min, cells were permeabilized with 0.5 % NP-40 for 5 min. Next, cells were blocked using 3 % BSA, 0.01 % TritonX-100 in PBS for 20 min. Then, cells were incubated with the indicated primary antibodies for 1 h followed by incubation with the fluorochrome-labeled secondary antibody (Alexa Fluor®, Invitrogen) for 30 min at room temperature. Nuclei were stained with 6-diamidino-2-phenylindole (DAPI) (Sigma-Aldrich) for 10 min. The coverslips were mounted (Fluorescent mounting medium, Dako) on microscope slides and imaged with a conventional immunofluorescence microscope (Leica DMI 4000) or a confocal microscope (Zeiss LSM 510 Meta). Confocal stacks were reconstructed with Imaris Software (Bitplane, Switzerland).

### *Immunoblotting*

Cells were lysed in RIPA buffer (150 mM NaCl, 2 mM MgCl<sub>2</sub>, 2 mM CaCl<sub>2</sub>, 0.5 % NaDOC, 1 % NP40, 0.1 % SDS, 10 % Glycerol, 50 mM Tris pH 8.0) containing 2 mM Na<sub>3</sub>VO<sub>4</sub>, 10 mM NaF, 1 mM DTT, and a 1:200 dilution of stock protease inhibitor cocktail for mammalian cells (Roche). Protein concentration was determined using the BCA assay kit (Pierce). Equal amounts of protein were diluted in SDS-PAGE loading buffer (10 % glycerol, 2 % SDS, 65 mM Tris, 1 mg/100 ml bromophenol blue, 1 % β-mercaptoethanol) and resolved by SDS-PAGE. Proteins were transferred to polyvinylidene fluoride (PVDF) membranes (Millipore) by semi-dry transfer, blocked with 5 % skim milk powder in TBS/ 0.05 % Tween 20 and incubated with the indicated antibodies. HRP conjugated secondary antibodies were detected by chemiluminescence using a Fusion Fx7 chemiluminescence reader (Vilber Lourmat, France).

### *Retroviral infection*

A cDNA encoding EGFP was subcloned from pEGFP-N3 (Clontech) into the retroviral vector pBabe-hygro (Morgenstern and Land, 1990). The resulting plasmid pBH-EGFP was transfected into the retroviral packaging cell line Plat-E (purchased from Cell Biolabs)(Morita et al., 2000) using FugeneHD (Roche). One day after transfection, medium was exchanged and retroviral supernatant was produced for 2 days. Viral supernatant was filtered through 0.45 μm pores and 8 ug/mL Polybrene was added. Py2T cells were plated into 6-well plates and were infected with viral supernatant one day after plating. For infection, 2 mL supernatant was added per well and plates were spun for 1 hour at 30°C at 1000xg and were subsequently incubated at 37°C with 5% CO<sub>2</sub> in a tissue culture incubator for 2 more hours. Viral

supernatant was then replaced by normal growth medium and one day later, selection with 500 µg/mL Hygromycin B (Invitrogen) was performed for 5 consecutive days.

#### *Lentiviral infection*

A cDNA encoding a human dominant-negative version of TGFβRII (K277R)(Oft et al., 1998) (kindly provided by M. Oft, Targenics Inc., San Francisco) was subcloned into the lentiviral expression vector pLentiCMV (a kind gift from O. Pertz, University of Basel). Lentiviral particles were produced by transfecting HEK293T cells with the lentiviral expression vector pLentiTBRDN or empty vector as a control, in combination with the helper vectors pHDM-HGPM2, pHDM-Tat1b, pRC-CMV-RaII and the envelope encoding vector pVSV using Fugene HD. After two days of virus production, lentivirus-containing supernatants were harvested, filtered (0.45 µm) and added to target cells in the presence of polybrene (8 µg/ml). Cells were spun for 1 hour at 30°C at 1000xg and were subsequently incubated at 37°C with 5% CO<sub>2</sub> in a tissue culture incubator for 2 more hours. Viral supernatant was then replaced by normal growth medium and one day later, selection with 5 µg/mL Puromycin (Sigma-Aldrich) was performed for 3 consecutive days.

#### *Boyden chamber migration and invasion assay*

Cells pre-treated or not with TGFβ were trypsinized, washed once with PBS, and resuspended in growth medium containing 0.2% FBS and 2 ng/mL TGFβ where appropriate. 2.5x10<sup>4</sup> cells in 500 µL were seeded into cell culture insert chambers containing 8 µm pores (migration chambers: 353097, BD Falcon; invasion chambers with ECM coating: 354483, BD Falcon) in triplicate. Subsequently, the bottoms of chambers were filled with 700 µL of growth medium containing 20% FBS, and cells were incubated in a tissue culture incubator at 37°C with 5% CO<sub>2</sub>. After 24 hours, inserts were fixed with 4% PFA/PBS for 10 min. Cells that had not crossed the membrane were removed with a cotton swab, and cells on the bottom of the membrane were stained with DAPI. Images of five fields per insert were taken with a Leica DMI 4000 microscope and stained cells were counted using an ImageJ software plugin developed in-house. Subsequently, inserts were stained in crystal violet solution (0.125% crystal violet, 20%MeOH) for 10 minutes, followed by washing in a large volume of dH<sub>2</sub>O and drying over night. Images of crystal violet stained inserts were taken with an AxioVert microscope (Zeiss, Germany).

*Scratch wound closure assay*

$3 \times 10^5$  untreated Py2T cells and  $3 \times 10^5$  Py2T cells treated with TGF $\beta$  for 13 days were seeded into 24-well plates with or without TGF $\beta$ . Normal growth medium was replaced by starving medium containing 2% FBS with or without TGF $\beta$  on the next day. After starvation over night, a wound was scratched into confluent monolayers and plates were transferred to an Incucyte™ live imaging instrument (Essen BioScience).

*3D matrigel culture and in-gel immunofluorescence staining*

Growth factor-reduced matrigel (356230, BD) stock was thawed on ice and diluted to 4 mg/mL protein with ice-cold, serum-free growth medium. Cells were trypsinized, resuspended in ice-cold normal growth medium and counted using a CASY cell counter (Roche, Switzerland). A pellet of 2500 cells was resuspended in 10  $\mu$ L of pre-diluted matrigel and transferred to one well of a  $\mu$ -slide angiogenesis microscopy slide (ibidi, Martinsried, Germany). After an incubation of 20 min in a tissue culture incubator to allow solidification of the gel, 50  $\mu$ L of normal growth medium containing or not 2 ng/mL TGF $\beta$  was added to each well. Growth medium was replenished every third day. After 6 days of growth, structures were prepared for immunofluorescence analysis directly in the matrix. Structures were fixed with 4% PFA/PBS for 10 min and washed with 20 mM Glycine/PBS for 5 min. After a second wash with PBS, cells were permeabilized and blocked with IF buffer (0.2% TritonX-100/0.1% BSA/0.05% Tween20/PBS) containing 10% goat serum. Samples were incubated with primary antibodies diluted in IF buffer for 2 hours at room temperature in a humid chamber. After 2 washes with IF buffer, secondary antibodies diluted in IF buffer were incubated for 45 minutes, and nuclei were stained with DAPI solution for 20 minutes. After 2 final washes with IF buffer, samples were topped with fluorescent mounting medium (Dako) and imaged with a confocal microscope (LSM 510 Meta, Zeiss).

*Orthotopic tumor cell transplantation*

Cells were trypsinized, washed twice and resuspended in ice-cold PBS. Eight weeks old female BALB/c nude mice or FVB/N mice were anaesthetized with isoflurane/oxygen and injected with  $1 \times 10^6$  Py2T cells in 100  $\mu$ L PBS into mammary gland number 9. Tumor volumes were calculated according to the formula  $V = 0.5 * D * d^2$ , where D represents length and d represents width of tumors measured by a digital caliper. Mice were sacrificed by CO<sub>2</sub> and tumors were isolated and further processed.

*Histology and immunostaining*

For immunohistochemistry (IHC) and Hematoxylin & Eosin (H&E) stainings, tumors were fixed at 4°C in 4% phosphate-buffered paraformaldehyde (PFA) for 12 hours and then embedded in paraffin after ethanol/xylene dehydration. H&E staining was performed as previously described (Perl et al., 1998; Wicki et al., 2006). For immunofluorescence analysis of frozen sections, organs were fixed at 4°C in 4% PFA for 2 hours, and cryopreserved for 10 hours in 20% sucrose in PBS prior to embedding in OCT freezing matrix. For IHC stainings of PFA-fixed, paraffin-embedded specimens, antigen epitopes were retrieved by boiling slides in 10mM Na-Citrate buffer (pH6.0) in a PrestigeMedical Z2300 antigen retriever. Stainings with mouse and rabbit antibodies were performed using the Dako EnVision plus Kit (K4065) according to the manufacturer's recommendations. Cytokeratin 8/18 staining was performed using the Vectastain ABC kit (PK-6100 standard, Vector). Stainings were revealed by incubation with biotinylated secondary antibodies and ABC Elite detection kit using AEC substrate (all from Vector Laboratories) according to the manufacturer's instructions and counterstained using hematoxylin. Cryosections were cut 7µm thick and dried for 30' prior to rehydration in PBS. Slides were permeabilized with in PBS/0.2% TritonX-100 and blocked for 30 min in PBS/5% normal goat serum and then incubated with the primary antibody in blocking buffer for 1 hour at room temperature. Immunofluorescence (IF) stainings were revealed by incubation with Alexa488 or Alexa568 labeled secondary antibodies (Molecular Probes) and nuclei were stained with DAPI (SIGMA). IHC stainings were evaluated on an AxioVert microscope (Zeiss, Germany) and IF stainings on a Leica DMI 4000 microscope (Leica Microsystems, Germany).

*Statistical analysis*

Statistical analysis and graphs were generated using the GraphPad Prism software (GraphPad Software Inc, San Diego, CA). All statistical analysis was performed by unpaired, two-sided t-test.

## ***3.2 Critical roles of Tead transcription factors in the EMT process***

### **3.2.1 Abstract**

Activation of cellular programs associated with epithelial-mesenchymal transition (EMT) can empower tumor cells with migratory, invasive and stem cell-like properties, thereby supporting tumor progression and malignancy. These phenotypic changes are driven by broad changes in gene expression, and we therefore sought to identify critical transcription factors (TFs) mediating these changes. To do so, we have chosen a genome-wide approach to search for TF DNA-binding motifs that are overrepresented in promoters of EMT-regulated genes. We have performed time-resolved gene expression profiling of normal murine mammary gland (NMG) cells undergoing EMT in response to TGF $\beta$ -treatment, and have subjected these data to computational motif-activity-response analysis (MARA). This analysis has predicted a prominent role for Tead transcription factors in the upregulation of a large number of genes during the EMT process. Here, show experimental evidence that endogenous Tead transcriptional activity is elevated during EMT. Moreover, Tead family members display an increase in their expression during EMT, and ectopic expression of wild type Tead2, or a constitutive active version of Tead2, leads to an increase in Tead transcriptional activity and is sufficient to induce EMT. Furthermore, we show that Tead2 can control the subcellular localization of Yap and Taz, indicating that during EMT, elevated levels of Tead2 may recruit additional Yap/Taz molecules to the nucleus to achieve increased transcriptional activity. MARA analysis has also provided us with candidate Tead target genes. We here demonstrate that Zyxin, a focal adhesion component and regulator of actin remodeling that has been previously shown to be required for EMT-induced migration, is a direct target gene of Tead2 during EMT.

### 3.2.2 Introduction

Epithelial-mesenchymal transition (EMT) is a cell-biological program that is required at various stages during development. Activation of EMT in epithelial cells induces a loss of cell-cell adhesions and apical-basal polarity and promotes transdifferentiation into a mesenchymal state which is characterized by a migratory and invasive phenotype (Kalluri and Weinberg, 2009; Nieto, 2011). During solid tumor progression, a reactivation of some of these features in epithelial tumor cells (oncogenic EMT) is regarded as one of the mechanisms that facilitate metastatic spread (Thiery et al., 2009; Chaffer and Weinberg, 2011). Oncogenic EMT not only provides tumor cells with invasive properties that permit dissemination from the primary tumor, but also results in the acquisition of stem cell-like traits, which has implications for cancer therapy and may also be important for colonization of distant organs (Polyak and Weinberg, 2009; Chaffer and Weinberg, 2011; Magee et al., 2012; Scheel and Weinberg, 2012). Oncogenic EMT can be driven by the same players that control developmental EMT, and transcription factors are major coordinators of the EMT program (Thiery and Sleeman, 2006; Moreno-Bueno et al., 2008; Acloque et al., 2009; Nieto, 2011). To gain more insight into the transcriptional regulation of EMT, we sought to identify transcription factors that differentially regulate the expression of a wide range of target genes during this process. To do so, we first performed time-resolved gene expression profiling of the EMT process utilizing normal murine mammary gland (NMuMG) cells, which undergo EMT upon TGF $\beta$  treatment, as a model (Maeda et al., 2005). Gene expression profiles of different timepoints of TGF $\beta$ -induced EMT were then analyzed by motif-activity-response-analysis (MARA) (FANTOM Consortium et al., 2009). This computational analysis is based on a collection of ~200 transcription factor (TF) binding motifs, which represent the DNA binding sites of ~340 TFs. The MARA algorithm ranks all of these binding motifs according to their overrepresentation in promoters of genes that are differentially regulated, in this case during EMT. Thereby, the transcription factors corresponding to the motifs at the top of the list are predicted to regulate the highest number of target genes. The MCAT motif, which corresponds to the DNA binding motif of Tead family TFs, ranked among the top of this list. In mammals, four Tead family members (Tead1-4) exist (Jacquemin et al., 1996; Kaneko and DePamphilis, 1998). Teads are ubiquitously expressed and have partially redundant roles in regulating the development of various tissues such as neural crest, notochord and trophoectoderm (Milewski et al., 2004; Sawada et al., 2005; Yagi et al., 2007; Sawada et al.,

2008). In the adult, Teads have mainly been implicated in muscle-specific gene expression (Chen et al., 1994; Stewart et al., 1994; Gupta et al., 1997; Butler and Ordahl, 1999; Ueyama et al., 2000; Milewski et al., 2004; Zhao et al., 2006; Benhaddou et al., 2012). Transcriptional activity of Teads is mediated by direct binding of the transcriptional co-activators Yap or Taz (Vassilev et al., 2001; Mahoney et al., 2005), which controls proliferation in epithelial cells and fibroblasts (Ota and Sasaki, 2008; Zhao et al., 2008b; Zhang et al., 2009a). Yap and Taz nuclear localization and Tead activation is inhibited by the Hippo tumor suppressor signaling pathway: when Hippo signaling is activated by high cell density, the Hippo core component Lats phosphorylates Yap/Taz, thereby creating a binding site for 14-3-3 proteins that act to sequester Yap/Taz in the cytoplasm. As a result, target gene expression is discontinued and the result is growth arrest (Pan, 2010; Zhao et al., 2010; 2011b). Interestingly, recent studies have shown binding of Yap/Taz to intact adherens junctions (Kim et al., 2011; Schlegelmilch et al., 2011; Silvis et al., 2011), tight junctions (Wang et al., 2011a; Zhao et al., 2011a) and polarity complexes (Varelas et al., 2010) in densely grown epithelial cells, which can contribute to cytoplasmic retention and inhibition of Tead activity. Several recent studies also established that Yap/Taz nuclear localization and Tead activity is positively regulated by cell spreading and the presence of stress fibers, however whether this is dependent on Hippo signaling is currently debated (Dupont et al., 2011; Fernández et al., 2011; Sansores-Garcia et al., 2011; Wada et al., 2011; Zhao et al., 2012). Interestingly, Yap/Taz overexpression was shown to be sufficient to induce EMT of MCF10A cells in a Tead-dependent manner (Lei et al., 2008; Zhao et al., 2008b; Zhang et al., 2009a). Moreover, a recent report established that Yap/Taz nuclear accumulation in Eph4 cells treated with TGF $\beta$  is required for these cells to undergo EMT (Varelas et al., 2010). Even though these studies clearly suggest a crucial role of Teads in mediating EMT induction, the mechanisms involved remain elusive. Thus, on the basis of our bioinformatics analysis that proposed an increase in Tead transcriptional activity during EMT of NMuMG cells, we chose to investigate the role of Tead transcription factors in the EMT process.

Here, we make use of several cellular model systems of EMT, and experimentally demonstrate that endogenous Tead activity is increased upon EMT in these systems. Moreover, we find that the expression levels of several Tead family members concomitantly increase with their transcriptional activity. In particular, Tead2 is upregulated during EMT in all three model systems investigated, and we show that ectopic expression of wild type Tead2



or of a constitutively active form (Tead2-VP16) is sufficient to induce EMT, while knockdown of Teads or overexpression of a dominant-negative form of Tead2 attenuates EMT. We further provide evidence that Tead2 can regulate Yap/Taz nuclear localization. Conversely, we show that Tead2 is exported from the nucleus in densely grown cells along with Yap/Taz. Finally, we identify Zyxin, a component of focal adhesions and an actin cytoskeleton remodeling protein which has previously been implicated in EMT (Mori et al., 2009; Sperry et al., 2010), as a novel downstream target gene of Tead2.

### 3.2.3 Results

#### 3.2.3.1 Increase of Tead transcriptional activity during EMT

To identify key transcription factors (TFs) that mediate the vast changes in gene expression during EMT, we screened for TFs that change their activity during EMT. To do so, we initially chose to employ the widely used normal murine mammary gland (NMuMG) cell line, which gradually undergoes EMT when stimulated with TGF $\beta$ , as a model system (Maeda et al., 2005). We performed gene expression profiling of five different time points during the transition from epithelial to mesenchymal cells and subjected the resulting data to Motif Activity Response Analysis (MARA); (Pachkov et al., 2007; FANTOM Consortium et al., 2009). MARA contains a collection of ~200 regulatory motifs representing the DNA binding sites of ~350 TFs, which are mapped to genome-wide, CAGE-defined promoters of genes (Balwierz et al., 2009). Briefly, the algorithm predicts changes in transcription factor activity by analyzing the presence of regulatory motifs in promoters of genes that are differentially regulated across different samples, in our case different time points of EMT. One of the top scoring regulatory motifs that was overrepresented in differentially expressed genes during EMT was the MCAT motif, corresponding to the DNA binding site of Tead transcription factors (Figure 1A).

MARA analysis revealed an increase in activity of this motif during EMT; in other words, the genes containing such a motif in their promoters were upregulated during EMT. Figure 1B shows the mean expression changes of these genes. To experimentally validate these findings, we constructed a luciferase reporter construct bearing 8 repeats of the MCAT core motif (CATTCCT), flanked by additional sequences that allow activation of expression in non-muscle cells (Figure 1C); (Larkin et al., 1996). To determine background luciferase activity, we used the same construct lacking MCAT and flanking sequences. We determined Tead activity during EMT in two different cellular model systems of EMT in addition to NMuMG cells (Figure 1D, *bottom panels*). Py2T cells are described in this thesis and undergo EMT upon TGF $\beta$  stimulation. The mammary tumor (MT) system consists of epithelial cells (MTflEcad) derived from an MMTV-Neu breast cancer mouse model (Muller et al., 1988), in which the E-cadherin gene is flanked by Lox-P sites (Derksen et al., 2006). The mesenchymal MT $\Delta$ Ecad cells in this system were derived from MTflEcad cells by cre-recombinase mediated deletion of the E-cadherin gene (Lehembre et al., 2008). Measurement of luciferase

activities revealed a gradual increase in Tead reporter activity during EMT of NMuMG and Py2T cells, and a marked increase in activity in mesenchymal MTΔEcad cells compared to epithelial MTfEcad cells (Figure 1D, *top panels*). Notably, MARA prediction from gene expression profiles of the MT system also showed higher Tead activity in MTΔEcad cells compared to epithelial MTfEcad cells (data not shown). We confirmed these findings using a previously described Tead reporter (Supplementary figure S1) (Ota and Sasaki, 2008). Therefore, the experimental data provided here suggests that Tead activity is increased during EMT and is high in mesenchymal cells, corroborating the findings obtained from *in silico* MARA analysis.

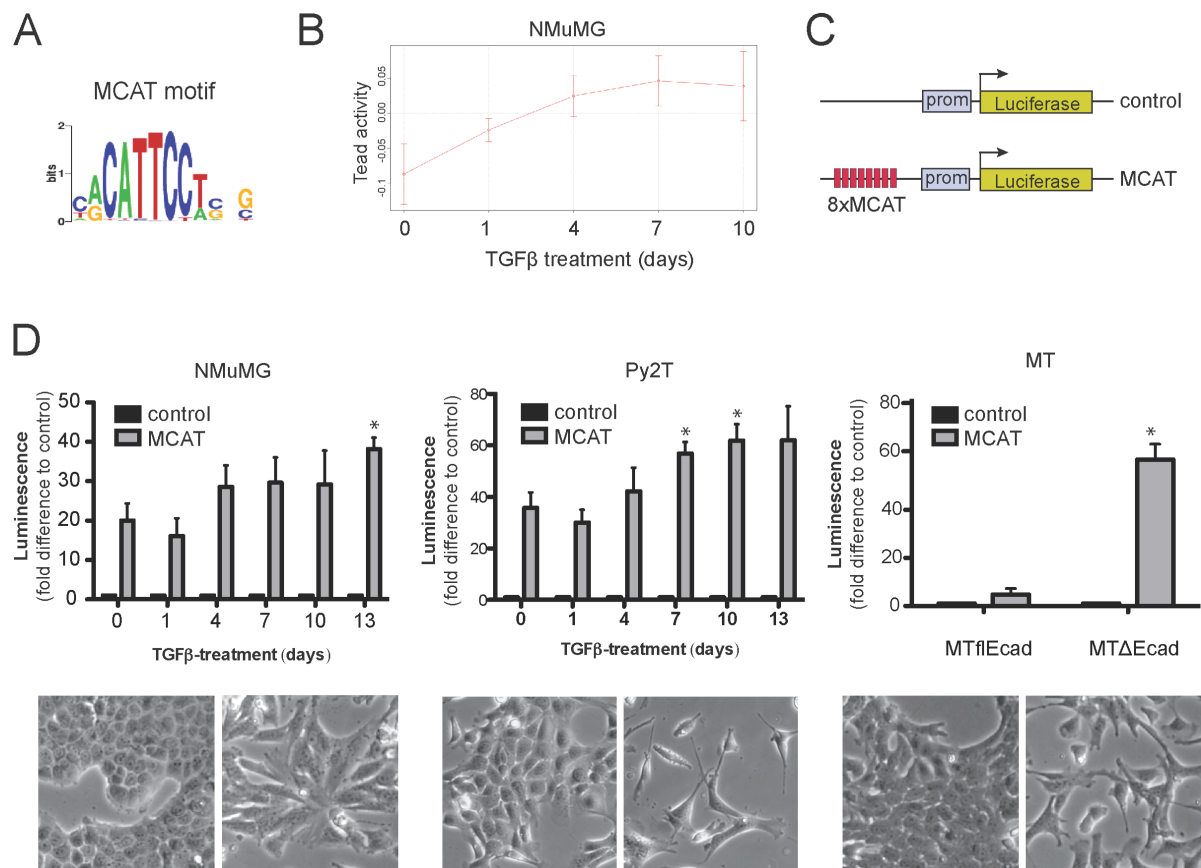


**Figure 1. Tead transcriptional activity increases during EMT.**

(A) Position weight matrix used for motif activity response analysis (MARA), representing the Tead DNA binding motif. (B) MARA analysis of Tead activity during TGFβ-induced EMT of NMuMG cells. NMuMG cells were induced to undergo EMT by TGFβ treatment and RNA was harvested at the timepoints indicated. Gene expression profiling of each timepoint was performed using affymetrix microarrays and data was subjected to MARA analysis. The curve shows averaged expression changes of all mRNAs containing a species-conserved MCAT motif in their promoters. Data shown is from three independent experiments. (C) Scheme of the luciferase reporter constructs engineered to measure Tead activity in cells. Eight repeats of the core MCAT Tead DNA binding motif (CATTCCT) including flanking sequences were cloned in front of a basal promoter followed by the firefly luciferase gene (MCAT reporter). A construct not containing the 8xMCAT sequences was used as a control.

**(D)** Measurement of Tead activity in three cellular EMT systems. Normal murine mammary gland (NMuMG) and Py2T cells undergo EMT in response to TGF $\beta$  treatment. Stably mesenchymal MT $\Delta$ Ecad cells were derived from epithelial Mtf1Ecad by Cre-recombinase mediated knockout of the E-cadherin gene. NMuMG and Py2T cells were treated with TGF $\beta$  for the indicated times prior to simultaneous lysis and luminescence analysis. Reporter constructs were transfected one day before lysis, along with a Renilla luciferase construct for normalization. *Top panels:* Tead-reporter activity in the NmuMG (n=3), Py2T (n=5) and MT (n=2) EMT systems. *Bottom panels:* Bright-field images illustrating the morphological differences of cells at the endpoints of these experiments. Experiments were repeated n times and results are shown as mean  $\pm$  S.E.M, \*p-value < 0.05; \*\*p-value < 0.01.

### 3.2.3.2 *Tead2 expression levels are upregulated during EMT*

The Tead family of transcription factors consists of the four members Tead1-4 in mammalian cells (Kaneko and DePamphilis, 1998). To determine which of these factors are expressed and whether they are regulated during EMT, we first measured mRNA levels of all four Tead family members (Figure 2A). Transcripts of all four members could be detected by quantitative RT-PCR. Interestingly, Tead2 mRNA levels were found to be upregulated consistently in all three EMT systems analyzed. We therefore chose to focus our attention on this member of the family, even though we do not exclude a possible role of the other three family members in the EMT process. Consequently, we generated a polyclonal antibody against Tead2 by immunizing rabbits with an N-terminal peptide of murine Tead2 that is conserved in humans. We confirmed that the antibody specifically detects Tead2 and not other family members by immunoblotting (Figure S2). Analysis of endogenous Tead2 expression levels in all three EMT systems by immunoblotting revealed that Tead2 protein levels gradually increase during EMT and closely follow the mRNA expression profile over time (Figure 2B). In addition, we were able to determine exclusively nuclear subcellular localization in these systems by performing immunofluorescent staining using the same antibody (Figure 2C). Collectively, these results demonstrate that Tead2 is the only Tead family member whose expression is consistently upregulated during EMT in the systems tested here, and that its nuclear localization is unchanged during EMT.

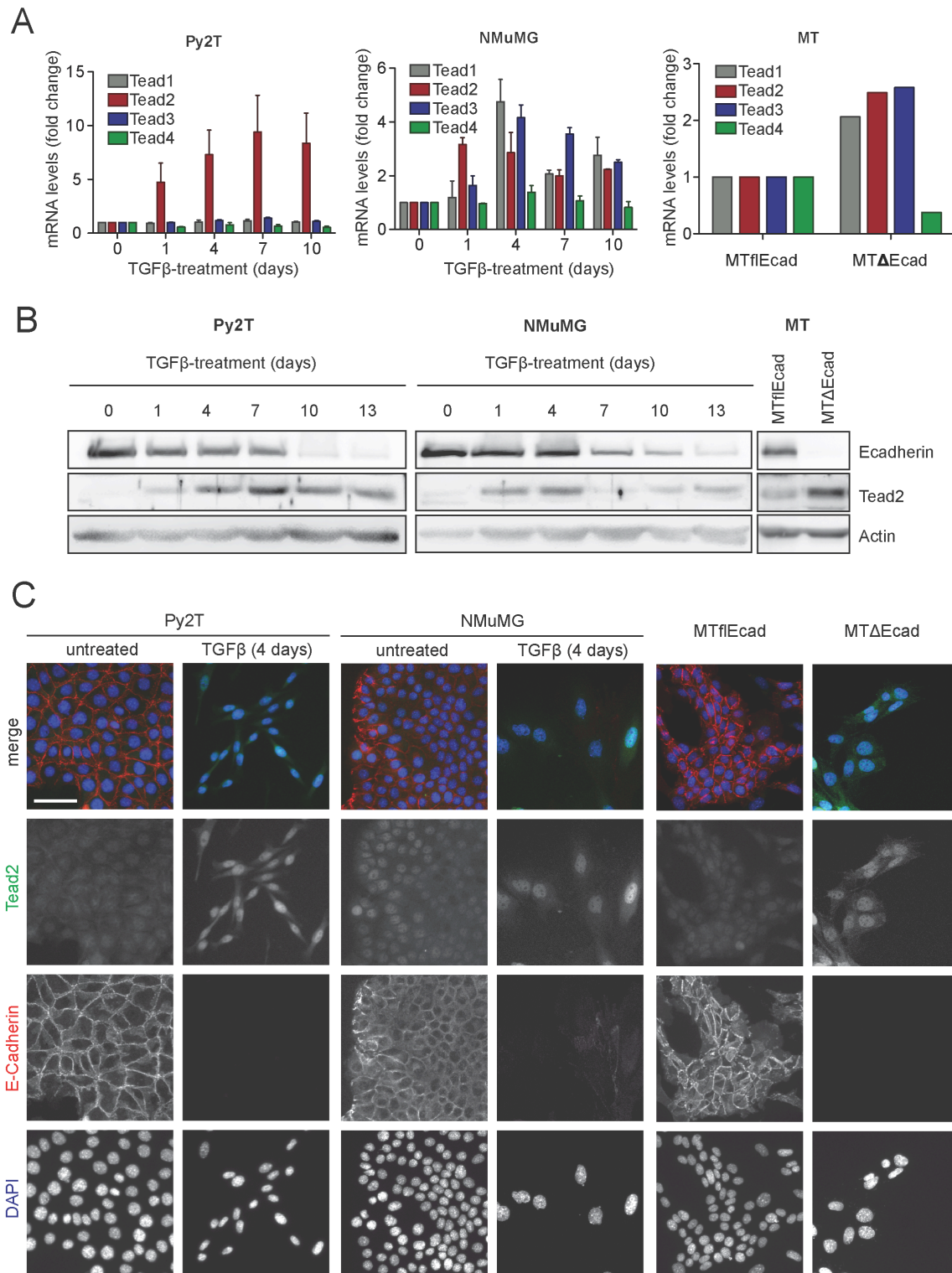


**Figure 2. Tead2 expression levels are increased during EMT.**

(A) Measurement of mRNA expression levels of Tead1-4 during EMT. Time-course experiments of TGF $\beta$  induced EMT were performed as described in Figure 1D and RNA was extracted at the indicated timepoints. Samples were analyzed by quantitative RT-PCR with primers specific for the individual Tead family members. Results are presented as mean fold difference  $\pm$  S.E.M of three independent experiments (Py2T and NMuMG). Expression changes in MT cells were determined once.

(B) Western blot analysis of Tead2 levels during EMT.

(C) Immunofluorescent staining for Tead2 showing subcellular localization. Cells were treated with TGF $\beta$  as indicated and stained with antibodies against Tead2 and E-cadherin as a control. Scale bar, 50  $\mu$ M.

### 3.2.3.3 Increase of Tead2 activity is sufficient to induce EMT

After having determined that Tead transcriptional activity and Tead2 expression levels increase during the EMT process, we next asked whether experimentally increasing Tead2 levels and/or Tead transcriptional activity could be sufficient to induce EMT. Notably, forced overexpression of the Tead co-factors Yap and Taz has been demonstrated to be sufficient to induce EMT in MCF10A cells (Overholtzer et al., 2006; Lei et al., 2008), which has later been shown to be dependent on Teads (Zhao et al., 2008b; Zhang et al., 2009a). Here we retrovirally transduced Py2T cells with either wild type, full-length Tead2 or with an activated version consisting of the TEA DNA-binding domain of Tead2, fused to the transcriptional activation domain of the herpes simplex virus protein VP16 (Figure 3A); (Ota and Sasaki, 2008). We next measured Tead activity in the resulting stable cell lines by a luciferase reporter assay, and observed increased transcriptional activity in cells stably expressing Tead2 FL, and an even greater increase in cells transduced with the activated version of Tead2 (Figure 3B). Activation of Tead activity resulted in morphological changes consistent with EMT (Figure 3C, *left*). Cells transduced with Tead2 FL appeared elongated, mostly lost cell-cell contact and formed filopodia. These effects were even more pronounced in cells expressing the fully activated version of Tead2 (Tead2-VP16). Cells overexpressing either version of Tead2 had lost intact adherens- and tight-junctions as revealed by immunofluorescence staining for E-cadherin and ZO-1, respectively. Furthermore, these cells expressed the mesenchymal marker vimentin, whose expression was absent in the epithelial control cells, and displayed remodeling of the actin cytoskeleton to stress fibers, whereas control cells showed cortical actin arrangement (Figure 3C). We additionally analyzed expression levels of EMT markers by immunoblotting (Figure 3D). Tead2 FL expressing cells displayed reduced levels of the epithelial marker E-cadherin and increased levels of the mesenchymal markers N-cadherin and Fibronectin. Expression of constitutively active Tead2-VP16 resulted in an even more pronounced downregulation of E-cadherin, however these cells failed to upregulate N-cadherin and Fibronectin, indicating that this artificial construct does not completely recapitulate the effects of the wild type version. Collectively, these results demonstrate that overexpression of Tead2 and a concomitant increase in Tead transcriptional activity in the absence of TGF $\beta$  stimulation is sufficient to induce EMT in Py2T breast cancer cells.

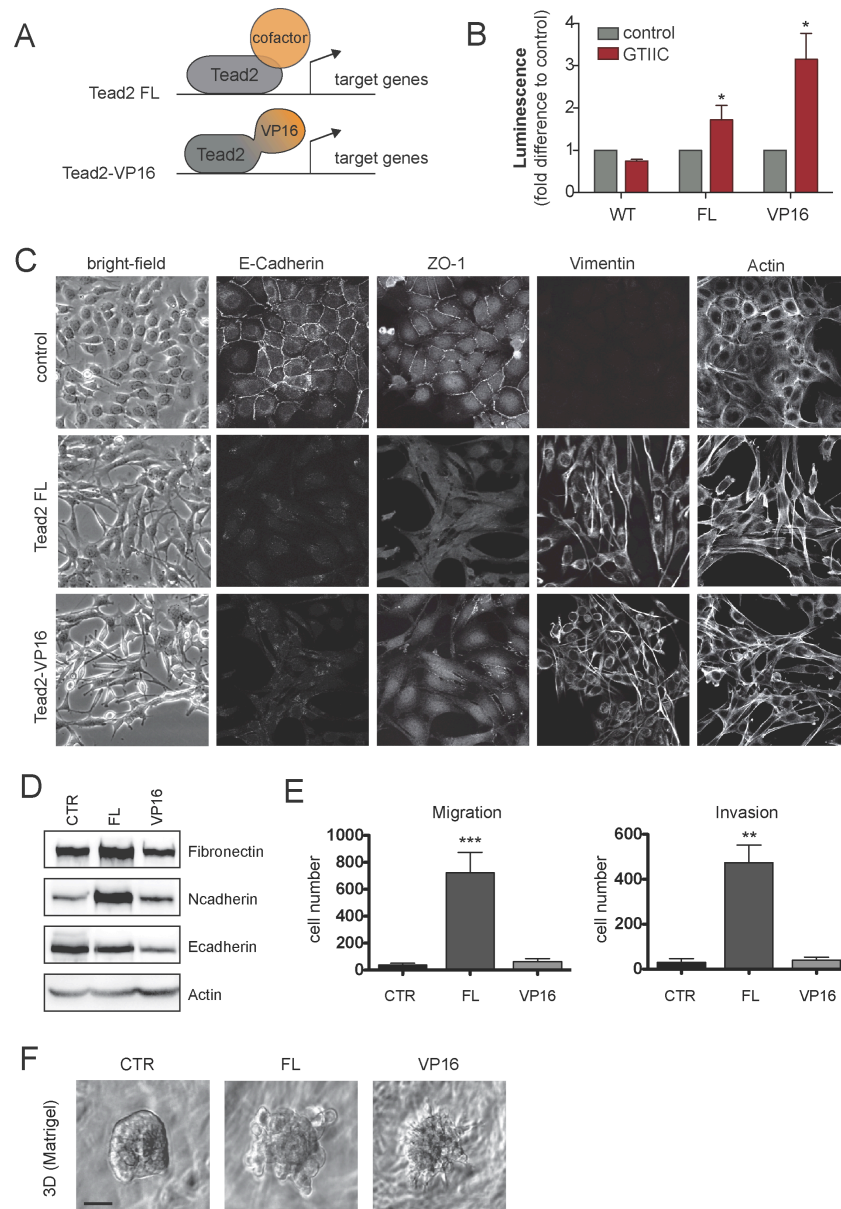


**Figure 3. Tead2 gain-of-function is sufficient to induce EMT.**

(A) Schematic representation of constructs used. Retroviral expression constructs were engineered coding for either full length Tead2 (FL) or a fusion protein consisting of the Tead2 DNA-binding domain fused to the VP16 transcriptional activation domain.

(B) Tead transcriptional activity in Py2T cells stably expressing Tead2 FL and Tead2-VP16. Cells were transfected with the indicated luciferase reporter constructs and luminescence was analyzed one day after transfection. Results from two independent experiments are represented as mean  $\pm$  SEM (\*p-value < 0.05).

(C) Morphological analysis for hallmarks of EMT. *Left*: Bright-field images showing changes in cell shape. Immunofluorescence analysis was performed using antibodies against the major adherens junction component E-cadherin, the tight-junction marker ZO-1 and the mesenchymal intermediate filament vimentin. Actin cytoskeleton was stained by phalloidin coupled to a fluorophore.

(D) Immunoblot analysis for EMT marker expression changes in the indicated cell lines. Membranes were probed with the epithelial marker E-cadherin and the mesenchymal markers N-cadherin and fibronectin.

(E) Modified Boyden chamber assay to determine chemotactic migration and invasion. 25'000 cells were seeded in starving medium (0.2% FBS) into porous cell culture inserts uncoated (migration) or coated with matrigel (invasion). Growth medium containing 20% FBS was filled in the bottom of wells as an attractant. Cells were allowed to pass through pores for 24 hours and were then fixed and cells at the bottom of inserts were counted. Data is shown as mean  $\pm$  S.E.M of three independent experiments (\*\*p-value < 0.01; \*\*\*p-value < 0.001).

(F) Three-dimensional culture in extracellular matrix (matrigel). Cells were embedded in matrigel and allowed to grow for 5 days. Scale bar, 50  $\mu$ M.



Another hallmark of cells that have undergone EMT is the acquisition of migratory and invasive properties (Yilmaz and Christofori, 2009; Nieto, 2011). We therefore performed modified Boyden chamber migration and invasion assays to test this notion. Py2T Tead2 FL cells exhibited a dramatic increase in migratory and invasive potential in these assays, while Py2T Tead2-VP16 cells did not (Figure 3E). When grown in a 3-dimensional environment consisting of extracellular matrix, Tead2 overexpressing cells invaded the surrounding matrix in contrast to control cells, which formed spheres. Tead2-VP16 expressing cells were able to project filopodia into the extracellular matrix indicative for increased invasiveness (Figure 3F). The differences in phenotypes between wild type Tead2 and Tead2-VP16 overexpressing cells could be due to the inability of Tead2-VP16 to form complexes with the appropriate co-factors and therefore activating sets of genes that slightly differ from physiologically relevant Tead2 target genes. An additional explanation could be that the constitutively activated Tead2-VP16 is not amenable to negative feedback, therefore not providing finely balanced expression of target genes, which might be crucial for a dynamic process like migration. Reinforcing this notion, we also observed differences in dynamic behavior of Tead2 FL and Tead2-VP16 overexpressing cells cultured on plastic. Tead2 FL overexpressing cells exhibited dynamic extension and retraction of filopodia and migrated on plastic, while Tead2-VP16 cells extended protrusions into various directions but were unable to move directionally (see Supplementary movies 1, 2 and 3). Together, these results indicate that a gain in Tead activity results in an activation of migratory and invasive machinery, consistent with EMT.

To get insight into the cellular programs activated by Tead2 and their possible relevance for biological processes in general, we performed gene expression profiling of Py2T Tead2 FL, Py2T-VP16 and control cells. We determined differentially expressed genes and subjected these gene lists to biological function and pathway enrichment analysis using Ingenuity pathway analysis software (IPA, Ingenuity systems, [www.ingenuity.com](http://www.ingenuity.com)); (Figure S3A). These analyses suggested that Tead activation affects genes involved in cellular movement and cell morphology, and that these genes contribute to biological processes such as tissue development, organ development, cancer and embryonic development. The data obtained is consistent with the observed role of Tead in EMT and with the role of Tead transcription factors as downstream effectors of the Hippo tumor suppressor pathway that controls organ size, tissue regeneration, stemness and self-renewal (Halder and Johnson, 2011; Zhao et al., 2011b). We also extended the IPA bioinformatics analysis to predict which



cellular signaling pathways might be most affected by the differentially regulated genes upon Tead2 activation in Py2T cells. Within the collection of pathways available in IPA, differentially expressed genes were largely overrepresented in pathways related to fibrosis, endocytosis and guidance of neuronal cells (Figure S3B).

3.2.3.4 Loss of Tead function attenuates EMT and inhibits migration and invasion

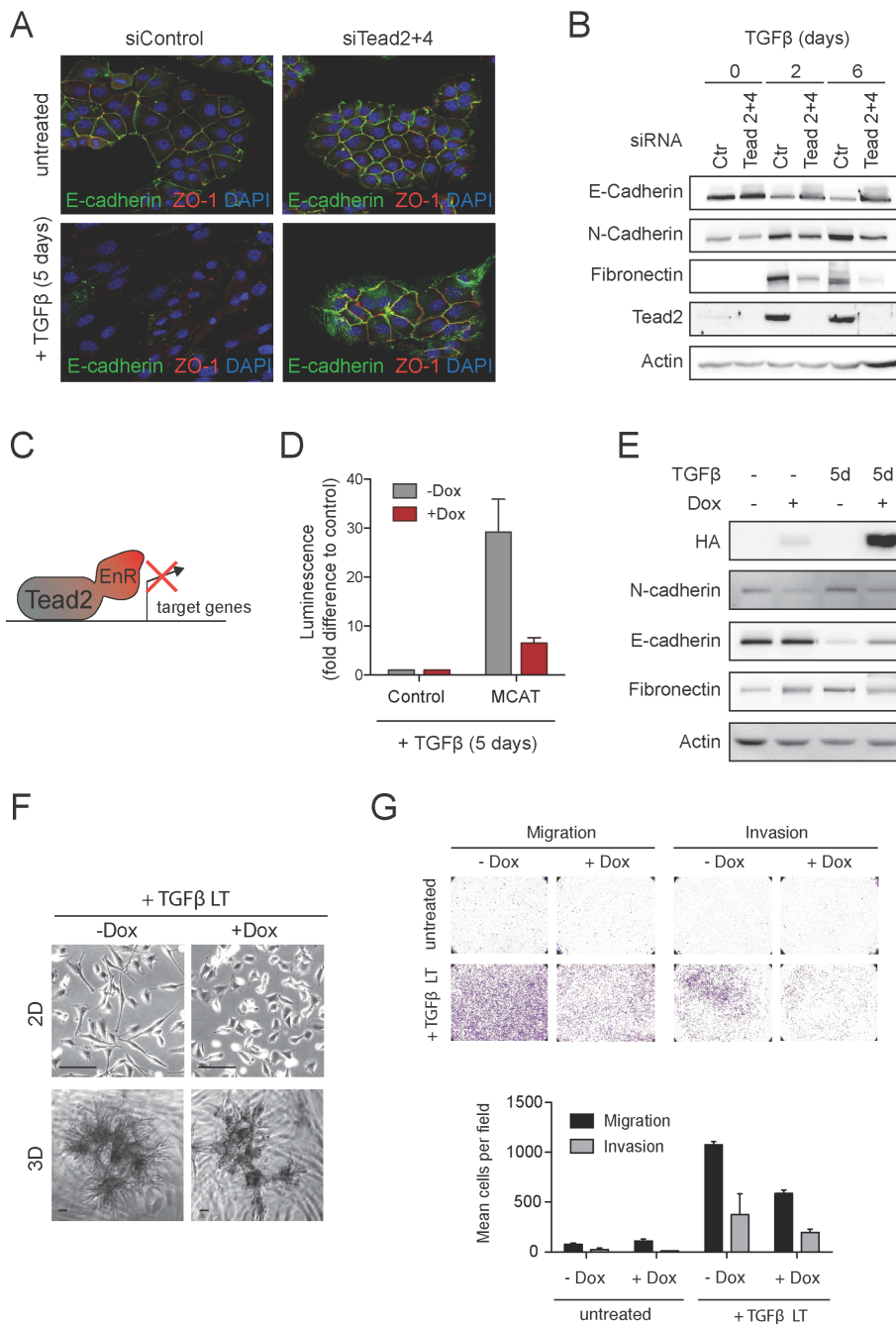


**Figure 4. Loss of Tead function attenuates EMT.**

(A) Effect of Tead knockdown on disassembly of adherens- and tight-junctions. NMuMG cells were transfected with siRNAs against Tead2 and Tead4. One day after transfection, cells were stimulated to undergo EMT by TGF $\beta$  treatment for 5 days. Cells were re-transfected every second day with the same siRNAs during TGF $\beta$  treatment. Images show immunofluorescence staining for the adherens junction marker E-cadherin and the tight-junction marker ZO-1.

(B) Western blot analysis to investigate the effect of Tead knockdown on EMT marker expression. The experiment was performed as described in (A), with different timepoints.

(C) Scheme of the dominant-negative construct used to block Tead activity. The Tead2 DNA-binding domain is fused to the transcriptional repression domain of *Drosophila* Engrailed (Tead2-EnR). A stable pool of Py2T cells expressing HA-tagged Tead2-EnR in a doxycycline-inducible fashion (Py2T-iTead2-EnR) was generated by lentiviral transduction.

(D) Analysis of Tead activity in parallel to the experiment described in (D). Cells were transfected one day before lysis with either control or MCAT Tead reporter along with a Renilla luciferase construct for normalization. Results are presented as mean  $\pm$  S.E.M. from two independent experiments.

(E) Effect of dominant-negative Tead2 on TGF $\beta$ -induced EMT of Py2T cells. Cells were pre-treated with doxycycline for 3 days to allow expression of dominant-negative Tead2, and were then treated or not with TGF $\beta$  for 5 days. Expression of HA-Tead2-EnR, E-cadherin, N-cadherin and fibronectin was determined by immunoblotting.

(F) Effect of Tead activity downregulation on morphology and invasiveness of mesenchymal cells. Mesenchymal Py2T-iTead2-EnR cells were generated by long-term (LT) treatment with TGF $\beta$  for 20 days. Bright-field images show the morphology of cells grown in standard cell culture dishes (2D), and in matrigel (3D) after 6 days of growth. Doxycycline treatment was done for 3 days (2D) or for the whole growth period of 6 days (3D). Scale bars, 50 $\mu$ M.

(G) Effect of Tead activity downregulation on migratory and invasive capabilities. Migration and invasion assays were performed as described in Figure 3E. Untreated and long-term TGF $\beta$ -treated Py2T-iTead2-EnR cells were pre-treated or not with doxycycline for 3 days, trypsinized, seeded into chambers and allowed to pass through pores for 24 hours. *Top*: Crystal violet staining of migrated/invaded cells. *Bottom*: quantification. Results are presented as mean  $\pm$  SD of biological duplicates.

To assess whether Teads are required for EMT, we first silenced Tead family members by siRNA in NMuMG cells and then induced EMT by TGF $\beta$  treatment. Knockdown of single Tead family members had no effect on EMT (data not shown), possibly because of functional compensation between family members, which has been observed previously (Zhang et al., 2009a). However, when cells undergoing EMT were treated with siRNA against Tead2 combined with siRNA against one other family member, in particular Tead4, we observed a striking stabilization of adherens and tight junctions in comparison to control cells, which completely lost these structures after 5 days of TGF $\beta$  treatment (Figure 4A). Indeed, in contrast to cells treated with control siRNA, which showed a marked downregulation of E-cadherin and upregulation of the mesenchymal markers N-cadherin and Fibronectin as expected, cells that were depleted of Tead2 and Tead4 showed much weaker changes in expression of these markers as determined by western blot (Figure 4B). These results suggested that in NMuMG cells, expression of Tead2 and Tead4 is required for EMT.

To confirm these results in a different cellular system, we assessed the requirement of Tead activity for EMT in Py2T cells. Knockdown of single Tead family members again did not have any effect on TGF $\beta$ -induced EMT in these cells (data not shown). As the knockdown efficiency was poor when we treated these cells with siRNA against more than one family member, we engineered Py2T cells that express a dominant-negative version of Tead2 (Figure 4C); (Ota and Sasaki, 2008) in a doxycycline-inducible manner (Py2T-iTead2-EnR).

Expression of this construct effectively suppressed Tead activity in cells treated with TGF $\beta$  (Figure 4D). Py2T cells undergoing EMT downregulated E-cadherin and upregulated the mesenchymal markers N-cadherin and Fibronectin as expected, however these changes were markedly attenuated in cells treated with doxycycline to express dominant-negative Tead2 (Figure 4E). However, a complete block of EMT was not observed as cells induced with doxycycline still lost most of their cell-cell contacts and scattered. Nevertheless, these results suggest that Tead transcriptional activity is also contributing to proper EMT in Py2T cells.

We next assessed whether Tead activity is required for migration and invasion in mesenchymal cells that had undergone full EMT. We therefore first generated mesenchymal Py2T-iTead2-EnR cells by long-term (LT) culture in TGF $\beta$ -containing medium for at least 20 days in the absence of doxycycline. Induction of Tead2-EnR in the derived mesenchymal cells resulted in rounder cell shapes with reduced filopodia formation as compared to cells that did not express the dominant-negative Tead construct (Figure 4F). When embedded in extracellular matrix, control cells formed highly invasive structures, in contrast to cells expressing Tead2-EnR which rather formed clumps and displayed less protrusions (Figure 4F). In Boyden chamber assays, migration and invasion of mesenchymal control cells was highly induced compared to cells not treated with TGF $\beta$  as expected. Expression of dominant-negative Tead2 drastically decreased the ability of mesenchymal cells to migrate and invade towards a chemotactic gradient (Figure 4G). From these experiments we concluded that Tead2 activity and therefore Tead2 target genes are an important determinant of mesenchymal migration and invasion. These findings are in line with the increased migration observed in Tead2 overexpressing cells, and the IPA bioinformatics analyses (Figure S3A) that suggested a role of Tead2 in cellular movement.

### *3.2.3.5 Tead2 is sufficient and required for Yap/Taz nuclear localization*

It has been well established that Yap and Taz directly bind to Tead transcription factors (Vassilev et al., 2001; Mahoney et al., 2005; Zhao et al., 2010). It has also been demonstrated that Taz mutants defective for interaction with Tead proteins fail to accumulate in the nucleus (Chan et al., 2009). Since Tead2 was upregulated in all our EMT systems, we hypothesized that increased levels of Tead2 in the nucleus may enhance Yap/Taz nuclear localization, which could explain the observed increase in Tead transcriptional activity during EMT (Figure 1). We first investigated whether overexpression of Tead2 results in Yap/Taz

recruitment to the nucleus. We therefore made use of a pool of Py2T cells that expresses wild type Tead2 in a doxycycline inducible fashion. Treatment with doxycycline for three days led to heterogeneous induction of Tead2 expression in these cells, as observed by immunofluorescence staining of Tead2 (Figure 5A).

We additionally co-stained Yap and Taz with an antibody that recognizes both of these highly similar proteins. Control cells expressing low endogenous levels of Tead2 showed Yap/Taz staining in the nucleus, as expected in proliferating cells, as well as prominent cytoplasmic staining consistent with Yap/Taz cytoplasmic sequestration by intercellular junctions and polarity complexes in polarized epithelial cells (Boggiano and Fehon, 2012). In cells that were induced to overexpress Tead2 by doxycycline for three days, we observed that already a moderate increase in Tead2 levels relative to endogenous levels resulted in depletion of Yap/Taz from the cytosol, indicating that both proteins may have relocated to the nucleus in response to elevated levels of Tead2. Notably, we observed that already 3 days after addition of doxycycline addition, cells that overexpressed Tead2 started to lose E-cadherin expression as revealed by triple staining with an antibody against E-cadherin, consistent with the EMT inducing capability established earlier.

To further investigate the possibility that Tead2 recruits Yap/Taz to the nucleus as an underlying mechanism of EMT induction, we also stained for these proteins in Py2T cells stably overexpressing Tead2 FL and Tead2-VP16. We could confirm the depletion of cytosolic Yap/Taz in cells stably overexpressing Tead2 FL. Interestingly, in cells overexpressing the Tead2-VP16 fusion protein that contains only the Tead2 DNA-binding domain but not the Yap binding domain, Yap/Taz localization was exclusively cytoplasmic. We propose that overexpression of Tead2-VP16, which is unable to bind Yap or Taz, competes with endogenous Tead2 for DNA binding. Therefore, wild type Tead2 binding to DNA and at the same to Yap/Taz seems to be necessary for Yap and Taz nuclear localization.

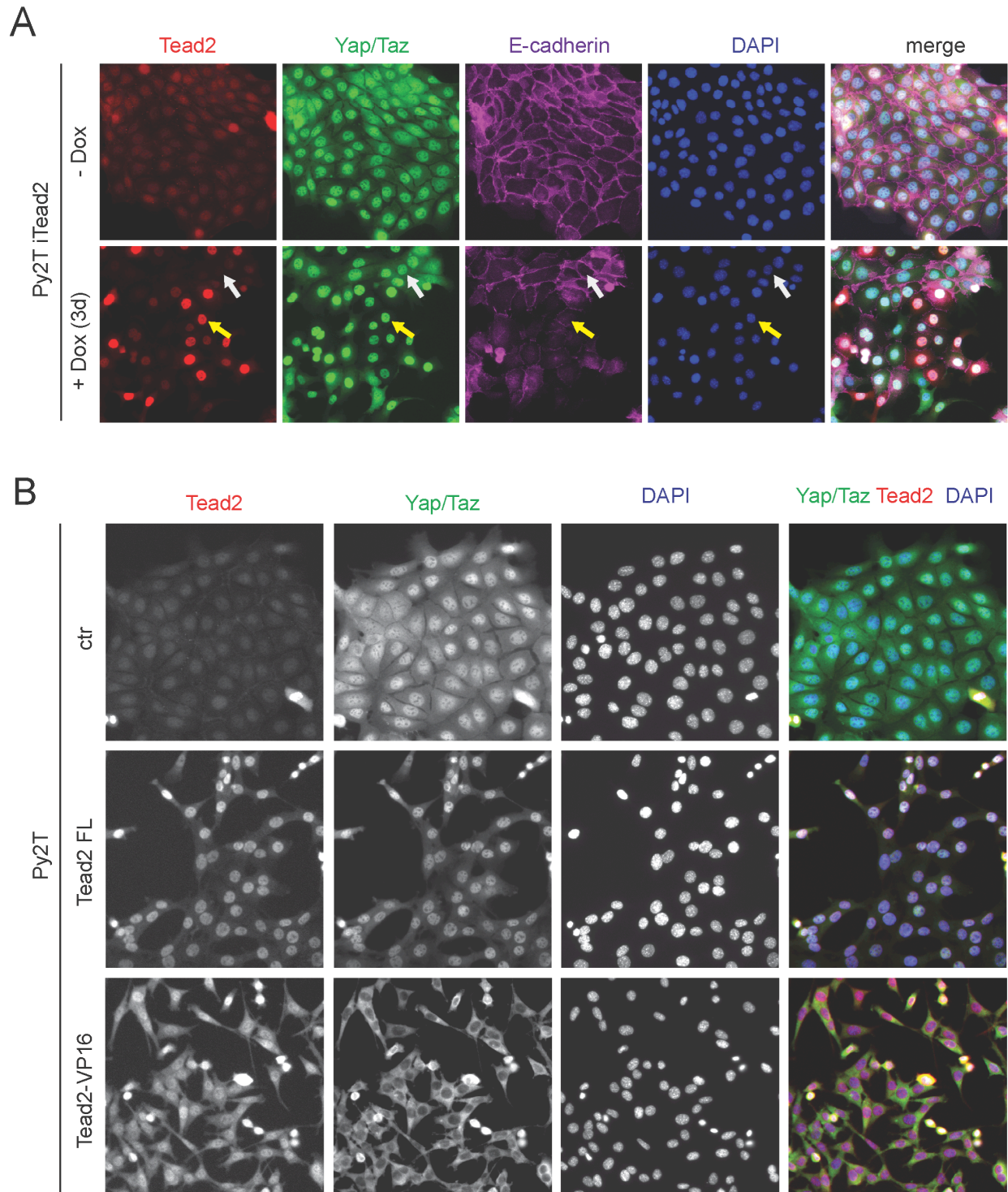


**Figure 5. Tead2 regulates nuclear/cytoplasmic localization of its co-factors Yap and Taz.**

(A) Forced expression of Tead2 in epithelial cells results in redistribution of Yap/Taz and reduced E-cadherin staining. A stable pool of Py2T cells expressing Tead2 in a doxycycline-inducible fashion (Py2T-iTead2) was generated by lentiviral transduction. Cells induced to express Tead2 or not were co-stained with an antibody against Tead2, an antibody recognizing both Yap and Taz, and an antibody directed against E-cadherin. Yellow and white arrows denote Tead2-overexpressing cells and cells with endogenous Tead2 levels, respectively.

(B) Full length Tead2 is required for redistribution and nuclear localization of Yap/Taz. Images show immunofluorescent stainings of Tead2 and Yap/Taz cellular localization in Py2T cells stably expressing full length Tead2 (Tead2 FL) or the Tead2-VP16 fusion protein consisting of the Tead2 DNA binding domain fused to the VP16 transcriptional activation domain.



To confirm this notion in the setting of EMT, during which Tead2 expression is upregulated (Figure 1 and 2), we assessed Yap/Taz localization in NMuMG and Py2T cells undergoing EMT and in the epithelial and mesenchymal counterparts of the MT system. These stainings showed that Yap/Taz was similarly distributed in all three epithelial cell types, with prominent nuclear and cytoplasmic staining (Figure 6A).

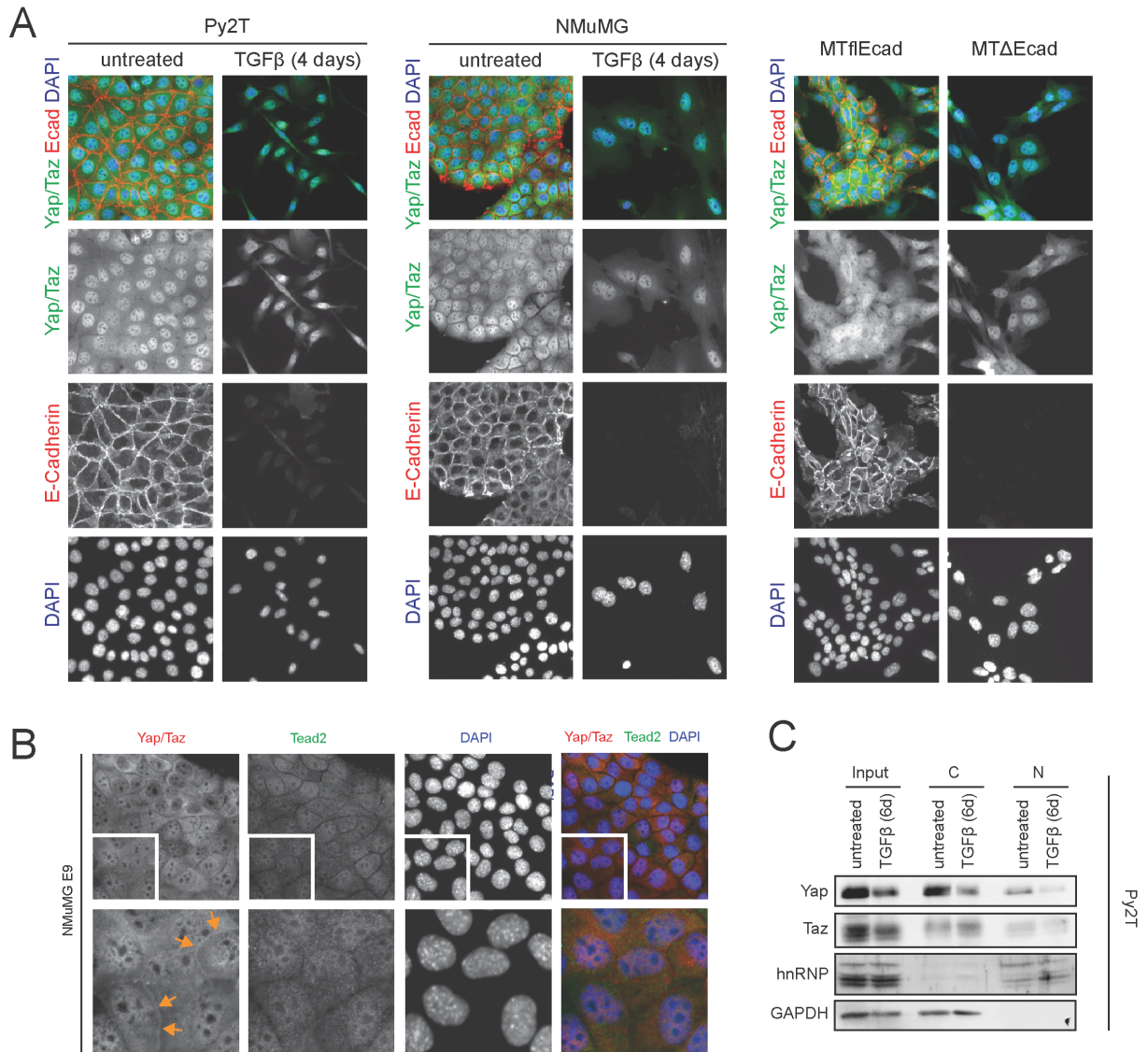


**Figure 6. Yap/Taz intracellular localization during EMT.**

(A) Immunofluorescent staining for Yap/Taz before, during or after EMT.

(B) Larger magnification showing membrane staining of Yap/Taz (marked by orange arrows).

(C) Nuclear/cytoplasmic fractionation to determine Yap/Taz compartmental localization during EMT. Py2T cells were treated or not with TGFβ for 6 days to induce EMT and nuclear/cytoplasmic protein fractions were separated and analyzed for the presence of Yap and Taz by immunoblot. (C=cytoplasmic fraction; N=nuclear fraction). Antibodies against heterogeneous nuclear ribonucleoproteins (hnRNP) and against GAPDH were used to control for purity of nuclear and cytoplasmic fractions, respectively.

A faint membrane staining could also be observed (Figure 6B), consistent with recent reports demonstrating Yap/Taz binding to adherens, tight junction and polarity complexes (Remue et al., 2010; Varelas et al., 2010; Kim et al., 2011; Robinson and Moberg, 2011; Schlegelmilch et al., 2011; Silvis et al., 2011). In cells undergoing EMT or in mesenchymal cells, Yap/Taz staining seemed to be more nuclear than cytoplasmic (Figure 6A). However, immunofluorescence imaging might be misleading because of the dramatic changes in cell shape during EMT. We therefore performed subcellular fractionation and analyzed Yap and Taz protein levels in nuclear and cytoplasmic fractions by immunoblotting. This analysis suggested that there is no collective shift of Yap/Taz proteins from the cytoplasm to the nucleus during EMT (Figure 6C). We suspect that only a fraction of Yap/Taz recruited to increased endogenous Tead2 during EMT is sufficient for activation. Co-immunoprecipitation of Tead2 and Yap to determine the amount of complex formation before, during and after EMT could resolve this open question.

### 3.2.3.6 *Tead2 localization is regulated by cell density*

It has been well established that Yap/Taz nuclear export is controlled by cell density, thereby leading to contact inhibition of proliferation (Zhao et al., 2010; Halder and Johnson, 2011). Since Tead2 seemed to regulate Yap/Taz subcellular localization, we wondered whether the opposite is also true.

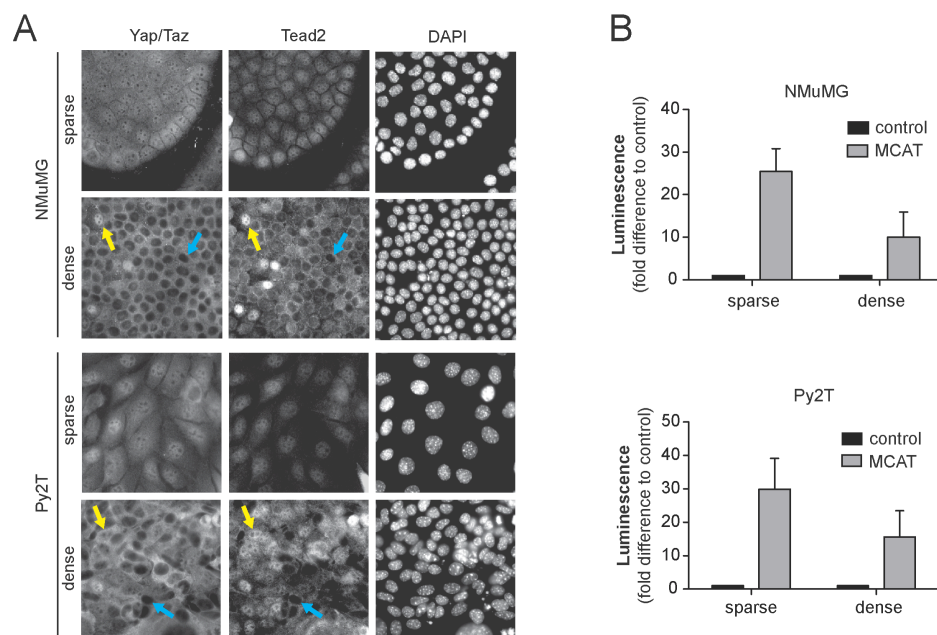


**Figure 7. Tead2 nuclear localization is regulated by cell density.**

(A) Tead relocation along with Yap/Taz in cells grown under dense conditions. Different cell numbers (factor 10 difference between sparse and dense) were seeded, grown for 5 days and co-stained for Yap/Taz and Tead2. Yellow arrows indicate nuclear localization; blue arrows denote cells with exclusively cytoplasmic staining.

(B) Measurement of Tead activity in sparse and dense cell cultures by luciferase reporter assay. The assay was performed as described in Figure 1D.

To investigate this, we grew NMuMG and Py2T cells to dense cultures, and performed double immunofluorescence labeling for Yap/Taz and Tead2. As shown in Figure 7A, dense culturing resulted in nuclear export of Yap and Taz in most cells. Strikingly, also Tead2 nuclear staining was absent in those cells and was concentrated in the cytoplasm, closely correlating with Yap/Taz localization at the single cell level. Consistent with this observation, Tead activity was decreased in densely grown cells (Figure 7B). These results suggest that Tead2 is exported from the nucleus upon cell density in a complex with Yap/Taz, and therefore establish a Hippo pathway dependent regulation of Tead activity by not only controlling localization of co-factors but also the transcription factor itself.

### 3.2.3.7 Identification of *Zyxin* as a novel *Tead2* target gene during EMT

Besides investigating upstream mechanisms that mediate the increase of Tead activity during EMT, we also sought to elucidate downstream effects mediated by the increase of Tead transcriptional activity. IPA analysis suggested that activation of Tead activity had a prominent effect on genes involved in cellular movement (Figure S3A). To identify direct Tead target genes, we made use of MARA predictions. By mapping the Tead DNA binding motif (MCAT) to genes that were upregulated during EMT of NMuMG cells, the MARA algorithm is able to predict direct Tead target genes during this process. Table I shows the top 50 candidates identified. Because *Zyxin*, which was one of the top candidates, has previously been shown to be upregulated during EMT and to be required for mediating actin reorganization and migration of these cells (Mori et al., 2009), we chose to validate a direct transcriptional induction of this gene by Tead2. To do so, we first evaluated *Zyxin* levels in response to increased Tead activity. We therefore overexpressed Tead2 FL, Tead2-VP16, and additionally Yap and Taz, together with Hippo signaling insensitive mutants of Yap and Taz. Western blot analysis of lysates from cells grown under sparse conditions revealed that *Zyxin* expression was induced by all of these factors except for Yap, in both Py2T cells and NMuMG cells (Figure 8A). These results suggest that Tead2 induces *Zyxin* expression via co-activation by Taz.



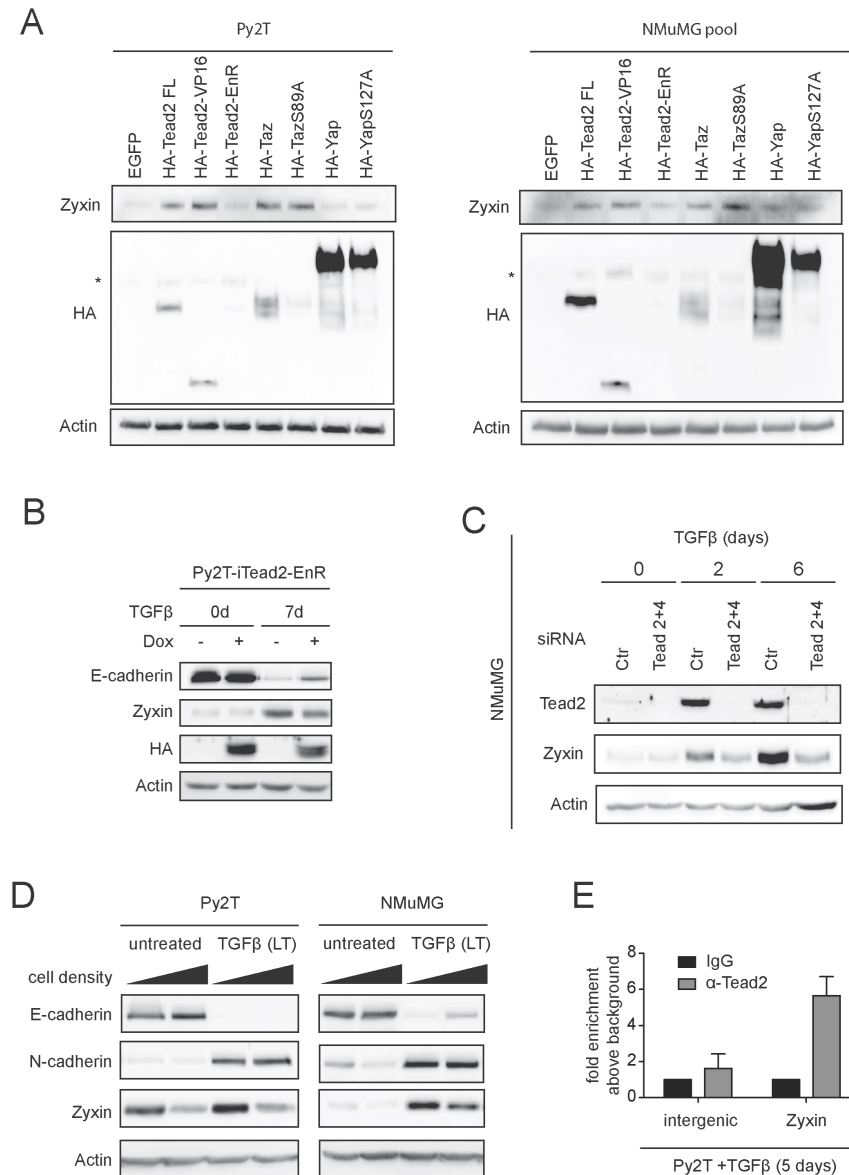


**Figure 8. Zyxin is a novel Tead target gene.**

(A) Western blot analysis of Zyxin expression in cells overexpressing different versions of Tead2 or Tead co-activators. Stable pools of cells overexpressing HA-tagged versions of indicated proteins were generated by retroviral infection. Note that HA-Tead2-EnR expression was not detected, possibly due to a selective disadvantage caused by the negative effect of Tead2-EnR expression on cell proliferation (data not shown). Taz and Yap Serine-to-Alanine point mutants are resistant to cell density mediated nuclear-cytoplasmic translocation. Lysates were prepared from cells grown under sparse conditions. A background band detected by the HA antibody is indicated with an asterisk.

(B) Zyxin expression levels in Py2T cells undergoing EMT in the absence (-Dox) or presence (+Dox) of HA-tagged dominant-negative Tead2-EnR. Cells were pretreated with doxycycline for three days before TGFβ treatment. Detection of the EMT marker E-cadherin is included as a control. See Supplementary figure 4A for Tead activity measurements done in parallel.

(C) Zyxin protein levels during an EMT timecourse of NMuMG cells depleted of Tead2 and Tead4 by siRNA or not. Membranes are from the experiment described in Figure 4b and were reprobbed with an antibody against Zyxin.

(D) Zyxin expression is regulated by cell density. Different cell numbers (factor 10 difference between sparse and dense) were seeded and grown for 5 days. Mesenchymal derivatives of Py2T and NMuMG cells included in this experiment were long term (LT) treated with TGFβ for at least 20 days. Epithelial (E-cadherin) and mesenchymal (N-cadherin) markers are included as controls. See Supplementary figure 4B for Tead activity measurements of this experiment.

(E) Chromatin immunoprecipitation (ChIP) experiment demonstrating direct binding of Tead2 to Zyxin intronic sequence containing an MCAT motif as predicted by MARA. Chromatin of Py2T cells treated with TGFβ for 5 days was used for ChIP with an antibody against endogenous Tead2 (see Supplementary figure 4C for ChIP validation of α-Tead2). Enrichment of Zyxin DNA was quantified by quantitative PCR. Results are presented as mean ± S.E.M of two independent experiments.

To determine whether Zyxin is indeed upregulated during EMT and whether this is dependent on Tead activity, we induced EMT in Py2T cells expressing dominant negative Tead2 (Tead2-EnR) or not. Immunoblotting analysis demonstrated that Zyxin was upregulated during EMT in a Tead-activity dependent manner (Figure 8B). A luciferase reporter assay performed in parallel to this experiment confirmed the increase in Tead activity upon EMT and the efficient reduction in activity due to expression of Tead2-EnR (Figure S4A). To confirm these results in NMuMG cells, we measured Zyxin levels in NMuMG cells undergoing EMT in the absence or presence of Tead2 and Tead4. Similar to the experiment performed with Py2T cells, we observed an upregulation of Zyxin during EMT only in the presence of Tead2 and Tead4 in NMuMG cells (Figure 8C). As Tead activity is regulated by cell density, Zyxin expression should also be regulated in a cell density dependent manner. To test this notion we grew epithelial and long term treated, mesenchymal NMuMG and Py2T cells to dense cultures and compared Zyxin levels in those cells to the levels expressed in sparsely growing cells. Immunoblot analysis showed that Zyxin levels were increased in mesenchymal cells as expected, and were reduced in cells that were grown to high density (Figure 8D), concomitant with Tead activity (Figure S4B), further indicating a direct regulation by Teads. MARA analysis found a Tead regulatory motif (MCAT) within the first intron of the Zyxin gene (data not shown). To prove a direct binding of Tead2 to this region, we performed chromatin immunoprecipitation (ChIP) of endogenous Tead2 with chromatin from Py2T cells treated with TGF $\beta$  for 5 days, a time point of EMT where Tead activity is increased (Figure 1D). We first validated the suitability of our antibody for ChIP and the ChIP protocol by analyzing the binding of Tead2 to the promoter of the established Tead target gene CTGF (Zhao et al., 2008b); (Figure S4C). We then tested for direct binding of Tead2 to the Zyxin gene region containing the MCAT motif and observed an enrichment of this DNA region in Tead2 immunoprecipitates but not in IgG samples, showing that Tead2 directly binds to this locus (Figure 8E). Together, these results suggest that Tead2 regulates Zyxin expression during EMT by direct binding to an MCAT motif in the Zyxin gene.

### 3.2.4 Discussion

The transdifferentiation of epithelial cells into a mesenchymal state involves changes in cell architecture and the establishment and activation of mesenchymal features, such as a remodeled cytoskeleton and an active migratory machinery, and relies on changes in gene expression orchestrated by transcription factors.

Here we have used a bioinformatic analysis (motif activity response analysis, MARA) to identify transcription factor binding motifs that display an overrepresentation in promoters of genes that are transcriptionally regulated during EMT, and therefore may explain the regulation of a large subset of totally regulated genes. This analysis identified the Tead DNA-binding motif MCAT to be among the most significant motifs.

By analyzing the average expression change of all genes carrying the MCAT motif in their promoters, MARA suggested an increase in Tead transcriptional activity upon EMT induction. This genome-wide analysis, together with complementary measurements of Tead activity using Tead-responsive luciferase reporter constructs, clearly demonstrates that overall Tead transcriptional activity increases during EMT. These results also validate that MARA analysis can accurately predict Tead activity from gene expression profiles. The same analysis could therefore be applied to datasets of human breast cancer samples to determine whether Tead activity is associated with tumor progression and whether it has prognostic value, as suggested by our results which demonstrated that an increase in Tead transcriptional activity is sufficient to induce EMT. Evidence that this could indeed be the case has been presented recently: one study showed that Taz is overexpressed in ~20% of breast cancers, most of which represent invasive ductal carcinomas (IDC), and that expression of this Tead co-activator is responsible for migration and invasiveness in cultured breast cancer cell lines (Chan et al., 2008). Another study defined that the response of breast cancer cell lines to Taxol, a cytostatic chemotherapeutic drug used for breast cancer treatment, is decreased by Yap/Taz/Tead mediated transcription of CTGF and Cyr61 (Lai et al., 2011). Interestingly, Cordenonsi and colleagues found that a species-conserved Yap/Taz target gene signature, established from various gene expression profiling experiments (Dong et al., 2007; Ota and Sasaki, 2008; Zhao et al., 2008b), correlates with normal breast and breast cancer stem cell signatures, and also with metastasis-free survival in patients (Cordenonsi et al., 2011).

Our findings that increased Tead activity induced by overexpression of wild type Tead2 or

of an activated version (Tead2-VP16) (Figure 3B) is sufficient to induce *bona fide* EMT in murine Py2T breast cancer cells (Figure 3C) is in line with previous reports which demonstrated that ectopic expression of Yap/Taz induces EMT via Teads in normal human MCF10A cells (Lei et al., 2008; Zhao et al., 2008b). As expected from cells that have undergone EMT, Tead2 overexpressing cells display dramatically increased migration and invasion capabilities in comparison to control cells (Figure 3E). Similarly, cells overexpressing constitutively active Tead2-VP16 undergo EMT, however these cells are unable to migrate, even though their gene expression profile displays a signature consistent with cellular movement (Figure 3A, *middle*). One explanation for these differences could be that the Tead2-VP16 fusion protein over-activates migration-related genes due to its constitutive activity, while in wild type Tead2 overexpressing cells negative feedback may occur, and, therefore, Tead target gene expression is finely balanced to allow proper function of the migration machinery. Interestingly, some predicted Tead target genes (Table I) are compatible with this hypothesis and could play a role in a negative feedback control: LATS2 is one of the core components of the Hippo pathway, and can inactivate Yap by phosphorylation leading to nuclear exit (Zhao et al., 2010). CAPZB (capping protein, muscle-Z line, beta) is another predicted Tead target gene. Capping proteins have been shown to negatively regulate Yki in *Drosophila* via prevention of extra F-actin formation (stress fibers), which normally activates Yki/Yap (Dupont et al., 2011; Fernández et al., 2011; Sansores-Garcia et al., 2011; Wada et al., 2011).

We observed an attenuation of the EMT process when we inhibited endogenous Tead activity during EMT by expression of a dominant-negative Tead2 (Tead2-EnR) in Py2T cells (Figure 3 C-E). This effect was even more pronounced when we depleted NMuMG cells of Tead family members by siRNA knockdown (Figure 4A, B), demonstrating that the presence and transcriptional activity of Teads is required for proper execution of the TGF $\beta$ -induced EMT program, and it also seems to be required to sustain the migratory and invasive phenotype of mesenchymal cells (Figure 4F-G).

As Tead transcriptional activity is mainly controlled by binding of the co-factors Yap and Taz (Vassilev et al., 2001; Mahoney et al., 2005; Zhao et al., 2008b; Zhang et al., 2009a), we wished to elucidate whether this is also true in the setting of EMT. We first attempted to test this possibility by transient knockdown experiments. However, knockdown of either Yap or Taz in cells undergoing EMT resulted in a complete proliferation arrest and apoptosis in all

cell types tested, consistent with the pro-proliferative function of these two factors (Zhao et al., 2010). Nuclear localization of Yap/Taz is negatively regulated by cell density via the Hippo tumor suppressor pathway (Zhao et al., 2010). The experiments evaluating Tead activity upon EMT however were all performed under sparse conditions with proliferating cells, and we therefore did not observe changes in Hippo-mediated Yap phosphorylation (data not shown). Consistent with the role of Yap/Taz in mediating proliferation under sparse conditions, we observed nuclear staining of these factors in all cells before, during and after EMT, with no obvious differences in nuclear staining intensity (Figure 6A). Cytoplasmic Yap/Taz appeared to be diminished in cells undergoing EMT (Figure 6A, *left, middle*) or in stable mesenchymal cells (Figure 6A, *right*) compared to cells that reside in the epithelial state. However, a direct comparison of cytoplasmic staining intensity is difficult to interpret due to the significant differences in cell shape. Moreover, we did not observe a major shift in Yap/Taz subcellular localization as determined by nuclear/cytoplasmic fractionation (Figure 6C). Together, these observations showed that the nuclear/cytoplasmic distribution of Yap/Taz was not extensively changed during EMT. Interestingly, in addition to nuclear and cytoplasmic staining, we observed a membranous staining pattern of Yap/Taz in epithelial cells reminiscent of tight junctions (Figure 6B). This observation is consistent with a series of recent studies that demonstrated inhibition of Yap/Taz transcriptional activity by direct binding to tight-junction localized angiotensin/angiotensin-like proteins, an inhibitory mechanism that is independent of canonical Hippo signaling (Chan et al., 2011; Wang et al., 2011a; Zhao et al., 2011a). It is therefore tempting to speculate that the membrane bound pool of Yap/Taz in epithelial cells, presumably a minor fraction of total levels, is released from angiotensins during EMT-induced tight-junction breakdown to enter the nucleus in order to stimulate Tead activity. Consistent with this hypothesis, knockdown of angiotensin-like 2 (Amotl2) is sufficient to induce EMT in MCF10A cells (Wang et al., 2011a). Furthermore, an earlier study established that mutation of Yap WW domains, the domain responsible for physical binding to angiotensins, increases the ability of Yap to activate Teads in MCF10A cells, and promotes cell migration (Zhang et al., 2009b). Furthermore, Taz has been shown to be able to interact with the tight-junction proteins zonula occludens 1 and 2 (ZO-1, 2), also via its WW domain (Remue et al., 2010). Remarkably, we observed a loss of tight-junction staining and nuclear accumulation of ZO-1 upon EMT induction in our cellular systems (data not shown), which supports a model in which membrane-localized Taz could translocate into the nucleus during EMT, possibly in a complex with ZO-1. Further along this line, Yap/Taz

have been shown to strongly bind to Pals1 and other crumbs polarity complex proteins (Varelas et al., 2010), and we observed nuclear accumulation of Pals1 upon EMT induction in our cellular systems (data not shown). Intriguingly, the crumbs polarity complex and tight junctions have been shown to be linked via Pals1 (Roh et al., 2002), indicating that the separate identification of Yap/Taz in the crumbs complex and its association with tight-junction proteins could be based on the presence of Yap/Taz in a multiprotein complex encompassing both tight-junction and polarity complex proteins that both localize to the apical part of the cell membrane. Collectively, these considerations would be compatible with the hypothesis that a small pool of apically sequestered Yap/Taz is released from the cell membrane and redistributes to the nucleus upon EMT, which might be sufficient for mediating the increased Tead activity we have observed.

An alternative mechanism could be envisioned that controls the increase in Tead activity: as Yap and Taz are already present in the nucleus in epithelial cells, the amount of Teads present may be the limiting factor for transcriptional activation of EMT-related target genes. Indeed, Tead2 and, depending on the cell type investigated, also other Tead family members display increased expression during EMT (Figure 2A, B). Moreover, increasing Tead2 levels by ectopic expression increases Tead activity (Figure 3B) and leads to EMT (Figure 3C, D), consistent with a “bottleneck” function of Tead expression levels. It is thus conceivable that the “bottleneck” mechanism and the relocalization of a membrane bound pool of Yap/Taz proposed above cooperate to increase Tead transcriptional activity.

However, a third mechanistic aspect would be unclear: how are Yap/Taz, once released from the apical membrane into the cytoplasm, recruited into the nucleus to serve as Tead co-activators? Much research has been directed towards the elucidation of how Yap/Taz are exported from the nucleus, however what determines their nuclear localization remains unexplored. Notably, Teads all carry a nuclear localization signal, while Yap and Taz do not. One report demonstrated that an ectopically expressed GFP-Taz fusion protein, carrying a point mutation that disrupts Tead binding, is more inefficiently shuttled to the nucleus after photobleaching in comparison to “wild-type” GFP-Taz that can bind to Teads (Chan et al., 2009). This observation suggests that Teads are able to mediate Taz (and presumably also Yap) accumulation in the nucleus. Indeed, we show here that ectopic expression of Tead2 is sufficient for a collective redistribution of Yap/Taz from the cytoplasm into the nucleus (Figure 5), suggesting that during EMT, the increasing amounts of Tead molecules in the

nucleus may recruit additional co-factors from the cytoplasm to ensure saturation and effective target gene transcription.

Interestingly, the reverse is also true, at least for Tead2: when Yap/Taz are shuttled into the cytoplasm in response to high cell density, Tead2 is also excluded from the nucleus. This observation suggests that Tead2 target genes are regulated by cell density, regardless whether co-activation is mediated by the Hippo pathway components Yap/Taz or by any other co-activators.

MARA analysis provided us with a rated list of potential Tead target genes. These genes all carry a species-conserved MCAT motif in their promoter-regions and their mRNA levels are upregulated during EMT. We confirmed that Zyxin, one of the target genes with the highest prediction score (Table I), is upregulated during EMT in a Tead-dependent manner (Figure 8B, C), and our data also suggests that this regulation is mediated via activation of Teads by Taz but not Yap (Figure 8A). Furthermore, we validated direct binding of Tead2 to the promoter-region of Zyxin, however final proof of actual regulation will have to be determined by luciferase assays with Zyxin promoter reporters carrying either a wild type or a mutant MCAT motif.

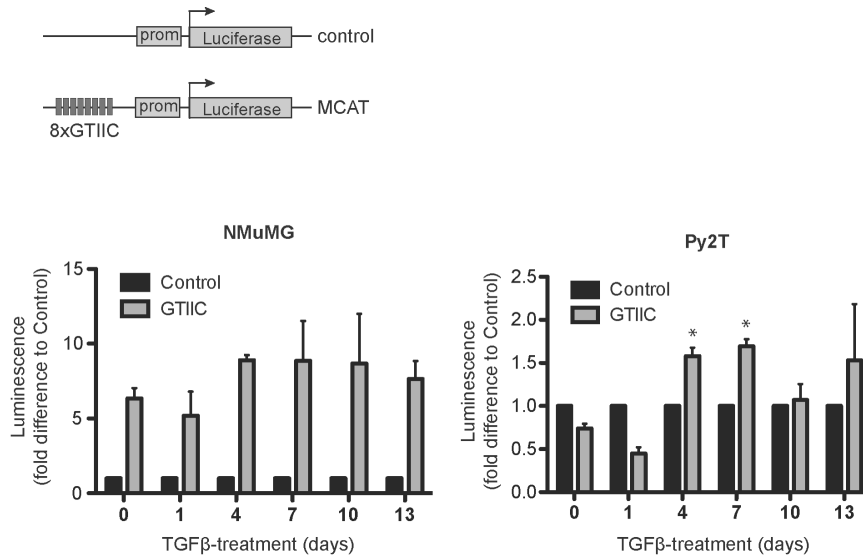
Zyxin belongs to the family of LIM proteins and associates with the actin cytoskeleton and therefore can be localized at the apical membrane, in focal adhesions and on stress fibers (Beckerle, 1997). Notably, Zyxin was previously shown to be upregulated and to be required for rearrangement of the actin cytoskeleton during TGF $\beta$ -induced EMT of NMuMG cells, thereby enabling migration (Mori et al., 2009). Zyxin upregulation could therefore be at least one of the mechanisms how Tead activity controls the induction of a migratory phenotype during EMT. Notably, the study of Mori and colleagues showed that Zyxin upregulation is dependent on the transcription factor Twist, indicating that Tead activation occurs downstream of the action of Twist. Interestingly, a connection between Zyxin and the Hippo pathway has been established recently. Zyxin localizes to the apical membrane at intercellular junctions of the wing disc epithelium, can interact with Wts (Lats in *Drosophila*) and the presence of Zyxin positively regulates Yki (Yap in *Drosophila*), because loss of Zyxin leads to diminished nuclear localization of Yki and reduced organ growth (Rauskolb et al., 2011). The mechanisms involved however have not been elucidated and it is unclear whether a similar role of Zyxin also exists in mammalian cells.

To gain further insight into the functional consequences of increased Tead activity during EMT, we are currently performing more extensive validation of genome-wide direct Tead2 target genes by combining chromatin immunoprecipitation with high-throughput sequencing (ChIP-seq), and functional sites will be evaluated by their mapping to gene promoters and comparison with the gene expression profiles of Tead2 gain-of-function experiments.

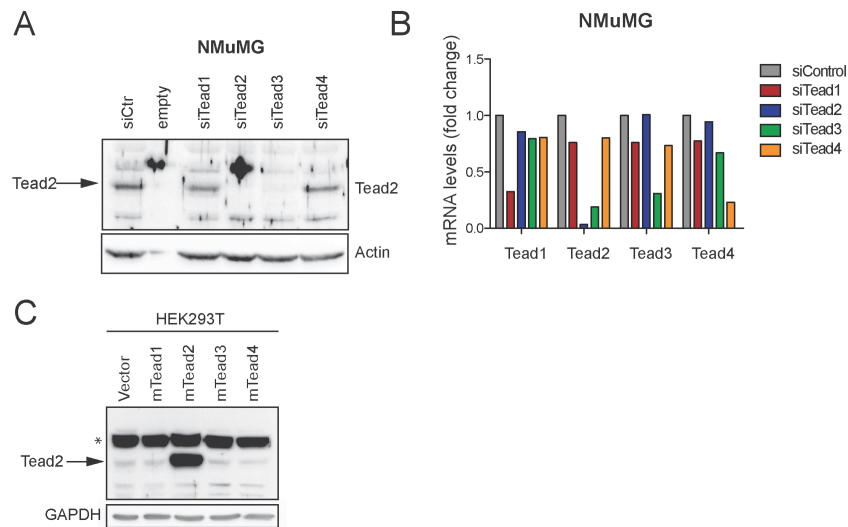
Collectively, our results establish a crucial regulatory role for Tead transcription factors in the EMT process, and provide first insights into the regulatory mechanisms that are involved in mediating enhanced transcriptional activation of Teads during EMT, and also provide a basis for the further investigation of downstream processes.



## 3.2.5 Supplementary Data

**Supplementary Figure 1. Tead activity during EMT as measured by a GTIIC Tead luciferase reporter.**

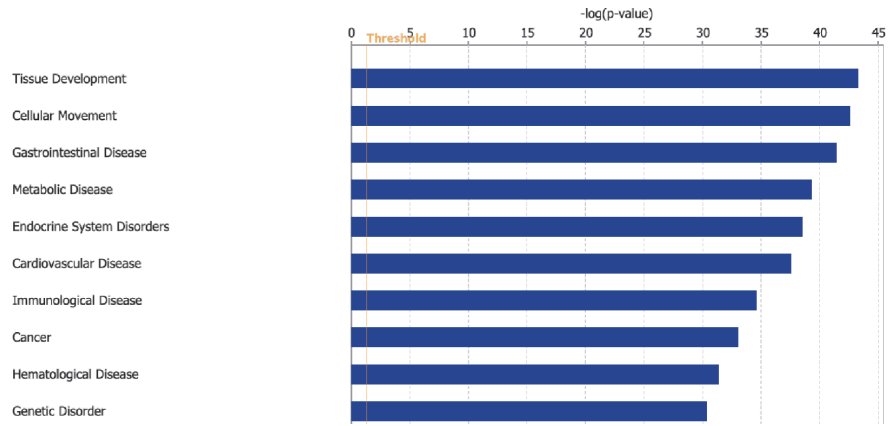
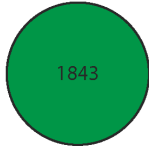
Measurement of Tead activity in NMuMG and Py2T cells using a luciferase reporter bearing a Tead response element termed GTIIC. Eight copies of the core GTIIC Tead DNA binding motif (CATTCCA) plus flanking sequences were cloned in front of a basal promoter followed by the firefly luciferase gene (GTIIC reporter). Cells were treated with TGFβ for the indicated times prior to simultaneous lysis and luminescence analysis. Reporter constructs were transfected one day before lysis, along with a Renilla luciferase construct for normalization. Reporter activities are shown as mean ± S.E.M of two independent experiments (\*p-value < 0.05).

**Supplementary Figure 2. Characterization of Tead2 antibody.**

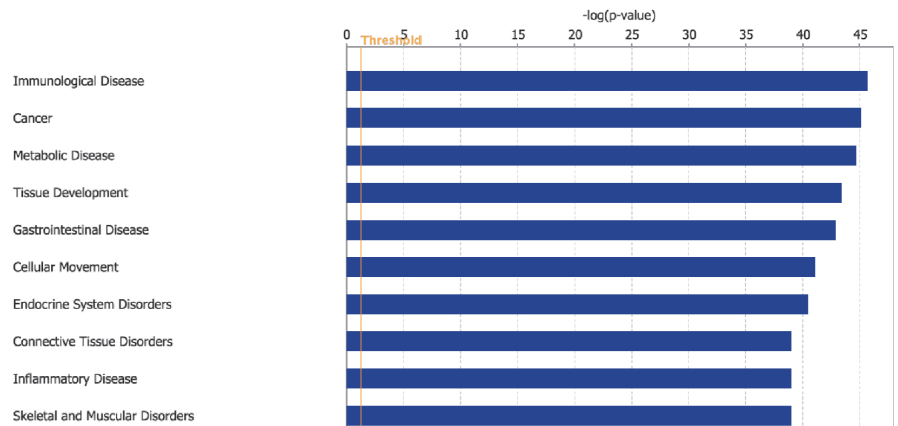
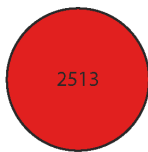
(A) Tead2 antibody does not detect Tead family members other than Tead2. Lysates of NMuMG cells transfected with siRNAs against all known Tead family members were probed with α-Tead2 by western blot. Note the disappearance of the band representing Tead2 in lysates of Tead2 knockdown cells. This band was also weaker when siTead3 was used, which is due to the fact that siTead3 also led to a knockdown of Tead2 (see below). (B) Quantification of siRNA efficiency in the experiment described in (A). Downregulation of targeted mRNAs was at least 60% and family member specific, with the exception of siTead3, which led to efficient double knockdown of Tead2 and Tead3. (C) Tead2 antibody does not detect overexpressed murine Tead family members other than Tead2. Tead family members were transiently overexpressed in HEK293 cells, and lysates were probed with α-Tead2 by western blot. Fugene HD (Roche) was used for transfection according to the manufacturers instruction. The asterisk denotes a band detected that is not specific for Tead2.

3A

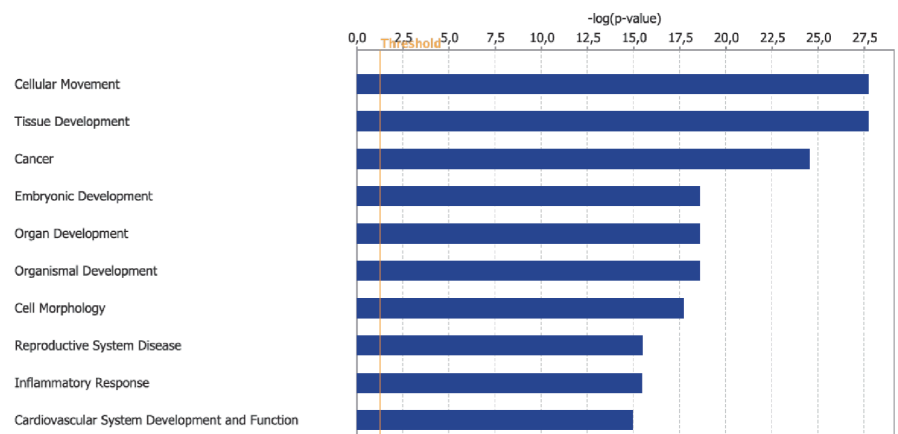
CTR vs Tead2 FL



CTR vs Tead2-VP16

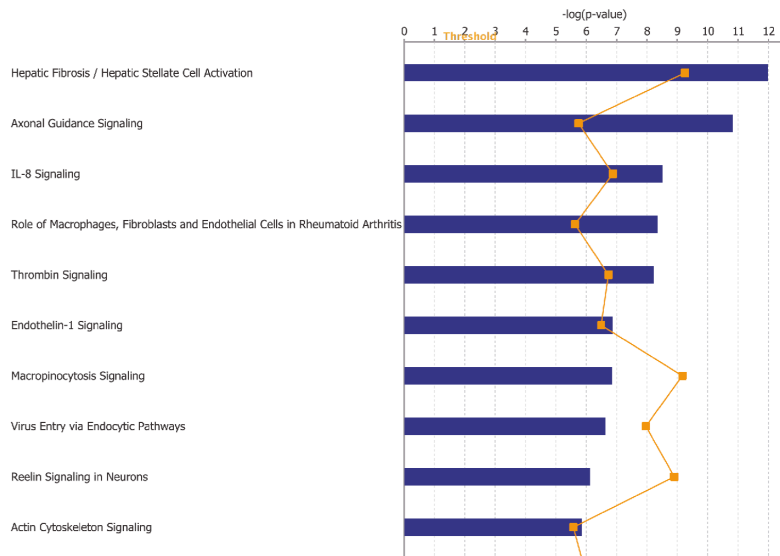
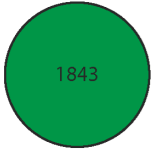


Tead2 FL vs Tead2-VP16

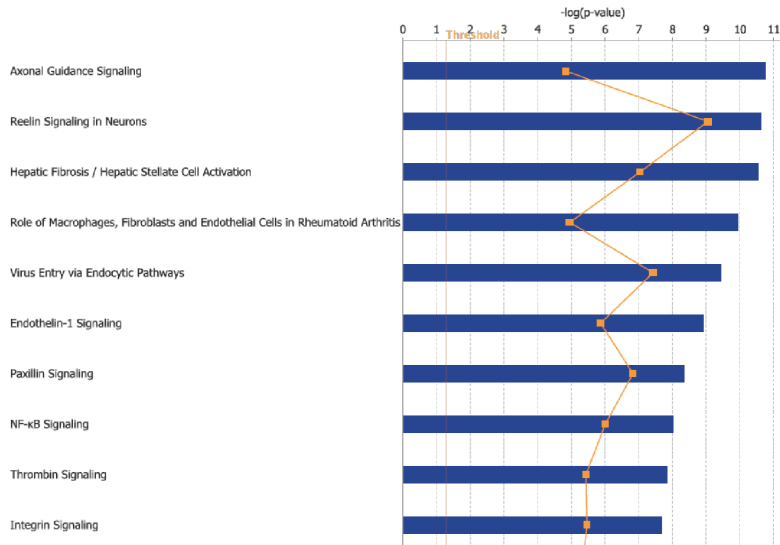
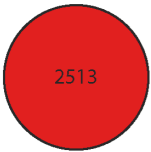


3B

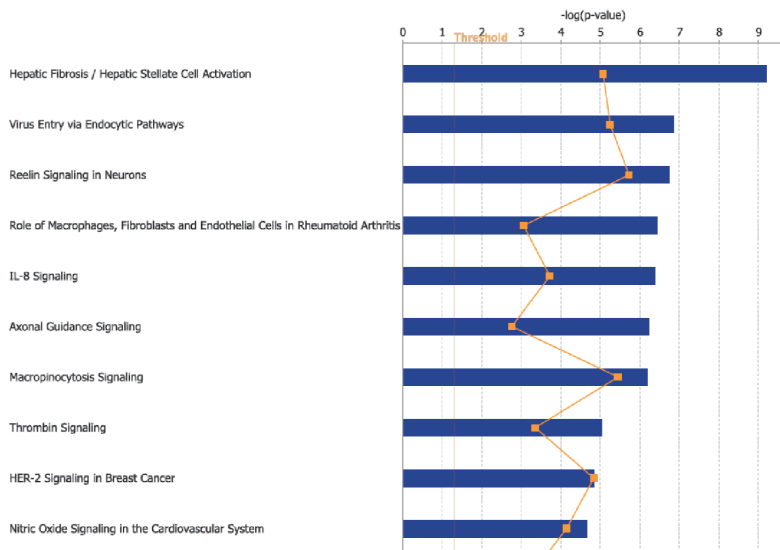
CTR vs Tead2 FL



CTR vs Tead2-VP16



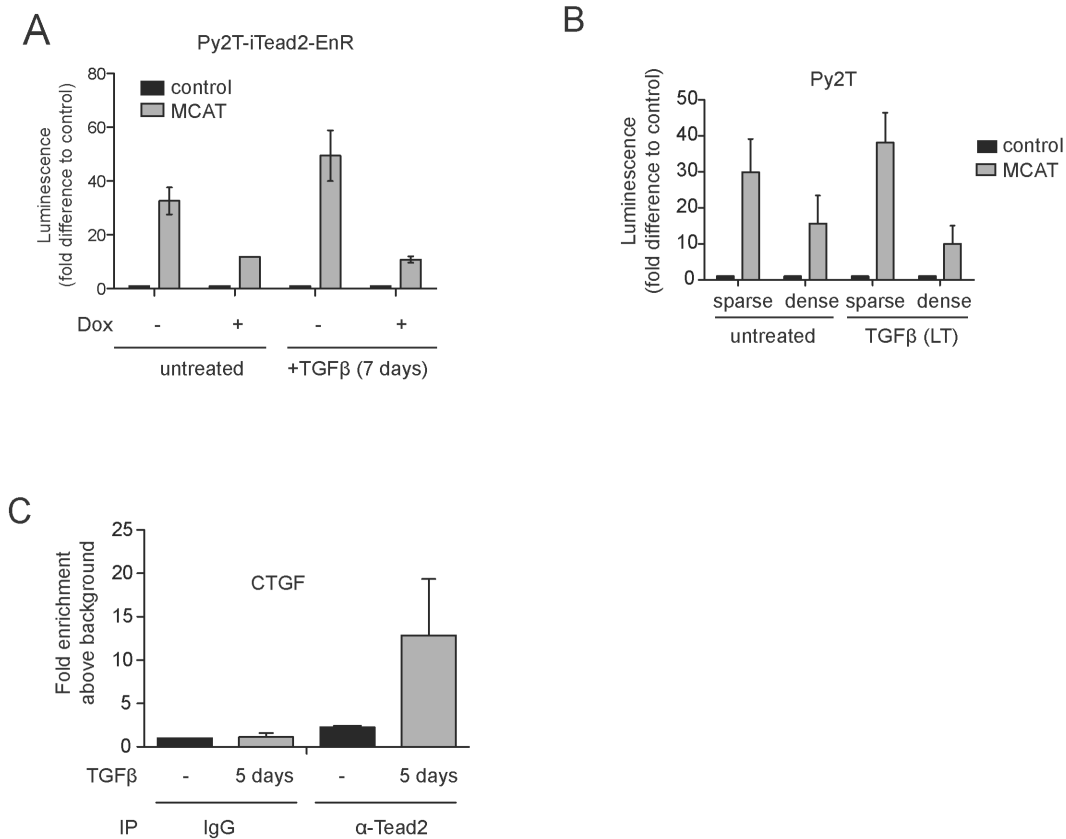
Tead2 FL Tead2-VP16



**Supplementary Figure 3. Gene expression profile analysis of Tead2 gain-of-function cell lines.**

(A) Enrichment of differentially expressed genes in distinct biological functions. Differentially expressed genes in Tead2 FL (top), Tead2-VP16 (middle) or in both (bottom) cell lines compared to control cells were determined by Partek microarray analysis software and uploaded into Ingenuity Pathway Analysis software (IPA, see Materials and Methods section). A cutoff of 2-fold up- or down-regulation with p-values  $\leq 0.05$  was applied for Partek analysis (see Supplementary files for full lists). Numbers in circles represent the number of genes with significant differential expression after upload to IPA. IPA core analysis was performed to assign a possible enrichment of the differentially regulated genes in distinct biological processes (left). In other words, the determined differentially expressed genes are overrepresented in the indicated biological function categories. Only the top 10 significant processes are shown. Orange lines represent a p-value cutoff of 0.05.

(B) Overrepresentation of differentially expressed genes in a non-exhaustive set of canonical pathways available within IPA. Data was processed as described in (A). Only the top 10 significant processes are shown. Orange data points represent the ratio of differentially regulated genes that map to the specific pathway, divided by the total number of genes contained within this pathway. Straight orange lines represent a p-value cutoff of 0.05.



**Supplementary Figure 4. Control experiments**

(A) Measurement of Tead activity in the experiment described in Figure 8B. Results are shown as mean  $\pm$  S.E.M. of two independent experiments.

(B) Tead activity measurements in the experiment described in Figure 8D. Data represents mean  $\pm$  S.E.M. (n=2).

(C) Validation of  $\alpha$ -Tead2 antibody for ChIP use. Chromatin of Py2T cells treated with TGFβ was subjected to ChIP with  $\alpha$ -Tead2. The DNA locus containing a Tead binding site was amplified by quantitative PCR and enrichment was calculated relative to ChIP with IgG antibody (mean  $\pm$  S.E.M. of two independent experiments).

z-Value	Target Gene	Gene Name
8.52	TNFAIP3	tumor necrosis factor, alpha-induced protein 3
6.77	CNN2	calponin 2
6.58	ZYX	zyxin
6.47	TPM1	tropomyosin 1, alpha
5.88	PRKCI	protein kinase C, iota
5.85	NPPB	natriuretic peptide precursor type B
5.58	TGM2	transglutaminase 2, C polypeptide
5.52	MYL7	myosin, light polypeptide 7, regulatory
5.45	PLEKHG2	pleckstrin homology domain containing, family G (with RhoGef domain) member 2
5.43	CYR61	cysteine rich protein 61
5.40	ITGB1	integrin beta 1 (fibronectin receptor beta)
5.37	ACTA1	actin, alpha 1, skeletal muscle
5.29	MGAT4B	mannoside acetylglucosaminyltransferase 4, isoenzyme B
5.08	AEBP2	AE binding protein 2
5.08	AEBP2	
5.05	2900073G15RIK	RIKEN cDNA 2900073G15 gene; predicted gene 6517
5.05	PDGFC	platelet-derived growth factor, C polypeptide
4.91	GPX1	glutathione peroxidase 1
4.88	FHOD3	formin homology 2 domain containing 3
4.86	PRKRIR	protein-kinase, interferon-inducible double stranded RNA dependent inhibitor
4.81	WISP1	WNT1 inducible signaling pathway protein 1
4.76	SMARCD3	SWI/SNF related, matrix associated, actin dependent regulator of chromatin,subfamily d,member 3
4.63	AMMECR1L	AMME chromosomal region gene 1-like
4.56	CTGF	connective tissue growth factor
4.51	ACTA2	actin, alpha 2, smooth muscle, aorta
4.48	PTPRK	protein tyrosine phosphatase, receptor type, K
4.41	SPARC	secreted acidic cysteine rich glycoprotein; similar to Secreted acidic cysteine rich glycoprotein
4.41	EXT1	exostoses (multiple) 1
4.40	NFKBIZ	nuclear factor of kappa light polypeptide gene enhancer in B-cells inhibitor, zeta
4.35	ZEB1	zinc finger E-box binding homeobox 1
4.31	JUN	Jun oncogene
4.27	CPE	carboxypeptidase E; similar to carboxypeptidase E
4.06	WWC2	WW, C2 and coiled-coil domain containing 2
4.05	KPNA4	karyopherin (importin) alpha 4
3.95	RBMS1	RNA binding motif, single stranded interacting protein 1
3.91	BDNF	brain derived neurotrophic factor
3.91	BDNF	
3.91	CAPZB	capping protein (actin filament) muscle Z-line, beta
3.90	ZBTB1	similar to Zinc finger and BTB domain containing 1; zinc finger and BTB domain containing 1
3.90	ZBTB1	
3.80	RNF111	predicted gene 6162; similar to ring finger 111; ring finger 111
3.67	OSBPL11	oxysterol binding protein-like 11
3.59	SLC12A4	solute carrier family 12, member 4
3.52	ABL1	c-abl oncogene 1, receptor tyrosine kinase
3.50	RAB34	RAB34, member of RAS oncogene family
3.45	KIF3C	kinesin family member 3C
3.44	LATS2	large tumor suppressor 2
3.41	TBC1D10B	TBC1 domain family, member 10b
3.33	ZFP295	zinc finger protein 295
3.31	JUB	ajuba
3.31	PPP1R10	protein phosphatase 1, regulatory subunit 10
3.27	TIMP1	tissue inhibitor of metalloproteinase 1
3.25	PSAP	prosaposin

**Supplementary table I. Tead target genes predicted by MARA analysis.**

Gene expression profiles of NMuMG cells undergoing EMT were subjected to MARA analysis as described in Figure 1B. Tead target genes were calculated and rated by z-Values based on occurrence of a Tead DNA binding motif (MCAT motif) in their promoters, the conservation of this motif in different species and their regulation during EMT. The top 50 predicted target genes are shown (see Supplementary files for an extended list).

Supplementary movies and supplementary data files mentioned in the text are available upon request.

### 3.2.6 Materials and Methods

#### *Antibodies and reagents*

Antibodies: Affinity purified, polyclonal rabbit Tead2 antibody was generated by immunizing rabbits with a peptide corresponding to the N-terminus of Tead2 (AAs 16-32), which is conserved in human and mouse. Actin (sc-1616, SantaCruz Biotechnology), E-cadherin (610182, Transduction Laboratories), N-cadherin (M142, Takara Bio), fibronectin (F3648 Sigma-Aldrich), GAPDH (G8795, Sigma), vimentin (V2258, Sigma-Aldrich), ZO-1 (617300, Zymed), Yap/Taz (101199, SantaCruz Biotechnology), hnRNP (sc-15386, SantaCruz Biotechnology), Zyxin (sc6437, SantaCruz Biotechnology), HA (MMS-101R, Covance), Phalloidin Alexa-Fluor 568 (A12380, Invitrogen).

Reagents: recombinant human TGF $\beta$ 1 (240-B-010, R&D Systems); Matrigel, growth factor reduced (356230, BD); Doxycycline (631311, Clontech).

#### *Cells and cell lines*

A subclone of NMuMG cells (NMuMG/E9; hereafter NMuMG) has been previously described (Maeda et al., 2005). MT $\Delta$ Ecad and MTfIEcad have been described previously (Lehembre et al., 2008). Py2T cells are described in this Thesis. All cells were cultured in DMEM supplemented with glutamine, penicillin, streptomycin, and 10% FBS (Sigma).

#### *Plasmids*

The GTIIC luciferase reporter construct was generated by subcloning of a cDNA fragment encompassing eight repeats of a GTIIC Tead DNA-binding motif with flanking sequences, followed by a basal promoter (kindly provided by Dr. H. Sasaki, RIKEN Center for Developmental Biology, Kobe, Japan) into the luciferase reporter plasmid pGL4 (Promega) (Davidson et al., 1988; Ota and Sasaki, 2008). MCAT reporter was generated by replacement of 8xGTIIC with eight copies of the sequence CCTGACACCACATTCCTCAGCT (8xMCAT), where the MCAT core motif is underlined, and flanking sequences were according to (Larkin et al., 1996). The total length 8xMCAT sequence was commercially synthesized with flanking restriction sites for subcloning (Mr. Gene GmbH, Regensburg, Germany). The control reporter construct was created by excision of 8xGTIIC and subsequent ligation. Renilla Luciferase expressing vector (pRL-CMV) was from Promega. Murine Tead1-4 in pcDNA3.1

for transient transfection were kindly provided by Dr. J. Carvajal (The Institute of Cancer Research, London, UK). Retroviral Tead2 FL and Tead2-VP16 constructs have been described previously (Ota and Sasaki, 2008). Retroviral HA-tagged Tead2, Tead2-VP16, Tead2-EnR, Taz and Yap were created by inserting the respective cDNAs into the pBabe-derived retroviral vector pRFTO containing an N-terminal HA tag (kindly provided by Dr. R. Kohler, FMI, Basel, Switzerland). cDNAs were kind gifts from Drs. H. Sasaki (Tead2, Tead2-VP16), R. Kohler (Yap and YapS127A) and K. Guan (Department of Pharmacology and Moores Cancer Center, UCSD, La Jolla, USA) (Taz and TazS89A). The lentiviral, doxycycline-inducible HA-Tead2 and HA-Tead2-EnR constructs were generated by subcloning from pRFTO into pLVX-tight-puro (Clontech).

#### *siRNA*

5 nM siGENOME smart pool siRNAs (Dharmacon) against murine Tead1 (M-048419-01), Tead2 (M-060552-00), Tead3 (M-044127-01) and Tead4 (M-057322-01) were used for transient knockdown experiments. Transfection was performed with Lipofectamine RNAiMax according to the manufacturer's instructions. A reverse transfection protocol was used at the start of each experiment, and forward re-transfection was done every second day where appropriate.

#### *Quantitative RT-PCR*

Total RNA was prepared using Tri Reagent (Sigma-Aldrich), reverse transcribed with M-MLV reverse transcriptase (Promega, Wallisellen, Switzerland), and transcripts were quantified by PCR using SYBR-green PCR MasterMix (Applied Biosystems, Rotkreuz, Switzerland). Riboprotein L19 primers were used for normalization. PCR assays were performed in triplicates, and fold induction was calculated using the comparative Ct method ( $\Delta\Delta$  Ct). Primers used for quantitative RT-PCR were: Tead1 (forward: 5'-ccaggatcctcacaagacg-3', reverse: 5'-gaatgggggctgtgactg-3'), Tead2 (forward: 5'-ctgaggacaggggaagacgag-3', reverse: 5'-cttcgagccaaaacctgaat-3'), Tead3 (forward: 5'-gagctgattgcccgtac-3', reverse: 5'-tgtatgtggtggacacctg-3'), Tead4 (forward: 5'-tcaaacacctaccctgtcca-3', reverse: 5'-gccctgcaggagactcaa-3'), RPL19 (forward: 5'-ctcgttgccggaaaaaca-3', reverse: 5'-tcattccaggtcaccttctca-3').

*Luciferase reporter assay*

Cells were plated in triplicate in a 24 well plate. One day after plating, cells were transfected with 800ng reporter and 5ng Renilla encoding plasmids using Lipofectamine 2000. Fresh growth medium was added after 5 hours of transfection. One or two days after transfection, cells were lysed directly in plates using 1x passive lysis buffer (#E194, Promega) and lysates were analyzed using the Dual-Luciferase Reporter Assay System (#E1960, Promega) and a Berthold Luminometer LB960. Measured luciferase values were normalized to internal Renilla control and fold difference to control reporter was calculated.

*Immunofluorescence staining of cultured cells*

Cells were plated on glass coverslips and treated for the indicated times with TGF $\beta$ . The following steps were all done at room temperature. After fixation using 4 % paraformaldehyde /PBS for 15 min, cells were permeabilized with 0.5 % NP-40 for 5 min. Next, cells were blocked using 3 % BSA, 0.01 % TritonX-100 in PBS for 20 min. Then, cells were incubated with the indicated primary antibodies for 1 h followed by incubation with the fluorochrome-labeled secondary antibody (Alexa Fluor®, Invitrogen) for 30 min at room temperature. Nuclei were stained with 6-diamidino-2-phenylindole (DAPI) (Sigma-Aldrich) for 10 min. The coverslips were mounted (Fluorescent mounting medium, Dako) on microscope slides and imaged with a conventional immunofluorescence microscope (Leica DMI 4000) or a confocal laser-scanning microscope (Zeiss LSM 510 Meta).

*Chromatin immunoprecipitation*

ChIP experiments were performed as previously described (Weber et al., 2007). In brief, crosslinked chromatin was sonicated to achieve an average fragment size of 500 bp. Starting with 150  $\mu$ g of chromatin and 5  $\mu$ g of antibody, 0.5  $\mu$ l of ChIP material and 0.5  $\mu$ l of input material were used for quantitative real-time PCR using specific primers covering the MCAT motif in the Zyxin gene. Primers covering an intergenic region were used as a control. The efficiencies of PCR amplification were normalized between the primer pairs. The following primers were used for ChIP-qPCR: Zyxin (forward: 5'-ccctgtcctgagcagatgtt-3', reverse: 5'-agaacgagccaggttgaaga-3'); Intergenic (forward: 5'-gctccgggtcctattctgt-3', reverse: 5'-tcttggttccaggagatgc-3').



*Nuclear/cytoplasmic fractionation*

All steps were performed on ice or at 4°C. Cells were scraped in cold PBS and pelleted, followed by swelling in RSB Buffer (10 mM HEPES, 10 mM NaCl, 1.5 mM MgCl<sub>2</sub>) containing phosphatase and protease inhibitors for 30 min. Cells were passed 5 times through a 26 gauge needle, protein content was measured, adjusted to the same levels in all samples and input samples were collected. Nuclei were then pelleted by centrifugation at 400xg for 2 min and cytoplasmic supernatant was collected. Nuclear pellet was washed 3 times with RSB Buffer containing inhibitors. Nuclei were lysed with EBC Buffer (50 mM Tris, 250 mM NaCl, 1 % Triton X-100) containing inhibitors by vortexing followed overhead shaking for 1 hour. Finally, nuclear and cytoplasmic fractions were centrifuged at full speed for 15 min in a tabletop centrifuge and supernatant was collected, and all samples were diluted in SDS-PAGE loading buffer (10 % glycerol, 2 % SDS, 65 mM Tris, 1 mg/100 ml bromophenol blue, 1 % β-mercaptoethanol).

*Immunoblotting*

Cells were lysed in RIPA buffer (150 mM NaCl, 2 mM MgCl<sub>2</sub>, 2 mM CaCl<sub>2</sub>, 0.5 % NaDOC, 1 % NP40, 0.1 % SDS, 10 % Glycerol, 50 mM Tris pH 8.0) containing 2 mM Na<sub>3</sub>VO<sub>4</sub>, 10 mM NaF, 1 mM DTT, and a 1:200 dilution of stock protease inhibitor cocktail for mammalian cells (Roche). Protein concentration was determined using the BCA assay kit (Pierce). Equal amounts of protein were diluted in SDS-PAGE loading buffer (10 % glycerol, 2 % SDS, 65 mM Tris, 1 mg/100 ml bromophenol blue, 1 % β-mercaptoethanol) and resolved by SDS-PAGE. Proteins were transferred to polyvinylidene fluoride (PVDF) membranes (Millipore) by semi-dry transfer, blocked with 5 % skim milk powder in TBS/ 0.05 % Tween 20 and incubated with the indicated antibodies. HRP conjugated secondary antibodies were detected by chemiluminescence using a Fusion Fx7 chemiluminescence reader (Vilber Lourmat, France).

*Retroviral infection*

Retroviral plasmids containing the cDNA of interest were transfected into the retroviral packaging cell line Plat-E (purchased from Cell Biolabs); (Morita et al., 2000) using FugeneHD (Roche). One day after transfection, medium was exchanged and retroviral supernatant was produced for 2 days. Viral supernatant was filtered through 0.45 μm pores

and 8  $\mu\text{g}/\text{mL}$  polybrene was added. Target cells were plated into 6-well plates and were infected with viral supernatant one day after plating. For infection, 2 mL supernatant was added per well and plates were spun for 1 hour at  $30^{\circ}\text{C}$  at  $1000\times g$  and were subsequently incubated at  $37^{\circ}\text{C}$  with 5%  $\text{CO}_2$  in a tissue culture incubator for 2 more hours. Viral supernatant was then replaced by normal growth medium and one day later, selection was performed with the appropriate antibiotics or cells were FACS sorted for GFP expression.

#### *Lentiviral infection*

The Lenti-X Tet-On Advanced system (Clontech) was used to generate stable pools of cells capable of expressing Tead2 FL or Tead2-EnR in a doxycycline-inducible fashion. Lentiviral particles were produced by transfecting HEK293T cells with the lentiviral expression vectors pLVX-Tet-On Advanced or pLVX-HA-Tead2 or pLVX-HA-Tead2-EnR or pLVX-tight-puro-luc as a control, in combination with the helper vectors pHDM-HGPM2, pHDM-Tat1b, pRC-CMV-RaII and the envelope encoding vector pVSV using Fugene HD. After two days of virus production, lentivirus-containing supernatants were harvested, filtered ( $0.45\ \mu\text{m}$ ) and stored at  $-80^{\circ}\text{C}$ . For infection, viral supernatants were added to target cells in the presence of polybrene ( $8\ \mu\text{g}/\text{ml}$ ). Cells were spun for 1 hour at  $30^{\circ}\text{C}$  at  $1000\times g$  and were subsequently incubated at  $37^{\circ}\text{C}$  with 5%  $\text{CO}_2$  in a tissue culture incubator for 2 more hours. Viral supernatant was then replaced by normal growth medium and one day later, selection with the appropriate antibiotics was performed for 3 consecutive days.

#### *Boyden chamber migration and invasion assay*

Cells were trypsinized, washed once with PBS, and resuspended in growth medium containing 0.2% FBS and 2  $\text{ng}/\text{mL}$   $\text{TGF}\beta$  where appropriate.  $2.5\times 10^4$  cells in 500  $\mu\text{L}$  medium were seeded into cell culture insert chambers containing 8  $\mu\text{m}$  pores (migration chambers: 353097, BD Falcon; invasion chambers with ECM coating: 354483, BD Falcon) in triplicate. Subsequently, the bottoms of chambers were filled with 700  $\mu\text{L}$  of growth medium containing 20% FBS, and cells were incubated in a tissue culture incubator at  $37^{\circ}\text{C}$  with 5%  $\text{CO}_2$ . After 24 hours, inserts were fixed with 4% PFA/PBS for 10 min. Cells that had not crossed the membrane were removed with a cotton swab, and cells on the bottom of the membrane were stained with DAPI. Images of five fields per insert were taken with a Leica DMI 4000 microscope and stained cells were counted using an ImageJ software plugin developed in-house. Subsequently, inserts were stained in crystal violet solution (0.125% crystal violet,

20%MeOH) for 10 minutes, followed by washing in a large volume of dH<sub>2</sub>O and drying over night. Images of crystal violet stained inserts were taken with an AxioVert microscope (Zeiss, Germany).

### *3D matrigel culture*

Growth factor-reduced matrigel (356230, BD) stock was thawed on ice and diluted to 4 mg/mL protein with ice-cold, serum-free growth medium. Cells were trypsinized, resuspended in ice-cold normal growth medium and counted using a CASY cell counter (Roche, Switzerland). A pellet of 2500 cells was resuspended in 10  $\mu$ L of pre-diluted matrigel and transferred to one well of a  $\mu$ -slide angiogenesis microscopy slide (ibidi, Martinsried, Germany). After an incubation of 20 min in a tissue culture incubator to allow solidification of the gel, 50  $\mu$ L of normal growth medium was added to each well. Growth medium was replenished every third day. After 5 days of growth, structures were photographed using a Leica DMIL microscope.

### *Affymetrix gene expression profiling*

RNA was isolated using Quiazol lysis reagent (Quiagen). RNA quality and quantity was evaluated using an Agilent 2100 Bioanalyzer (Agilent Technologies). The manufacturer's protocols for the GeneChip platform by Affymetrix were followed. Methods included synthesis of the first- and second-strand cDNA followed by synthesis of cRNA by *in vitro* transcription, subsequent synthesis of single-stranded cDNA, biotin labeling and fragmentation of cDNA and hybridization with the microarray slide (GeneChip® Mouse Gene 1.0 ST array), posthybridization washings and detection of the hybridized cDNAs using a streptavidin-coupled fluorescent dye. Hybridized Affimetric GeneChips were scanned using an Affimetric GeneChip 3000 scanner. Image generation and feature extraction were performed using Affimetric GCOS Software and quality control was performed using Affimetric Expression Console Software. Raw microarray data were normalized with Robust Multi-Array (RMA) and analyzed using Partek® Genomics Suite Software (Partek Inc.). One-way analysis of variance (ANOVA) and asymptotic analysis were used to identify significantly differentially expressed genes. Ingenuity pathway analysis software (IPA) was used for further analyses.

*Ingenuity Pathway analysis*

The functional analysis identified the biological functions and/or diseases that were most significant to the data set. Molecules from the dataset that met the fold change cutoff of 2 were considered for the analysis and were associated with biological functions in the Ingenuity Knowledge Base. Right-tailed Fisher's exact test was used to calculate a p-value determining the probability that each biological function assigned to that data set is due to chance alone. Canonical pathways analysis identified the pathways from the IPA library of canonical pathways that were most significant to the data set. Molecules from the data set that met the fold change cutoff of 2 were considered for the analysis were associated with canonical pathways in the Ingenuity Knowledge Base. The significance of the association between the data set and the canonical pathway was measured in 2 ways: 1) A ratio of the number of molecules from the data set that map to the pathway divided by the total number of molecules that map to the canonical pathway is displayed. 2) Fisher's exact test was used to calculate a p-value determining the probability that the association between the genes in the dataset and the canonical pathway is explained by chance alone.

*Statistical analysis*

Statistical analysis and graphs were generated using the GraphPad Prism software (GraphPad Software Inc, San Diego, CA). All statistical analyses were performed by unpaired, two-sided t-test

---

## 4. References

- Acloque, H., Adams, M.S., Fishwick, K., Bronner-Fraser, M., and Nieto, M.A. (2009). Epithelial-mesenchymal transitions: the importance of changing cell state in development and disease. *J. Clin. Invest.* *119*, 1438–1449.
- Al-Hajj, M., Wicha, M.S., Benito-Hernandez, A., Morrison, S.J., and Clarke, M.F. (2003). Prospective identification of tumorigenic breast cancer cells. *Proc Natl Acad Sci USA* *100*, 3983–3988.
- Alcorn, J.F., Guala, A.S., van der Velden, J., McElhinney, B., Irvin, C.G., Davis, R.J., and Janssen-Heininger, Y.M.W. (2008). Jun N-terminal kinase 1 regulates epithelial-to-mesenchymal transition induced by TGF-beta1. *J Cell Sci* *121*, 1036–1045.
- Anbanandam, A., Albarado, D.C., Nguyen, C.T., Halder, G., Gao, X., and Veeraraghavan, S. (2006). Insights into transcription enhancer factor 1 (TEF-1) activity from the solution structure of the TEA domain. *Proc Natl Acad Sci USA* *103*, 17225–17230.
- Andrechek, E.R., White, D., and Muller, W.J. (2005). Targeted disruption of ErbB2/Neu in the mammary epithelium results in impaired ductal outgrowth. *Oncogene* *24*, 932–937.
- Asiedu, M.K., Ingle, J.N., Behrens, M.D., Radisky, D.C., and Knutson, K.L. (2011). TGFbeta/TNF(alpha)-mediated epithelial-mesenchymal transition generates breast cancer stem cells with a claudin-low phenotype. *Cancer Res* *71*, 4707–4719.
- Badouel, C., Gardano, L., Amin, N., Garg, A., Rosenfeld, R., Le Bihan, T., and McNeill, H. (2009). The FERM-domain protein Expanded regulates Hippo pathway activity via direct interactions with the transcriptional activator Yorkie. *Dev Cell* *16*, 411–420.
- Bakin, A.V., Rinehart, C., Tomlinson, A.K., and Arteaga, C.L. (2002). p38 mitogen-activated protein kinase is required for TGFbeta-mediated fibroblastic transdifferentiation and cell migration. *J Cell Sci* *115*, 3193–3206.
- Bakin, A.V.A., Tomlinson, A.K.A., Bhowmick, N.A.N., Moses, H.L.H., and Arteaga, C.L.C. (2000). Phosphatidylinositol 3-kinase function is required for transforming growth factor beta-mediated epithelial to mesenchymal transition and cell migration. *J Biol Chem* *275*, 36803–36810.
- Balwiercz, P.J., Carninci, P., Daub, C.O., Kawai, J., Hayashizaki, Y., Van Belle, W., Beisel, C., and van Nimwegen, E. (2009). Methods for analyzing deep sequencing expression data: constructing the human and mouse promoterome with deepCAGE data. *Genome Biol* *10*, R79.
- Barrallo-Gimeno, A., and Nieto, M.A. (2005). The Snail genes as inducers of cell movement and survival: implications in development and cancer. *Development* *132*, 3151–3161.
- Beckerle, M.C. (1997). Zyxin: Zinc fingers at sites of cell adhesion - Beckerle - 2005 - BioEssays - Wiley Online Library. *Bioessays* *19*, 949–957.
- Belandia, B., and Parker, M.G. (2000). Functional interaction between the p160 coactivator proteins and the transcriptional enhancer factor family of transcription factors. *J Biol Chem* *275*, 30801–30805.
- Benhaddou, A., Keime, C., Ye, T., Morlon, A., Michel, I., Jost, B., Mengus, G., and Davidson, I. (2012). Transcription factor TEAD4 regulates expression of myogenin and the unfolded protein response genes during C2C12 cell differentiation. *Cell Death & Differentiation* *19*, 220–231.
- Bertos, N.R., and Park, M. (2011). Breast cancer - one term, many entities? *J. Clin. Invest.* *121*, 3789–3796.
- Bhowmick, N.A., Ghiassi, M., Bakin, A., Aakre, M., Lundquist, C.A., Engel, M.E., Arteaga, C.L., and Moses, H.L. (2001). Transforming growth factor-beta1 mediates epithelial to mesenchymal transdifferentiation through a RhoA-dependent mechanism. *Mol Biol Cell* *12*, 27–36.

- 
- Biddle, A., and Mackenzie, I.C. (2012). Cancer stem cells and EMT in carcinoma. *Cancer Metastasis Rev.* Pubmed ID 22302111
- Biswas, S., Guix, M., Rinehart, C., Dugger, T.C., Chytil, A., Moses, H.L., Freeman, M.L., and Arteaga, C.L. (2007). Inhibition of TGF-beta with neutralizing antibodies prevents radiation-induced acceleration of metastatic cancer progression. *J Clin Invest* 117, 1305–1313.
- Blanpain, C., Horsley, V., and Fuchs, E. (2007). Epithelial stem cells: turning over new leaves. *Cell* 128, 445–458.
- Blatt, C., and DePamphilis, M.L. (1993). Striking homology between mouse and human transcription enhancer factor-1 (TEF-1). *Nucleic Acids Res* 21, 747–748.
- Boggiano, J.C., and Fehon, R.G. (2012). Growth control by committee: intercellular junctions, cell polarity, and the cytoskeleton regulate hippo signaling. *Dev Cell* 22, 695–702.
- Boulanger, C.A., and Smith, G.H. (2001). Reducing mammary cancer risk through premature stem cell senescence. *Oncogene* 20, 2264–2272.
- Brabletz, T., Jung, A., Spaderna, S., Hlubek, F., and Kirchner, T. (2005). Opinion: migrating cancer stem cells - an integrated concept of malignant tumour progression. *Nat Rev Cancer* 5, 744–749.
- Breasted, J. (1930). *Breasted: The Edwin Smith Surgical Papyrus*. University... - Google Scholar (University of Chicago Press).
- Brook, W.J., Diaz-Benjumea, F.J., and Cohen, S.M. (1996). Organizing spatial pattern in limb development. *Annu Rev Cell Dev Biol* 12, 161–180.
- Burk, U., Schubert, J., Wellner, U., Schmalhofer, O., Vincan, E., Spaderna, S., and Brabletz, T. (2008). A reciprocal repression between ZEB1 and members of the miR-200 family promotes EMT and invasion in cancer cells. *EMBO Rep* 9, 582–589.
- Butler, A.J., and Ordahl, C.P. (1999). Poly(ADP-ribose) polymerase binds with transcription enhancer factor 1 to MCAT1 elements to regulate muscle-specific transcription. *Mol Cell Biol* 19, 296–306.
- Campbell, L.L., and Polyak, K. (2007). Breast Tumor Heterogeneity: Cancer Stem Cells or Clonal Evolution? *Cell Cycle* 6, 2332–2338.
- Campbell, S., Inamdar, M., Rodrigues, V., Raghavan, V., Palazzolo, M., and Chovnick, A. (1992). The scalloped gene encodes a novel, evolutionarily conserved transcription factor required for sensory organ differentiation in *Drosophila*. *Genes Dev* 6, 367–379.
- Cardiff, R.D. (2010). The pathology of EMT in mouse mammary tumorigenesis. *J Mammary Gland Biol Neoplasia* 15, 225–233.
- Cardiff, R.D., Anver, M.R., Gusterson, B.A., Hennighausen, L., Jensen, R.A., Merino, M.J., Rehm, S., Russo, J., Tavassoli, F.A., Wakefield, L.M., et al. (2000). The mammary pathology of genetically engineered mice: the consensus report and recommendations from the Annapolis meeting. *Oncogene* 19, 968–988.
- Cardiff, R.D., Couto, S., and Bolon, B. (2011). Three interrelated themes in current breast cancer research: gene addiction, phenotypic plasticity, and cancer stem cells. *Breast Cancer Res* 13, 216.
- Cavallaro, U., and Christofori, G. (2004). Cell adhesion and signalling by cadherins and Ig-CAMs in cancer. *Nat Rev Cancer* 4, 118–132.
- Chaffer, C.L., and Weinberg, R.A. (2011). A perspective on cancer cell metastasis. *Science* 331, 1559–1564.

- 
- Chan, S.W., Lim, C.J., Chong, Y.F., Pobbati, A.V., Huang, C., and Hong, W. (2011). Hippo Pathway-independent Restriction of TAZ and YAP by Angiomotin. *Journal of Biological Chemistry* 286, 7018–7026.
- Chan, S.W., Lim, C.J., Guo, K., Ng, C.P., Lee, I., Hunziker, W., Zeng, Q., and Hong, W. (2008). A role for TAZ in migration, invasion, and tumorigenesis of breast cancer cells. *Cancer Res* 68, 2592–2598.
- Chan, S.W., Lim, C.J., Loo, L.S., Chong, Y.F., Huang, C., and Hong, W. (2009). TEADs mediate nuclear retention of TAZ to promote oncogenic transformation. *J Biol Chem* 284, 14347–14358.
- Chen, Z., Friedrich, G.A., and Soriano, P. (1994). Transcriptional enhancer factor 1 disruption by a retroviral gene trap leads to heart defects and embryonic lethality in mice. *Genes Dev* 8, 2293–2301.
- Clevers, H. (2011). The cancer stem cell: premises, promises and challenges. *Nature Medicine* 17, 313–319.
- Colombo, P.-E., Milanezi, F., Weigelt, B., and Reis-Filho, J.S. (2011). Microarrays in the 2010s: the contribution of microarray-based gene expression profiling to breast cancer classification, prognostication and prediction. *Breast Cancer Research* 2007 9:R38 13, 212.
- Comijn, J., Berx, G., Vermassen, P., Verschuere, K., van Grunsven, L., Bruyneel, E., Mareel, M., Huylebroeck, D., and Van Roy, F. (2001). The two-handed E box binding zinc finger protein SIP1 downregulates E-cadherin and induces invasion. *Mol Cell* 7, 1267–1278.
- Cordenonsi, M., Zanconato, F., Azzolin, L., Forcato, M., Rosato, A., Frasson, C., Inui, M., Montagner, M., Parenti, A.R., Poletti, A., et al. (2011). The Hippo Transducer TAZ Confers Cancer Stem Cell-Related Traits on Breast Cancer Cells. *Cell* 147, 759–772.
- Creighton, C.J., Li, X., Landis, M., Dixon, J.M., Neumeister, V.M., Sjolund, A., Rimm, D.L., Wong, H., Rodriguez, A., Herschkowitz, J.I., et al. (2009). Residual breast cancers after conventional therapy display mesenchymal as well as tumor-initiating features. *Proc Natl Acad Sci USA* 106, 13820–13825.
- Dalal, B.I., Keown, P.A., and Greenberg, A.H. (1993). Immunocytochemical localization of secreted transforming growth factor-beta 1 to the advancing edges of primary tumors and to lymph node metastases of human mammary carcinoma. *Am J Pathol* 143, 381–389.
- Damonte, P., Gregg, J.P., Borowsky, A.D., Keister, B.A., and Cardiff, R.D. (2007). EMT tumorigenesis in the mouse mammary gland. *Lab Invest* 87, 1218–1226.
- Dave, B., Mittal, V., Tan, N.M., and Chang, J.C. (2012). Epithelial-mesenchymal transition, cancer stem cells and treatment resistance. *Breast Cancer Res* 14, 202.
- Davidson, I., Xiao, J.H., Rosales, R., Staub, A., and Chambon, P. (1988). The HeLa cell protein TEF-1 binds specifically and cooperatively to two SV40 enhancer motifs of unrelated sequence. *Cell* 54, 931–942.
- Dennler, S., Itoh, S., Vivien, D., Dijke, ten, P., Huet, S., and Gauthier, J.M. (1998). Direct binding of Smad3 and Smad4 to critical TGF beta-inducible elements in the promoter of human plasminogen activator inhibitor-type 1 gene. *Embo J* 17, 3091–3100.
- Derksen, P.W.B., Liu, X., Saridin, F., van der Gulden, H., Zevenhoven, J., Evers, B., van Beijnum, J.R., Griffioen, A.W., Vink, J., Krimpenfort, P., et al. (2006). Somatic inactivation of E-cadherin and p53 in mice leads to metastatic lobular mammary carcinoma through induction of anoikis resistance and angiogenesis. *Cancer Cell* 10, 437–449.
- Deshpande, N., Chopra, A., Rangarajan, A., Shashidhara, L.S., Rodrigues, V., and Krishna, S. (1997). The human transcription enhancer factor-1, TEF-1, can substitute for *Drosophila* scalloped during wingblade development. *J Biol Chem* 272, 10664–10668.
- Dilworth, S.M. (2002). Polyoma virus middle T antigen and its role in identifying cancer-related molecules. *Nat Rev Cancer* 2, 951–956.
-

- 
- Dong, J., Feldmann, G., Huang, J., Wu, S., Zhang, N., Comerford, S.A., Gayyed, M.F., Anders, R.A., Maitra, A., and Pan, D. (2007). Elucidation of a universal size-control mechanism in *Drosophila* and mammals. *Cell* *130*, 1120–1133.
- Drasin, D.J., Robin, T.P., and Ford, H.L. (2011). Breast cancer epithelial-to-mesenchymal transition: examining the functional consequences of plasticity. *Breast Cancer Res* *13*, 226.
- Dupont, S., Morsut, L., Aragona, M., Enzo, E., Giulitti, S., Cordenonsi, M., Zanconato, F., Le Digabel, J., Forcato, M., Bicciato, S., et al. (2011). Role of YAP/TAZ in mechanotransduction. *Nature* *474*, 179–183.
- Dvorak, H.F. (1986). Tumors: Wounds That Do Not Heal. *New England Journal of Medicine* *315*, 1650–1659.
- Eger, A., Aigner, K., Sonderegger, S., Dampier, B., Oehler, S., Schreiber, M., Berx, G., Cano, A., Beug, H., and Foisner, R. (2005). DeltaEF1 is a transcriptional repressor of E-cadherin and regulates epithelial plasticity in breast cancer cells. *Oncogene* *24*, 2375–2385.
- FANTOM Consortium, Suzuki, H., Forrest, A.R.R., van Nimwegen, E., Daub, C.O., Balwierz, P.J., Irvine, K.M., Lassmann, T., Ravasi, T., Hasegawa, Y., et al. (2009). The transcriptional network that controls growth arrest and differentiation in a human myeloid leukemia cell line. *Nat. Genet.* *41*, 553–562.
- Fantozzi, A., and Christofori, G. (2006). Mouse models of breast cancer metastasis. *Breast Cancer Res* *8*, 212.
- Feng, X.-H., and Derynck, R. (2005). Specificity and versatility in tgf-beta signaling through Smads. *Annu Rev Cell Dev Biol* *21*, 659–693.
- Fernández, B.G., Gaspar, P., Brás-Pereira, C., Jezowska, B., Rebelo, S.R., and Janody, F. (2011). Actin-Capping Protein and the Hippo pathway regulate F-actin and tissue growth in *Drosophila*. *Development* *138*, 2337–2346.
- Friedl, P. (2004). Prespecification and plasticity: shifting mechanisms of cell migration. *Curr Opin Cell Biol* *16*, 14–23.
- Garg, A., Srivastava, A., Davis, M.M., O'Keefe, S.L., Chow, L., and Bell, J.B. (2007). Antagonizing scalloped with a novel vestigial construct reveals an important role for scalloped in *Drosophila melanogaster* leg, eye and optic lobe development. *Genetics* *175*, 659–669.
- Goulev, Y., Fauny, J.D., Gonzalez-Marti, B., Flagiello, D., Silber, J., and Zider, A. (2008). SCALLOPED interacts with YORKIE, the nuclear effector of the hippo tumor-suppressor pathway in *Drosophila*. *Curr Biol* *18*, 435–441.
- Gregory, P.A., Bert, A.G., Paterson, E.L., Barry, S.C., Tsykin, A., Farshid, G., Vadas, M.A., Khew-Goodall, Y., and Goodall, G.J. (2008). The miR-200 family and miR-205 regulate epithelial to mesenchymal transition by targeting ZEB1 and SIP1. *Nat Cell Biol* *10*, 593–601.
- Gupta, M.P., Amin, C.S., Gupta, M., Hay, N., and Zak, R. (1997). Transcription enhancer factor 1 interacts with a basic helix-loop-helix zipper protein, Max, for positive regulation of cardiac alpha-myosin heavy-chain gene expression. *Mol Cell Biol* *17*, 3924–3936.
- Guss, K.A., Nelson, C.E., Hudson, A., Kraus, M.E., and Carroll, S.B. (2001). Control of a genetic regulatory network by a selector gene. *Science* *292*, 1164–1167.
- Guttilla, I.K., Adams, B.D., and White, B.A. (2012). ER $\alpha$ , microRNAs, and the epithelial-mesenchymal transition in breast cancer. *Trends Endocrinol. Metab.* *23*, 73–82.
- Guy, C.T., Cardiff, R.D., and Muller, W.J. (1992). Induction of mammary tumors by expression of polyomavirus middle T oncogene: a transgenic mouse model for metastatic disease. *Mol Cell Biol* *12*, 954–961.
- Halder, G., and Johnson, R.L. (2011). Hippo signaling: growth control and beyond. *Development* *138*, 9–22.
-



- 
- Halder, G., Polaczyk, P., Kraus, M.E., Hudson, A., Kim, J., Laughon, A., and Carroll, S. (1998). The Vestigial and Scalloped proteins act together to directly regulate wing-specific gene expression in *Drosophila*. *Genes Dev* *12*, 3900–3909.
- Hamaratoglu, F., Willecke, M., Kango-Singh, M., Nolo, R., Hyun, E., Tao, C., Jafar-Nejad, H., and Halder, G. (2006). The tumour-suppressor genes NF2/Merlin and Expanded act through Hippo signalling to regulate cell proliferation and apoptosis. *Nat Cell Biol* *8*, 27–36.
- Hanahan, D., and Weinberg, R.A. (2000). The hallmarks of cancer. *Cell* *100*, 57–70.
- Hanahan, D., and Weinberg, R.A. (2011). Hallmarks of cancer: the next generation. *Cell* *144*, 646–674.
- Hennessy, B.T., Gonzalez-Angulo, A.-M., Stenke-Hale, K., Gilcrease, M.Z., Krishnamurthy, S., Lee, J.-S., Fridlyand, J., Sahin, A., Agarwal, R., Joy, C., et al. (2009). Characterization of a naturally occurring breast cancer subset enriched in epithelial-to-mesenchymal transition and stem cell characteristics. *Cancer Res* *69*, 4116–4124.
- Herreros, A.G., Peiró, S., Nassour, M., and Savagner, P. (2010). Snail Family Regulation and Epithelial Mesenchymal Transitions in Breast Cancer Progression. *J Mammary Gland Biol Neoplasia* *15*, 135–147.
- Herschkowitz, J.I., Simin, K., Weigman, V.J., Mikaelian, I., Usary, J., Hu, Z., Rasmussen, K.E., Jones, L.P., Assefnia, S., Chandrasekharan, S., et al. (2007). Identification of conserved gene expression features between murine mammary carcinoma models and human breast tumors. *Genome Biol* *8*, R76.
- Herschkowitz, J.I., Zhao, W., Zhang, M., Usary, J., Murrow, G., Edwards, D., Knezevic, J., Greene, S.B., Darr, D., Troester, M.A., et al. (2012). Comparative oncogenomics identifies breast tumors enriched in functional tumor-initiating cells. *Proc Natl Acad Sci USA* *109*, 2778–2783.
- Hoot, K.E., Lighthall, J., Han, G., Lu, S.-L., Li, A., Ju, W., Kulesz-Martin, M., Bottinger, E., and Wang, X.-J. (2008). Keratinocyte-specific Smad2 ablation results in increased epithelial-mesenchymal transition during skin cancer formation and progression. *J Clin Invest* *118*, 2722–2732.
- Huber, M.A., Kraut, N., and Beug, H. (2005). Molecular requirements for epithelial-mesenchymal transition during tumor progression. *Curr Opin Cell Biol* *17*, 548–558.
- Jacquemin, P., Hwang, J.J., Martial, J.A., Dollé, P., and Davidson, I. (1996). A novel family of developmentally regulated mammalian transcription factors containing the TEA/ATTS DNA binding domain. *J Biol Chem* *271*, 21775–21785.
- Janda, E., Lehmann, K., Killisch, I., Jechlinger, M., Herzig, M., Downward, J., Beug, H., and Grünert, S. (2002). Ras and TGF[ $\beta$ ] cooperatively regulate epithelial cell plasticity and metastasis: dissection of Ras signaling pathways. *J Cell Biol* *156*, 299–313.
- Janda, E., Nevolo, M., Lehmann, K., Downward, J., Beug, H., and Grieco, M. (2006). Raf plus TGF $\beta$ -dependent EMT is initiated by endocytosis and lysosomal degradation of E-cadherin. *Oncogene* *25*, 7117–7130.
- Jeanes, A., Gottardi, C.J., and Yap, A.S. (2008). Cadherins and cancer: how does cadherin dysfunction promote tumor progression? *Oncogene* *27*, 6920–6929.
- Jiang, S.W., and Eberhardt, N.L. (1996). TEF-1 transrepression in BeWo cells is mediated through interactions with the TATA-binding protein, TBP. *J Biol Chem* *271*, 9510–9518.
- Joyce, J.A., and Pollard, J.W. (2009). Microenvironmental regulation of metastasis. *Nat Rev Cancer* *9*, 239–252.
- Kalluri, R., and Weinberg, R.A. (2009). The basics of epithelial-mesenchymal transition. *J. Clin. Invest.* *119*, 1420–1428.
-

- 
- Kanai, F., Marignani, P.A., Sarbassova, D., Yagi, R., Hall, R.A., Donowitz, M., Hisaminato, A., Fujiwara, T., Ito, Y., Cantley, L.C., et al. (2000). TAZ: a novel transcriptional co-activator regulated by interactions with 14-3-3 and PDZ domain proteins. *Embo J* 19, 6778.
- Kaneko, K.J., and DePamphilis, M.L. (1998). Regulation of gene expression at the beginning of mammalian development and the TEAD family of transcription factors. *Dev. Genet.* 22, 43–55.
- Kaneko, K.J., Cullinan, E.B., Latham, K.E., and DePamphilis, M.L. (1997). Transcription factor mTEAD-2 is selectively expressed at the beginning of zygotic gene expression in the mouse. *Development* 124, 1963–1973.
- Kaneko, K.J., Kohn, M.J., Liu, C., and Depamphilis, M.L. (2007). Transcription factor TEAD2 is involved in neural tube closure. *Genesis* 45, 577–587.
- Keller, P.J., Lin, A., Arendt, L.M., Klebba, I., Jones, A.D., Rudnick, J.A., Dimeo, T.A., Gilmore, H., Jefferson, D.M., Graham, R.A., et al. (2010). Mapping the cellular and molecular heterogeneity of normal and malignant breast tissues and cultured cell lines. *Breast Cancer Res* 12, R87.
- Kim, N.-G., Koh, E., Chen, X., and Gumbiner, B.M. (2011). E-cadherin mediates contact inhibition of proliferation through Hippo signaling-pathway components. *Proc Natl Acad Sci USA* 108, 11930–11935.
- Klymkowsky, M.W., and Savagner, P. (2009). Epithelial-Mesenchymal Transition. A Cancer Researcher's Conceptual Friend and Foe. *Am J Pathol* 174, 1588–1593.
- Korpala, M., Lee, E.S., Hu, G., and Kang, Y. (2008). The miR-200 Family Inhibits Epithelial-Mesenchymal Transition and Cancer Cell Migration by Direct Targeting of E-cadherin Transcriptional Repressors ZEB1 and ZEB2. *J Biol Chem* 283, 14910–14914.
- Lai, D., Ho, K.C., Hao, Y., and Yang, X. (2011). Taxol resistance in breast cancer cells is mediated by the hippo pathway component TAZ and its downstream transcriptional targets Cyr61 and CTGF. *Cancer Res* 71, 2728–2738.
- Larkin, S.B., Farrance, I.K., and Ordahl, C.P. (1996). Flanking sequences modulate the cell specificity of M-CAT elements. *Mol Cell Biol* 16, 3742–3755.
- Lee, J.M., Dedhar, S., Kalluri, R., and Thompson, E.W. (2006). The epithelial-mesenchymal transition: new insights in signaling, development, and disease. *J Cell Biol* 172, 973–981.
- Lee, M.K., Pardoux, C., Hall, M.C., Lee, P.S., Warburton, D., Qing, J., Smith, S.M., and Derynck, R. (2007). TGF-beta activates Erk MAP kinase signalling through direct phosphorylation of ShcA. *Embo J* 26, 3957–3967.
- Lehembre, F., Yilmaz, M., Wicki, A., Schomber, T., Strittmatter, K., Ziegler, D., Kren, A., Went, P., Derksen, P.W.B., Berns, A., et al. (2008). NCAM-induced focal adhesion assembly: a functional switch upon loss of E-cadherin. *Embo J* 27, 2603–2615.
- Lei, Q.-Y., Zhang, H., Zhao, B., Zha, Z.-Y., Bai, F., Pei, X.-H., Zhao, S., Xiong, Y., and Guan, K.-L. (2008). TAZ promotes cell proliferation and epithelial-mesenchymal transition and is inhibited by the hippo pathway. *Mol Cell Biol* 28, 2426–2436.
- Lim, E., Vaillant, F., Wu, D., Forrest, N.C., Pal, B., Hart, A.H., Asselin-Labat, M.-L., Gyorki, D.E., Ward, T., Partanen, A., et al. (2009). Aberrant luminal progenitors as the candidate target population for basal tumor development in BRCA1 mutation carriers. *Nature Medicine* 15, 907–913.
- Lim, E., Wu, D., Pal, B., Bouras, T., Asselin-Labat, M.-L., Vaillant, F., Yagita, H., Lindeman, G.J., Smyth, G.K., and Visvader, J.E. (2010). Transcriptome analyses of mouse and human mammary cell subpopulations reveal multiple conserved genes and pathways. *Breast Cancer Res* 12, R21.
-

- Lin, E.Y., Jones, J.G., Li, P., Zhu, L., Whitney, K.D., Muller, W.J., and Pollard, J.W. (2003). Progression to malignancy in the polyoma middle T oncoprotein mouse breast cancer model provides a reliable model for human diseases. *Am J Pathol* *163*, 2113–2126.
- Maeda, M., Johnson, K.R., and Wheelock, M.J. (2005). Cadherin switching: essential for behavioral but not morphological changes during an epithelium-to-mesenchyme transition. *J Cell Sci* *118*, 873–887.
- Maeda, T., Chapman, D.L., and Stewart, A.F.R. (2002). Mammalian vestigial-like 2, a cofactor of TEF-1 and MEF2 transcription factors that promotes skeletal muscle differentiation. *J Biol Chem* *277*, 48889–48898.
- Magee, J.A., Piskounova, E., and Morrison, S.J. (2012). Cancer stem cells: impact, heterogeneity, and uncertainty. *Cancer Cell* *21*, 283–296.
- Maglione, J.E., Moghanaki, D., Young, L.J., Manner, C.K., Ellies, L.G., Joseph, S.O., Nicholson, B., Cardiff, R.D., and MacLeod, C.L. (2001). Transgenic Polyoma middle-T mice model premalignant mammary disease. *Cancer Res* *61*, 8298–8305.
- Mahler-Araujo, B., Savage, K., Parry, S., and Reis-Filho, J.S. (2008). Reduction of E-cadherin expression is associated with non-lobular breast carcinomas of basal-like and triple negative phenotype. *J. Clin. Pathol.* *61*, 615–620.
- Mahoney, W.M., Hong, J.-H., Yaffe, M.B., and Farrance, I.K.G. (2005). The transcriptional co-activator TAZ interacts differentially with transcriptional enhancer factor-1 (TEF-1) family members. *Biochem. J.* *388*, 217–225.
- Mani, S.A., Guo, W., Liao, M.-J., Eaton, E.N., Ayyanan, A., Zhou, A.Y., Brooks, M., Reinhard, F., Zhang, C.C., Shipitsin, M., et al. (2008). The epithelial-mesenchymal transition generates cells with properties of stem cells. *Cell* *133*, 704–715.
- Massagué, J. (2008). TGFbeta in Cancer. *Cell* *134*, 215–230.
- Massagué, J., and Gomis, R.R. (2006). The logic of TGFbeta signaling. *FEBS Lett* *580*, 2811–2820.
- May, C.D., Sphyris, N., Evans, K.W., Werden, S.J., Guo, W., and Mani, S.A. (2011). Epithelial-mesenchymal transition and cancer stem cells: a dangerously dynamic duo in breast cancer progression. *Breast Cancer Res* *13*, 202.
- McCoy, E.L., Iwanaga, R., Jedlicka, P., Abbey, N.-S., Chodosh, L.A., Heichman, K.A., Welm, A.L., and Ford, H.L. (2009). Six1 expands the mouse mammary epithelial stem/progenitor cell pool and induces mammary tumors that undergo epithelial-mesenchymal transition. *J. Clin. Invest.* *119*, 2663–2677.
- Meyer, D.S., Brinkhaus, H., Muller, U., Muller, M., Cardiff, R.D., and Bentires-Alj, M. (2011). Luminal Expression of PIK3CA Mutant H1047R in the Mammary Gland Induces Heterogeneous Tumors. *Cancer Res* *71*, 4344–4351.
- Micalizzi, D.S., Farabaugh, S.M., and Ford, H.L. (2010). Epithelial-mesenchymal transition in cancer: parallels between normal development and tumor progression. *J Mammary Gland Biol Neoplasia* *15*, 117–134.
- Miettinen, P.J., Ebner, R., Lopez, A.R., and Derynck, R. (1994). TGF-beta induced transdifferentiation of mammary epithelial cells to mesenchymal cells: involvement of type I receptors. *J Cell Biol* *127*, 2021–2036.
- Milewski, R.C., Chi, N.C., Li, J., Brown, C., Lu, M.M., and Epstein, J.A. (2004). Identification of minimal enhancer elements sufficient for Pax3 expression in neural crest and implication of Tead2 as a regulator of Pax3. *Development* *131*, 829–837.
- Moody, S.E., Sarkisian, C.J., Hahn, K.T., Gunther, E.J., Pickup, S., Dugan, K.D., Innocent, N., Cardiff, R.D., Schnall, M.D., and Chodosh, L.A. (2002). Conditional activation of Neu in the mammary epithelium of transgenic mice results in reversible pulmonary metastasis. *Cancer Cell* *2*, 451–461.

- 
- Morel, A.-P., Lièvre, M., Thomas, C., Hinkal, G., Ansieau, S., and Puisieux, A. (2008). Generation of breast cancer stem cells through epithelial-mesenchymal transition. *PLoS ONE* 3, e2888.
- Moreno-Bueno, G., Portillo, F., and Cano, A. (2008). Transcriptional regulation of cell polarity in EMT and cancer. *Oncogene* 27, 6958–6969.
- Morgenstern, J.P., and Land, H. (1990). Advanced mammalian gene transfer: high titre retroviral vectors with multiple drug selection markers and a complementary helper-free packaging cell line. *Nucleic Acids Res* 18, 3587–3596.
- Mori, M., Nakagami, H., Koibuchi, N., Miura, K., Takami, Y., Koriyama, H., Hayashi, H., Sabe, H., Mochizuki, N., Morishita, R., et al. (2009). Zyxin mediates actin fiber reorganization in epithelial-mesenchymal transition and contributes to endocardial morphogenesis. *Mol Biol Cell* 20, 3115–3124.
- Morin-Kensicki, E.M., Boone, B.N., Howell, M., Stonebraker, J.R., Teed, J., Alb, J.G., Magnuson, T.R., O'Neal, W., and Milgram, S.L. (2006). Defects in yolk sac vasculogenesis, chorioallantoic fusion, and embryonic axis elongation in mice with targeted disruption of Yap65. *Mol Cell Biol* 26, 77–87.
- Morita, S., Kojima, T., and Kitamura, T. (2000). Plat-E: an efficient and stable system for transient packaging of retroviruses. *Gene Ther.* 7, 1063–1066.
- Moses, H., and Barcellos-Hoff, M.H. (2011). TGF-beta biology in mammary development and breast cancer. *Cold Spring Harbor Perspectives in Biology* 3, a003277.
- Moustakas, A., and Heldin, C.-H. (2007). Signaling networks guiding epithelial-mesenchymal transitions during embryogenesis and cancer progression. *Cancer Sci* 98, 1512–1520.
- Muller, W.J., Sinn, E., Pattengale, P.K., Wallace, R., and Leder, P. (1988). Single-step induction of mammary adenocarcinoma in transgenic mice bearing the activated c-neu oncogene. *Cell* 54, 105–115.
- Nam, J.-S., Terabe, M., Mamura, M., Kang, M.-J., Chae, H., Stuelten, C., Kohn, E., Tang, B., Sabzevari, H., Anver, M.R., et al. (2008). An anti-transforming growth factor beta antibody suppresses metastasis via cooperative effects on multiple cell compartments. *Cancer Res* 68, 3835–3843.
- Neto-Silva, R.M., de Beco, S., and Johnston, L.A. (2010). Evidence for a growth-stabilizing regulatory feedback mechanism between Myc and Yorkie, the Drosophila homolog of Yap. *Dev Cell* 19, 507–520.
- Nieto, M.A. (2011). The ins and outs of the epithelial to mesenchymal transition in health and disease. *Annu Rev Cell Dev Biol* 27, 347–376.
- Nowell, P.C. (1976). The clonal evolution of tumor cell populations. *Science* 194, 23–28.
- Oft, M., Heider, K.H., and Beug, H. (1998). TGFbeta signaling is necessary for carcinoma cell invasiveness and metastasis. *Curr Biol* 8, 1243–1252.
- Oft, M., Peli, J., Rudaz, C., Schwarz, H., Beug, H., and Reichmann, E. (1996). TGF-beta1 and Ha-Ras collaborate in modulating the phenotypic plasticity and invasiveness of epithelial tumor cells. *Genes Dev* 10, 2462–2477.
- Oh, H., Reddy, B.V.V.G., and Irvine, K.D. (2009). Phosphorylation-independent repression of Yorkie in Fat-Hippo signaling. *Dev Biol* 335, 188–197.
- Onder, T.T., Gupta, P.B., Mani, S.A., Yang, J., Lander, E.S., and Weinberg, R.A. (2008). Loss of E-cadherin promotes metastasis via multiple downstream transcriptional pathways. *Cancer Res* 68, 3645–3654.
- Ota, M., and Sasaki, H. (2008). Mammalian Tead proteins regulate cell proliferation and contact inhibition as transcriptional mediators of Hippo signaling. *Development* 135, 4059–4069.

- 
- Overholtzer, M., Zhang, J., Smolen, G.A., Muir, B., Li, W., Sgroi, D.C., Deng, C.-X., Brugge, J.S., and Haber, D.A. (2006). Transforming properties of YAP, a candidate oncogene on the chromosome 11q22 amplicon. *Proc Natl Acad Sci USA* *103*, 12405–12410.
- Ozdamar, B., Bose, R., Barrios-Rodiles, M., Wang, H., Zhang, Y., and Wrana, J. (2005). Regulation of the polarity protein Par6 by TGF beta receptors controls epithelial cell plasticity. *Science* *307*, 1603–1609.
- Pachkov, M., Erb, I., Molina, N., and van Nimwegen, E. (2007). SwissRegulon: a database of genome-wide annotations of regulatory sites. *Nucleic Acids Res* *35*, D127–D131.
- Padua, D., and Massagué, J. (2009). Roles of TGF[ $\beta$ ] in metastasis. *Cell Res* *19*, 89.
- Pan, D. (2010). The hippo signaling pathway in development and cancer. *Dev Cell* *19*, 491–505.
- Parker, J.S., Mullins, M., Cheang, M.C.U., Leung, S., Voduc, D., Vickery, T., Davies, S., Fauron, C., He, X., Hu, Z., et al. (2009). Supervised risk predictor of breast cancer based on intrinsic subtypes. *J Clin Oncol* *27*, 1160–1167.
- Peinado, H., Olmeda, D., and Cano, A. (2007). Snail, Zeb and bHLH factors in tumour progression: an alliance against the epithelial phenotype? *Nat Rev Cancer* *7*, 415–428.
- Perl, A.K., Wilgenbus, P., Dahl, U., Semb, H., and Christofori, G. (1998). A causal role for E-cadherin in the transition from adenoma to carcinoma. *Nature* *392*, 190–193.
- Perou, C.M., Sørlie, T., Eisen, M.B., van de Rijn, M., Jeffrey, S.S., Rees, C.A., Pollack, J.R., Ross, D.T., Johnsen, H., Akslen, L.A., et al. (2000). Molecular portraits of human breast tumours. *Nature* *406*, 747–752.
- Petersen, O.W., Lind Nielsen, H., Gudjonsson, T., Villadsen, R., Rønnov-Jessen, L., and Bissell, M.J. (2001). The plasticity of human breast carcinoma cells is more than epithelial to mesenchymal conversion. *Breast Cancer Research* *2007* *9*:R38 *3*, 213–217.
- Polyak, K. (2007). Breast cancer: origins and evolution. *J Clin Invest* *117*, 3155–3163.
- Polyak, K., and Weinberg, R.A. (2009). Transitions between epithelial and mesenchymal states: acquisition of malignant and stem cell traits. *Nat Rev Cancer* *9*, 265–273.
- Postigo, A.A., Depp, J.L., Taylor, J.J., and Kroll, K.L. (2003). Regulation of Smad signaling through a differential recruitment of coactivators and corepressors by ZEB proteins. *Embo J* *22*, 2453–2462.
- Prat, A., and Perou, C.M. (2009). Mammary development meets cancer genomics. *Nature Medicine* *15*, 842–844.
- Prat, A., Parker, J.S., Karginova, O., Fan, C., Livasy, C., Herschkowitz, J.I., He, X., and Perou, C.M. (2010a). Phenotypic and molecular characterization of the claudin-low intrinsic subtype of breast cancer. *Breast Cancer Res* *12*, R68.
- Prat, A., Parker, J.S., Karginova, O., Fan, C., Livasy, C., Herschkowitz, J.I., He, X., and Perou, C.M. (2010b). Phenotypic and molecular characterization of the claudin-low intrinsic subtype of breast cancer. *Breast Cancer Res* *12*, R68.
- Ramalho-Santos, M., Yoon, S., Matsuzaki, Y., Mulligan, R.C., and Melton, D.A. (2002). “Stemness”: transcriptional profiling of embryonic and adult stem cells. *Science* *298*, 597–600.
- Rauskolb, C., Pan, G., Reddy, H., and Irvine, K.D. (2011). Zyxin links fat signaling to the hippo pathway. *PLoS Biol* *9*, e1000624.
-

- 
- Remue, E., Meerschaert, K., Oka, T., Boucherie, C., Vandekerckhove, J., Sudol, M., and Gettemans, J. (2010). TAZ interacts with zonula occludens-1 and -2 proteins in a PDZ-1 dependent manner. *FEBS Lett* *584*, 4175–4180.
- Robinson, B.S., and Moberg, K.H. (2011). Cell-Cell Junctions:  $\alpha$ -Catenin and E-Cadherin Help Fence In Yap1. *Curr Biol* *21*, R890–R892.
- Roh, M.H., Makarova, O., Liu, C.-J., Shin, K., Lee, S., Laurinec, S., Goyal, M., Wiggins, R., and Margolis, B. (2002). The Maguk protein, Pals1, functions as an adapter, linking mammalian homologues of Crumbs and Discs Lost. *J Cell Biol* *157*, 161–172.
- Sahai, E. (2005). Mechanisms of cancer cell invasion. *Curr Opin Genet Dev* *15*, 87–96.
- Sansores-Garcia, L., Bossuyt, W., Wada, K.-I., Yonemura, S., Tao, C., Sasaki, H., and Halder, G. (2011). Modulating F-actin organization induces organ growth by affecting the Hippo pathway. *Embo J* *30*, 2325–2335.
- Santibañez, J.F. (2006). JNK mediates TGF-beta1-induced epithelial mesenchymal transdifferentiation of mouse transformed keratinocytes. *FEBS Lett* *580*, 5385–5391.
- Sarrió, D., Rodríguez-Pinilla, S.M., Hardisson, D., Cano, A., Moreno-Bueno, G., and Palacios, J. (2008). Epithelial-mesenchymal transition in breast cancer relates to the basal-like phenotype. *Cancer Res* *68*, 989–997.
- Savagner, P. (2010). The epithelial-mesenchymal transition (EMT) phenomenon. *Annals of Oncology* *21*, vii89–vii92.
- Sawada, A., Kiyonari, H., Ukita, K., Nishioka, N., Imuta, Y., and Sasaki, H. (2008). Redundant roles of Tead1 and Tead2 in notochord development and the regulation of cell proliferation and survival. *Mol Cell Biol* *28*, 3177–3189.
- Sawada, A., Nishizaki, Y., Sato, H., Yada, Y., Nakayama, R., Yamamoto, S., Nishioka, N., Kondoh, H., and Sasaki, H. (2005). Tead proteins activate the Foxa2 enhancer in the node in cooperation with a second factor. *Development* *132*, 4719–4729.
- Scheel, C., and Weinberg, R.A. (2012). Cancer stem cells and epithelial–mesenchymal transition: Concepts and molecular links. *Seminars in Cancer Biology* *VL*.
- Schlegelmilch, K., Mohseni, M., Kirak, O., Pruszk, J., Rodriguez, J.R., Zhou, D., Kreger, B.T., Vasioukhin, V., Avruch, J., Brummelkamp, T.R., et al. (2011). Yap1 acts downstream of  $\alpha$ -catenin to control epidermal proliferation. *Cell* *144*, 782–795.
- Shimizu, N., Smith, G., and Izumo, S. (1993). Both a ubiquitous factor mTEF-1 and a distinct muscle-specific factor bind to the M-CAT motif of the myosin heavy chain beta gene. *Nucleic Acids Res* *21*, 4103–4110.
- Shirakihara, T., Saitoh, M., and Miyazono, K. (2007). Differential regulation of epithelial and mesenchymal markers by deltaEF1 proteins in epithelial mesenchymal transition induced by TGF-beta. *Mol Biol Cell* *18*, 3533–3544.
- Siegel, P.M., Shu, W., Cardiff, R.D., Muller, W.J., and Massagué, J. (2003). Transforming growth factor beta signaling impairs Neu-induced mammary tumorigenesis while promoting pulmonary metastasis. *Proc Natl Acad Sci USA* *100*, 8430–8435.
- Silvis, M.R., Kreger, B.T., Lien, W.-H., Klezovitch, O., Rudakova, G.M., Camargo, F.D., Lantz, D.M., Seykora, J.T., and Vasioukhin, V. (2011).  $\alpha$ -catenin is a tumor suppressor that controls cell accumulation by regulating the localization and activity of the transcriptional coactivator Yap1. *Science Signaling* *4*, ra33.
- Simmonds, A.J., Liu, X., Soanes, K.H., Krause, H.M., Irvine, K.D., and Bell, J.B. (1998). Molecular interactions between Vestigial and Scalloped promote wing formation in *Drosophila*. *Genes Dev* *12*, 3815–3820.
-

- 
- Singh, A., and Settleman, J. (2010). EMT, cancer stem cells and drug resistance: an emerging axis of evil in the war on cancer. *Oncogene* 29, 4741–4751.
- Sleeman, J.P., and Thiery, J.P. (2011). SnapShot: The epithelial-mesenchymal transition. *Cell* 145, 162.e1.
- Sleeman, J.P., Christofori, G., Fodde, R., Collard, J.G., Berx, G., Decraene, C., and Rüegg, C. (2012). Concepts of metastasis in flux: The stromal progression model.
- Sorrentino, A., Thakur, N., Grimsby, S., Marcusson, A., Bulow, von, V., Schuster, N., Zhang, S., Heldin, C.-H., and Landström, M. (2008). The type I TGF-beta receptor engages TRAF6 to activate TAK1 in a receptor kinase-independent manner. *Nat Cell Biol* 10, 1199–1207.
- Sperry, R.B., Bishop, N.H., Bramwell, J.J., Brodeur, M.N., Carter, M.J., Fowler, B.T., Lewis, Z.B., Maxfield, S.D., Staley, D.M., Vellinga, R.M., et al. (2010). Zyxin controls migration in epithelial-mesenchymal transition by mediating actin-membrane linkages at cell-cell junctions. *J Cell Physiol* 222, 612–624.
- Srivastava, A., Simmonds, A.J., Garg, A., Fossheim, L., Campbell, S.D., and Bell, J.B. (2004). Molecular and functional analysis of scalloped recessive lethal alleles in *Drosophila melanogaster*. *Genetics* 166, 1833–1843.
- Stewart, A.F., Larkin, S.B., Farrance, I.K., Mar, J.H., Hall, D.E., and Ordahl, C.P. (1994). Muscle-enriched TEF-1 isoforms bind M-CAT elements from muscle-specific promoters and differentially activate transcription. *J Biol Chem* 269, 3147–3150.
- Sørli, T., Perou, C.M., Tibshirani, R., Aas, T., Geisler, S., Johnsen, H., Hastie, T., Eisen, M.B., van de Rijn, M., Jeffrey, S.S., et al. (2001). Gene expression patterns of breast carcinomas distinguish tumor subclasses with clinical implications. *Proc Natl Acad Sci USA* 98, 10869–10874.
- Takebe, N., Warren, R.Q., and Ivy, S.P. (2011). Breast cancer growth and metastasis: interplay between cancer stem cells, embryonic signaling pathways and epithelial-to-mesenchymal transition. *Breast Cancer Res* 13, 211.
- Taube, J.H., Herschkowitz, J.I., Komurov, K., Zhou, A.Y., Gupta, S., Yang, J., Hartwell, K., Onder, T.T., Gupta, P.B., Evans, K.W., et al. (2010). Core epithelial-to-mesenchymal transition interactome gene-expression signature is associated with claudin-low and metaplastic breast cancer subtypes. *Proc Natl Acad Sci USA* 107, 15449–15454.
- Taylor, M.A., Parvani, J.G., and Schiemann, W.P. (2010). The Pathophysiology of Epithelial-Mesenchymal Transition Induced by Transforming Growth Factor-beta in Normal and Malignant Mammary Epithelial Cells. *J Mammary Gland Biol Neoplasia* 15, 169–190.
- Thiery, J.P. (2002). Epithelial-mesenchymal transitions in tumour progression. *Nat Rev Cancer* 2, 442–454.
- Thiery, J.P., Acloque, H., Huang, R.Y.J., and Nieto, M.A. (2009). Epithelial-mesenchymal transitions in development and disease. *Cell* 139, 871–890.
- Thiery, J.P., and Sleeman, J.P. (2006). Complex networks orchestrate epithelial-mesenchymal transitions. *Nat Rev Mol Cell Biol* 7, 131–142.
- Thuault, S., Valcourt, U., Petersen, M., Manfioletti, G., Heldin, C.-H., and Moustakas, A. (2006). Transforming growth factor-beta employs HMGA2 to elicit epithelial-mesenchymal transition. *J Cell Biol* 174, 175–183.
- Tiwari, N., Gheldof, A., Tatari, M., and Christofori, G. (2012). EMT as the ultimate survival mechanism of cancer cells. *Seminars in Cancer Biology* VL - 22, 194–207.
- Tomaskovic-Crook, E., Thompson, E.W., and Thiery, J.P. (2009). Epithelial to mesenchymal transition and breast cancer. *Breast Cancer Res* 11, 213.
-

- 
- Trimboli, A.J., Fukino, K., de Bruin, A., Wei, G., Shen, L., Tanner, S.M., Creasap, N., Rosol, T.J., Robinson, M.L., Eng, C., et al. (2008). Direct evidence for epithelial-mesenchymal transitions in breast cancer. *Cancer Res* 68, 937–945.
- Ueyama, T., Zhu, C., Valenzuela, Y.M., Suzow, J.G., and Stewart, A.F. (2000). Identification of the functional domain in the transcription factor RTEF-1 that mediates alpha 1-adrenergic signaling in hypertrophied cardiac myocytes. *J Biol Chem* 275, 17476–17480.
- Valastyan, S., and Weinberg, R.A. (2011). Tumor metastasis: molecular insights and evolving paradigms. *Cell* 147, 275–292.
- van Nimwegen, E. (2007). Finding regulatory elements and regulatory motifs: a general probabilistic framework. *BMC Bioinformatics* 8 *Suppl* 6, S4.
- Varelas, X., Sakuma, R., Samavarchi-Tehrani, P., Peerani, R., Rao, B.M., Dembowy, J., Yaffe, M.B., Zandstra, P.W., and Wrana, J.L. (2008). TAZ controls Smad nucleocytoplasmic shuttling and regulates human embryonic stem-cell self-renewal. *Nat Cell Biol* 10, 837–848.
- Varelas, X., Samavarchi-Tehrani, P., Narimatsu, M., Weiss, A., Cockburn, K., Larsen, B.G., Rossant, J., and Wrana, J.L. (2010). The Crumbs Complex Couples Cell Density Sensing to Hippo-Dependent Control of the TGF- $\beta$ -SMAD Pathway. *Dev Cell* 19, 831–844.
- Vargo-Gogola, T., and Rosen, J.M. (2007). Modelling breast cancer: one size does not fit all. *Nat Rev Cancer* 7, 659–672.
- Vassilev, A., Kaneko, K.J., Shu, H., Zhao, Y., and DePamphilis, M.L. (2001). TEAD/TEF transcription factors utilize the activation domain of YAP65, a Src/Yes-associated protein localized in the cytoplasm. *Genes Dev* 15, 1229–1241.
- Vaudin, P., Delanoue, R., Davidson, I., Silber, J., and Zider, A. (1999). TONDU (TDU), a novel human protein related to the product of vestigial (vg) gene of *Drosophila melanogaster* interacts with vertebrate TEF factors and substitutes for Vg function in wing formation. *Development* 126, 4807–4816.
- Virchow, R. (1871). *Cellularpathologie in ihrer Begründung auf Physiologische und Pathologische Gewebelehre*. 4th. edition.
- Visvader, J.E. (2009). Keeping abreast of the mammary epithelial hierarchy and breast tumorigenesis. *23*, 2563.
- Visvader, J.E. (2011). Cells of origin in cancer. *Nature* 469, 314–322.
- Visvader, J.E., and Lindeman, G.J. (2008). Cancer stem cells in solid tumours: accumulating evidence and unresolved questions. *Nat Rev Cancer* 8, 755–768.
- Vos, C.B., Cleton-Jansen, A.M., Berx, G., de Leeuw, W.J., Haar, ter, N.T., Van Roy, F., Cornelisse, C.J., Peterse, J.L., and van de Vijver, M.J. (1997). E-cadherin inactivation in lobular carcinoma in situ of the breast: an early event in tumorigenesis. *Br J Cancer* 76, 1131–1133.
- Wada, K.-I., Itoga, K., Okano, T., Yonemura, S., and Sasaki, H. (2011). Hippo pathway regulation by cell morphology and stress fibers. *Development* 138, 3907–3914.
- Wagner, K.U., McAllister, K., Ward, T., Davis, B., Wiseman, R., and Hennighausen, L. (2001). Spatial and temporal expression of the Cre gene under the control of the MMTV-LTR in different lines of transgenic mice. *Transgenic Res.* 10, 545–553.
- Wang, W., Huang, J., and Chen, J. (2011a). Angiomotin-like proteins associate with and negatively regulate YAP1. *Journal of Biological Chemistry* 286, 4364–4370.
-



- 
- Wang, W., Huang, J., and Chen, J. (2011b). Angiotensin-like Proteins Associate with and Negatively Regulate YAP1. *286*, 4364–4370.
- Weber, M., Hellmann, I., Stadler, M.B., Ramos, L., Pääbo, S., Rebhan, M., and Schübeler, D. (2007). Distribution, silencing potential and evolutionary impact of promoter DNA methylation in the human genome. *Nat. Genet.* *39*, 457–466.
- Weigelt, B., Mackay, A., A'hern, R., Natrajan, R., Tan, D.S., Dowsett, M., Ashworth, A., and Reis-Filho, J.S. (2010). Breast cancer molecular profiling with single sample predictors: a retrospective analysis. *The Lancet Oncology* *11*, 339–349.
- Weinberg, R.A. (2006). *The Biology of Cancer* (Garland Science).
- Weiss, L. (2000). Early concepts of cancer. *Cancer and Metastasis Reviews* *19*, 205–217.
- Wicki, A., Lehembre, F., Wick, N., Hantusch, B., Kerjaschki, D., and Christofori, G. (2006). Tumor invasion in the absence of epithelial-mesenchymal transition: podoplanin-mediated remodeling of the actin cytoskeleton. *Cancer Cell* *9*, 261–272.
- Wu, J., Duggan, A., and Chalfie, M. (2001). Inhibition of touch cell fate by *egl-44* and *egl-46* in *C. elegans*. *Genes Dev* *15*, 789–802.
- Wu, S., Liu, Y., Zheng, Y., Dong, J., and Pan, D. (2008). The TEAD/TEF family protein Scalloped mediates transcriptional output of the Hippo growth-regulatory pathway. *Dev Cell* *14*, 388–398.
- Xie, L., Law, B.K., Chytil, A.M., Brown, K.A., Aakre, M.E., and Moses, H.L. (2004). Activation of the Erk pathway is required for TGF-beta1-induced EMT in vitro. *Neoplasia* *6*, 603–610.
- Xie, W., Mertens, J.C., Reiss, D.J., Rimm, D.L., Camp, R.L., Haffty, B.G., and Reiss, M. (2002). Alterations of Smad signaling in human breast carcinoma are associated with poor outcome: a tissue microarray study. *Cancer Res* *62*, 497–505.
- Xu, J., Lamouille, S., and Derynck, R. (2009). TGF-beta-induced epithelial to mesenchymal transition. *Cell Res* *19*, 156–172.
- Yagi, R., Chen, L.F., Shigesada, K., Murakami, Y., and Ito, Y. (1999). A WW domain-containing yes-associated protein (YAP) is a novel transcriptional co-activator. *Embo J* *18*, 2551–2562.
- Yagi, R., Kohn, M.J., Karavanova, I., Kaneko, K.J., Vullhorst, D., Depamphilis, M.L., and Buonanno, A. (2007). Transcription factor TEAD4 specifies the trophoctoderm lineage at the beginning of mammalian development. *Development* *134*, 3827–3836.
- Yamashita, M., Fatyol, K., Jin, C., Wang, X., Liu, Z., and Zhang, Y.E. (2008). TRAF6 mediates Smad-independent activation of JNK and p38 by TGF-beta. *Mol Cell* *31*, 918–924.
- Yasunami, M., Suzuki, K., and Ohkubo, H. (1996). A novel family of TEA domain-containing transcription factors with distinct spatiotemporal expression patterns. *Biochemical and Biophysical Research Communications* *228*, 365–370.
- Yasunami, M., Suzuki, K., Houtani, T., Sugimoto, T., and Ohkubo, H. (1995). Molecular characterization of cDNA encoding a novel protein related to transcriptional enhancer factor-1 from neural precursor cells. *J Biol Chem* *270*, 18649–18654.
- Yi, J.Y., Shin, I., and Arteaga, C.L. (2005). Type I transforming growth factor beta receptor binds to and activates phosphatidylinositol 3-kinase. *J Biol Chem* *280*, 10870–10876.
- Yilmaz, M., and Christofori, G. (2009). EMT, the cytoskeleton, and cancer cell invasion. *Cancer Metastasis Rev* *28*, 15–33.
-

- Yockey, C.E., Smith, G., Izumo, S., and Shimizu, N. (1996). cDNA cloning and characterization of murine transcriptional enhancer factor-1-related protein 1, a transcription factor that binds to the M-CAT motif. *J Biol Chem* *271*, 3727–3736.
- Yoshida, T. (2008). MCAT elements and the TEF-1 family of transcription factors in muscle development and disease. *Arterioscler. Thromb. Vasc. Biol.* *28*, 8–17.
- Yu, L., Hébert, M.C., and Zhang, Y.E. (2002). TGF-beta receptor-activated p38 MAP kinase mediates Smad-independent TGF-beta responses. *Embo J* *21*, 3749–3759.
- Zavadil, J., and Böttinger, E.P. (2005). TGF-beta and epithelial-to-mesenchymal transitions. *Oncogene* *24*, 5764–5774.
- Zeng, Q., and Hong, W. (2008). The emerging role of the hippo pathway in cell contact inhibition, organ size control, and cancer development in mammals. *Cancer Cell* *13*, 188–192.
- Zhang, H., Liu, C.-Y., Zha, Z.-Y., Zhao, B., Yao, J., Zhao, S., Xiong, Y., Lei, Q.-Y., and Guan, K.-L. (2009a). TEAD transcription factors mediate the function of TAZ in cell growth and epithelial-mesenchymal transition. *J Biol Chem* *284*, 13355–13362.
- Zhang, L., Ren, F., Zhang, Q., Chen, Y., Wang, B., and Jiang, J. (2008). The TEAD/TEF Family of Transcription Factor Scalloped Mediates Hippo Signaling in Organ Size Control. *Dev Cell* *14*, 377–387.
- Zhang, X., Milton, C.C., Humbert, P.O., and Harvey, K.F. (2009b). Transcriptional output of the Salvador/warts/hippo pathway is controlled in distinct fashions in *Drosophila melanogaster* and mammalian cell lines. *Cancer Res* *69*, 6033–6041.
- Zhao, B., Lei, Q.-Y., and Guan, K.-L. (2008a). The Hippo-YAP pathway: new connections between regulation of organ size and cancer. *Curr Opin Cell Biol* *20*, 638–646.
- Zhao, B., Li, L., Lei, Q., and Guan, K.-L. (2010). The Hippo-YAP pathway in organ size control and tumorigenesis: an updated version. *Genes Dev* *24*, 862–874.
- Zhao, B., Li, L., Lu, Q., Wang, L.H., Liu, C.-Y., Lei, Q., and Guan, K.-L. (2011a). Angiotensin is a novel Hippo pathway component that inhibits YAP oncoprotein. *Genes Dev* *25*, 51–63.
- Zhao, B., Li, L., Wang, L., Wang, C.-Y., Yu, J., and Guan, K.-L. (2012). Cell detachment activates the Hippo pathway via cytoskeleton reorganization to induce anoikis. *Genes Dev* *26*, 54–68.
- Zhao, B., Tumaneng, K., and Guan, K.-L. (2011b). The Hippo pathway in organ size control, tissue regeneration and stem cell self-renewal. *Nat Cell Biol* *13*, 877–883.
- Zhao, B., Wei, X., Li, W., Udan, R.S., Yang, Q., Kim, J., Xie, J., Ikenoue, T., Yu, J., Li, L., et al. (2007). Inactivation of YAP oncoprotein by the Hippo pathway is involved in cell contact inhibition and tissue growth control. *Genes Dev* *21*, 2747–2761.
- Zhao, B., Ye, X., Yu, J., Li, L., Li, W., Li, S., Yu, J., Lin, J.D., Wang, C.-Y., Chinnaiyan, A.M., et al. (2008b). TEAD mediates YAP-dependent gene induction and growth control. *Genes Dev* *22*, 1962–1971.
- Zhao, P., Caretti, G., Mitchell, S., McKeehan, W.L., Boskey, A.L., Pachman, L.M., Sartorelli, V., and Hoffman, E.P. (2006). Fgfr4 is required for effective muscle regeneration in vivo. Delineation of a MyoD-Tead2-Fgfr4 transcriptional pathway. *J Biol Chem* *281*, 429–438.
- Ziosi, M., Baena-López, L.A., Grifoni, D., Frolidi, F., Pession, A., Garoia, F., Trotta, V., Bellosta, P., Cavicchi, S., and Pession, A. (2010). dMyc functions downstream of Yorkie to promote the supercompetitive behavior of hippo pathway mutant cells. *PLoS Genet* *6*.

## 5. Curriculum Vitae

### Personal Details

Date of birth: 25.7.1981  
Place of birth: Bern, Switzerland  
Citizenship: Swiss  
Status: not married

### Education and Professional Training

<b>Doctoral studies in tumor biology</b> Department of Biomedicine, Institute of Biochemistry and Genetics, University of Basel, Switzerland Lab of Prof. Dr. Gerhard Christofori	August 2007-present  Basel, Switzerland
<b>Master of science in molecular biology, major in cell biology</b> Biocenter, University of Basel  Field of research: Membrane Traffic Thesis title: "Characterization of the novel p24 family member CGI-100" Guidance: Prof. H. -P. Hauri	November 2005 Basel, Switzerland
<b>Bachelor of science in biology, major in molecular biology</b> Biocenter, University of Basel  Minor Subject: Informatics	November 2004 Basel, Switzerland
<b>Matura type C (Mathematics and natural sciences)</b> Deutsches Gymnasium Biel	1996-2001 Biel, Switzerland

### Foreign Tours

<b>Educational year in New Zealand</b> Hauraki Plains College, Ngatea, New Zealand	1998-99 Thames, New Zealand
---	--------------------------------

### Work Experience

<b>Master Thesis Supervisor</b> During doctoral studies	July 2009-Juli 2010
<b>IT support for Institute of Biochemistry and Genetics</b> During doctoral studies	January 2008-present
<b>Civil service duty as scientific associate in neurobiology lab</b> Universitäre Psychiatrische Kliniken (UPK) Basel, Switzerland Neurobiologisches Labor für Brain Aging and Mental Health Prof. Dr. rer. nat. Anne Eckert	April–September 06
<b>Civil service duty as scientific associate in human genetics lab</b> Department of Clinical Research, Inselspital, University of Bern, Switzerland Human Genetics Laboratory Prof. Dr. Sabina Gallati, PhD	November 06–April 07

**Attended Conferences**

<b>First FP7 metastasis summer school</b> Sesimbra, Portugal (Oral presentation)	5-9 <sup>th</sup> September 2009
<b>BioValley Science Day 2009</b> Basel, Switzerland (Oral presentation)	13 <sup>th</sup> October 2009
<b>European Cancer Center, 17th annual meeting</b> Strasbourg, France (Oral Presentation, Paul-Basset-Award for the best presentation)	May 7 <sup>th</sup> , 2010
<b>Metafight international workshop on metastasis research</b> Torino, Italy (Poster presentation)	2-3 <sup>rd</sup> December 2010
<b>ENDBC workshop on methods in mammary gland biology and breast cancer</b> Weggis, Switzerland (Poster presentation)	23-25 <sup>th</sup> April 2010
<b>8<sup>th</sup> BC2 Basel computational biology conference</b> Basel, Switzerland	24-25 June 2010
<b>1<sup>st</sup> international SystemsX.ch conference on systems biology</b> Basel, Switzerland	24-26 <sup>th</sup> October 2011

**Publications**

- Koegler E, Bonnon C, Waldmeier L, Mitrovic S, Halbeisen R, Hauri H-P. p28, a novel ERGIC/cis Golgi protein, required for Golgi ribbon formation. *Traffic*. 2010 Jan.;11(1):70–89.
- Yilmaz M\*, Maass DM\*, Tiwari N, Waldmeier L, Schmidt P, Lehembre F, et al. Transcription factor Dlx2 protects from TGF-beta-induced cell-cycle arrest and apoptosis. *EMBO J*. 2011 Sep. 6;:1–11.
- Waldmeier L, Meyer-Schaller N, Diepenbruck M, Christofori G. Py2T murine breast cancer cells, a versatile model of TGFβ-induced EMT *in vitro* and *in vivo* (submitted)
- Tiwari N, Waldmeier L, Pachkov M, Meyer-Schaller N, Arnold P, van Nimwegen E, Christofori G. Sox4 regulates epithelial-mesenchymal transition by directly controlling Ezh2 methyltransferase expression (submitted)

## 6. Acknowledgments

I would like to express my sincere gratitude to Gerhard Christofori for giving me the chance and freedom to pursue the research projects of my interest, while at the same time supporting me wherever and whenever needed. I much appreciated his uncomplicated and congenial way of collaboration, and I am grateful for the intensive and highly instructive time I could spend in his laboratory.

Special thanks go to Maren. As a former master student, her steep learning curve made supervision a pleasant and valuable experience for me. Sitting in the same (PhD) boat, she developed into an invaluable part of what is now a team that complements each other effectively. Her exceptional passion for science was always of high value, especially when I was in danger of losing steam. I greatly enjoyed working together, and I hope that I have the chance to meet more collaborators like this in my future career.

I would also like to thank ALL the former and present lab-members for (in no particular order): inspiration, teaching, helping me out, setting my boundaries, music, cakes, coffee, motivation, fun, drinks, smiles, laughs, mutual respect, Eureka! moments, cash, anticipation, challenges, crosswords, ideas and sharing dreams.

I am tremendously thankful and truly blessed to be able to count on the profound love and support of my family. This one goes to you.

Most importantly, I thank Carole for the life we live, for her love, joyfulness and patience, and for the harmony that lets us conquer the rat race.